The Syntheses and Photochromic Properties of Several Substituted and Condensed Benzo[e]dimethyldihydropyrenes

Yunxia Wang

B.Sc. University of Science and Technology of China, Hefei, 1988
M.Sc. University of Science and Technology of China, Hefei, 1991

A Dissertation Submitted in Partial Fulfillment of the
Requirements for the Degree of

DOCTOR OF PHILOSOPHY

in the Department of Chemistry

We accept this dissertation as conforming
to the required standard

Dr. R. H. Mitchell (Department of Chemistry)

Dr. T. M. Fyles (Department of Chemistry)

Dr. R. G. Hicks (Department of Chemistry)

Dr. R. W. Olafson (Department of Biochemistry)

Dr. R. R. Tykwinski (Department of Chemistry, University of Alberta)

Supervisor: Dr. R. H. Mitchell

ABSTRACT

The symmetric multistate photo-switchable molecule **72**, which contains two DHP units with a dibenzocyclophane as a spacer, was successfully synthesized by different routes using aryne-furan type Diels-Alder reactions. In the course of making **72**, the intermediate furan **79** was synthesized, which upon deoxygenation gave photo-switchable furan **82**.

In a study of substitution effects on benzo[e]pyrene **21**, the substituents phenyl, acetyl, nitro and phenylethynyl were attached to the 4,5-positions. The acetyl and nitro groups were introduced by direct substitution of **21**, while coupling methodology were used for the phenyl and phenylethynyl groups. In the later case, a Suzuki coupling was used on bromide **69**, followed by bromination, or a Sonogashira coupling was used on the bromoiodide **100**, and then an aryne-furan Diels-Alder reaction and deoxygenation were used to give the final substituted benzo[e]pyrenes **105** and **103**.

The successful synthesis of the phenylbenzo[e]pyrene **105** enabled us to access the monosubstituted tris-pyrene system **120** through the reaction of bromophenylpyrene **107** and furan **79**.

The thermal return reactions (cyclophanediene to dihydropyrene) were studied on the benzo[e]pyrene derivatives and multistate photoswitch systems. Although the activation energies and enthalpies do not change much with substitution, the thermal return rates do appear to decrease with an electron withdrawing substituent.

Photochromic studies were performed on **72** and **120**. They both opened in a stepwise manner with one DHP ring opening and then the other, though the intermediate could not be isolated.

A simple comparison of the photo opening and closing rates relative to benzo[e]pyrene **21** was performed under excess light conditions. All the derivatives of **21** synthesized in this thesis had faster visible opening rates than the parent **21**; the UV closing rates did not change much however.

Examiners:

Dr. R. H. Mitchell (Department of Chemistry)

Dr. T. M. Fyles (Department of Chemistry)

Dr. R. G. Hicks (Department of Chemistry)

Dr. R. W. Olafson (Department of Biochemistry)

Dr. R. R. Tykwinski (Department of Chemistry, University of Alberta)

Table of Contents

Chapter One Introduction

Chapter Two Syntheses

Chapter Three

Photochemical and Thermochemical Results and Discussion

List of Tables

List of Figures

List of Numbered Compounds

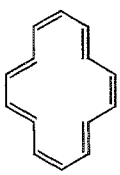
1

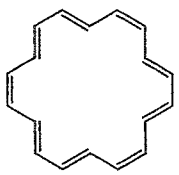
2

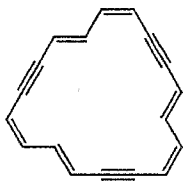
3


4


5


6


7


8


9


10


11

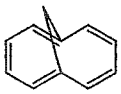
12

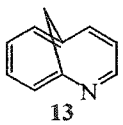
13

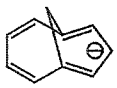
14

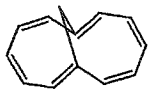
15

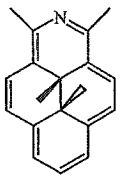
16

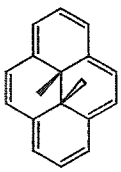
17

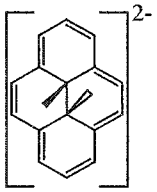
18

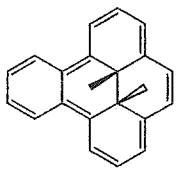
19

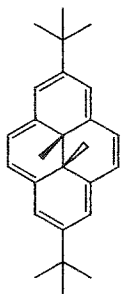
20

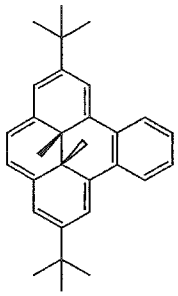
21

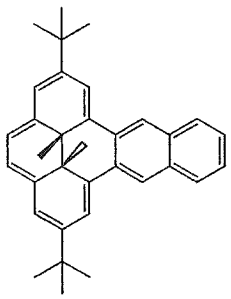
22

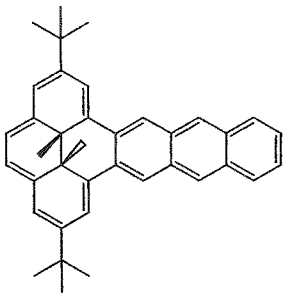
23

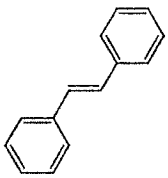
24

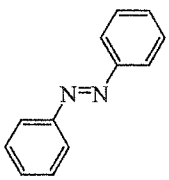
25

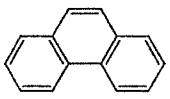
26

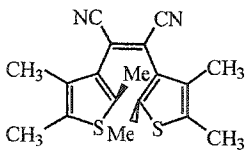
27

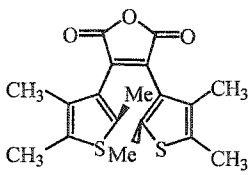
28

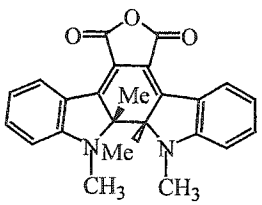
29

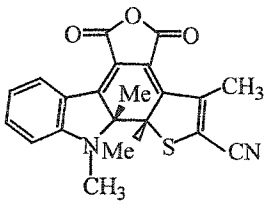
30

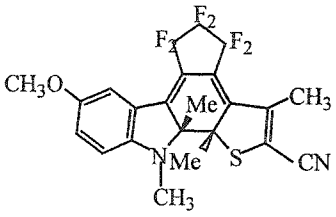
31

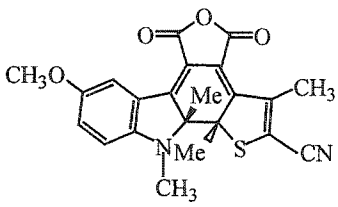
32

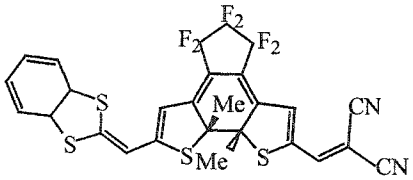
33

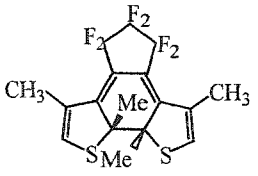

34

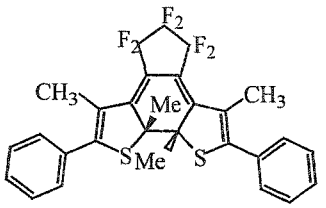

35

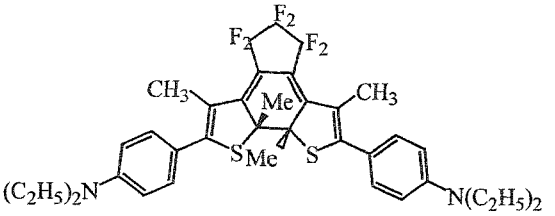

36

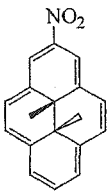

37

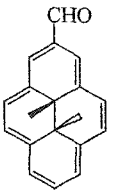

38

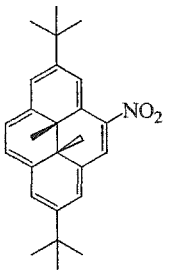

39

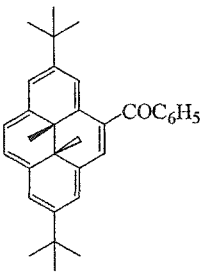

40

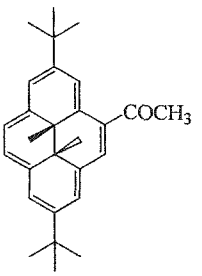

41

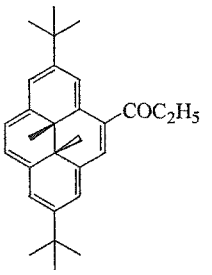

42

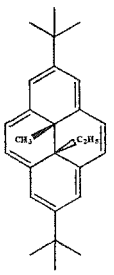

43

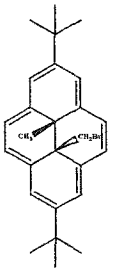

44

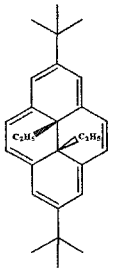

45

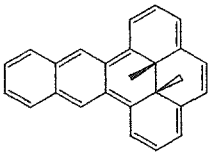

46

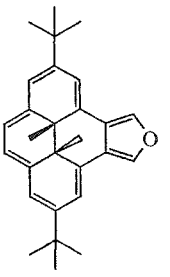

47

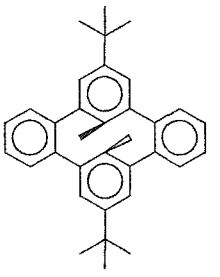

48

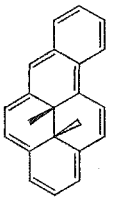

49

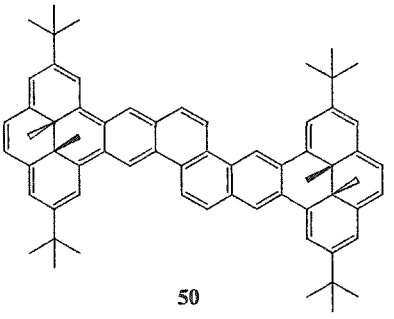

50

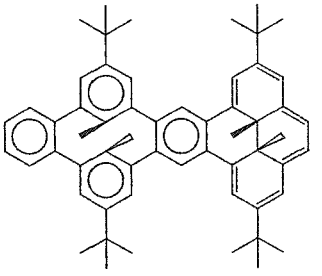

51

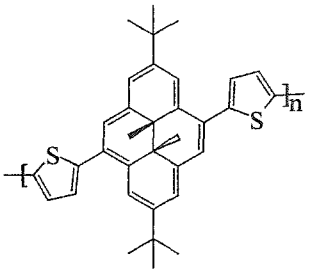

52

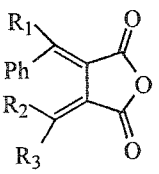

53

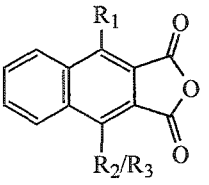

54

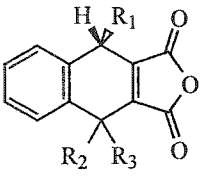

55

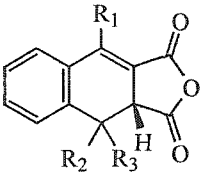

56

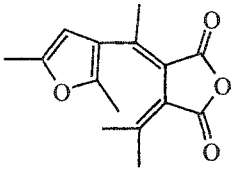

57

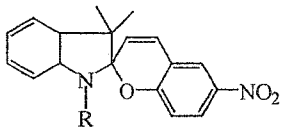

58

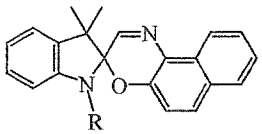

59

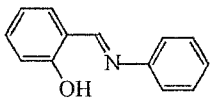

60

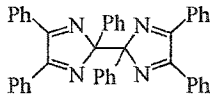

61

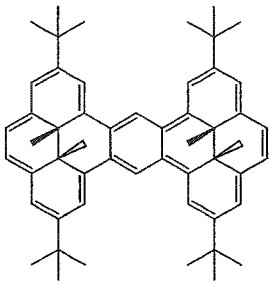

62

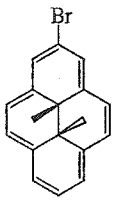

63

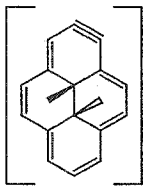

64

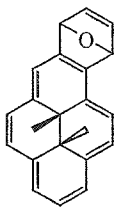

65

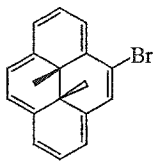

66

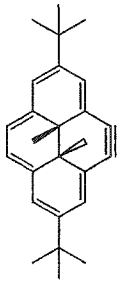

67

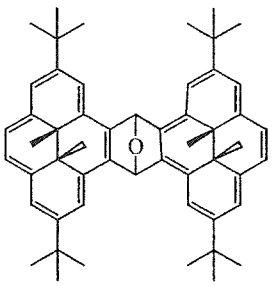

68

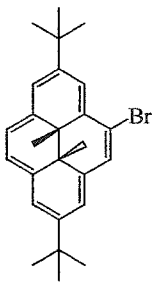

69

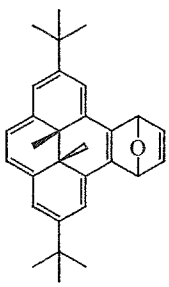

70

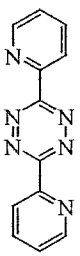

71

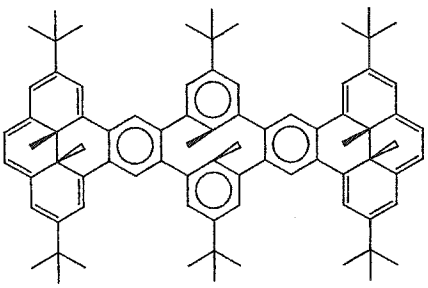

72

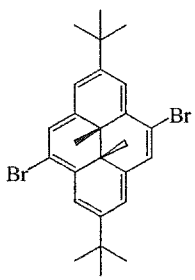

73

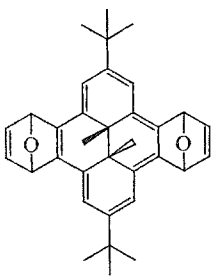

74

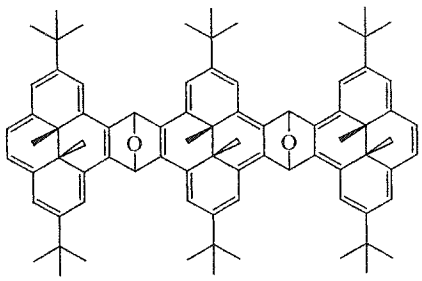

75

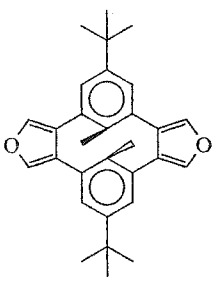

76

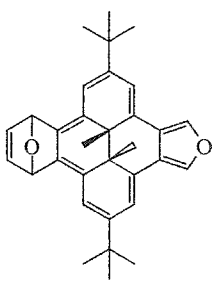

77

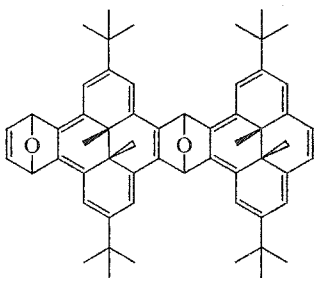

78

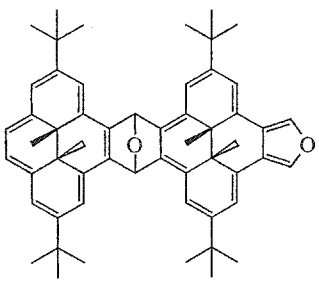

79

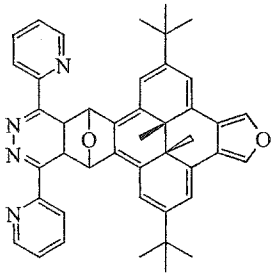

80

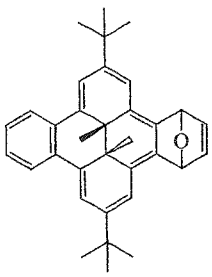

81

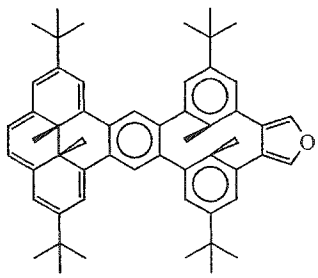

82

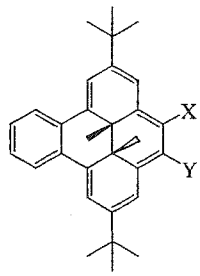

83

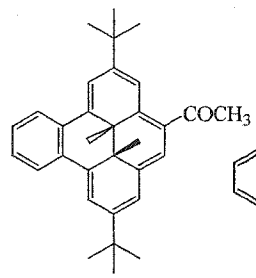

84

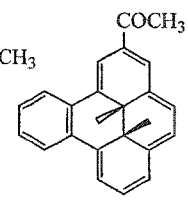

85

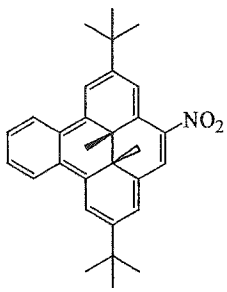

86

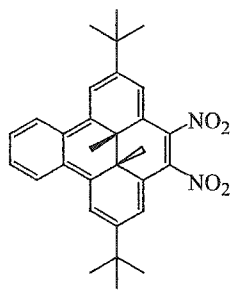

87

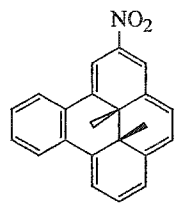

88

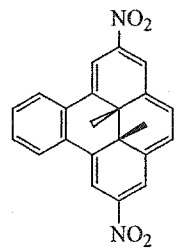

89

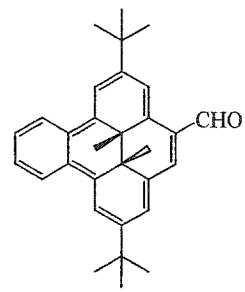

90

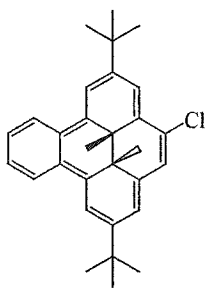

91

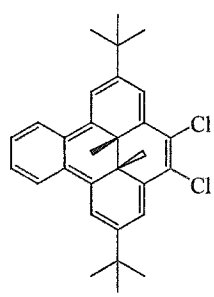

92

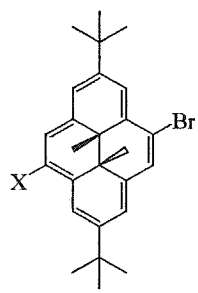

93

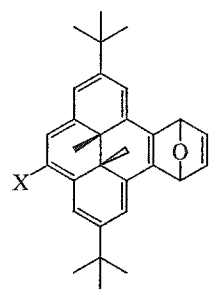

94

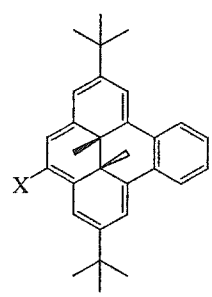

95

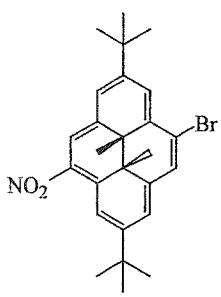

96

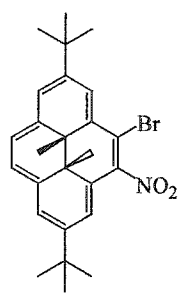

97

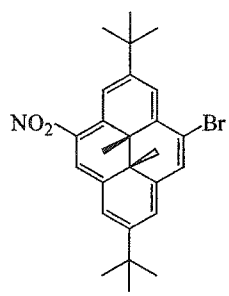

98

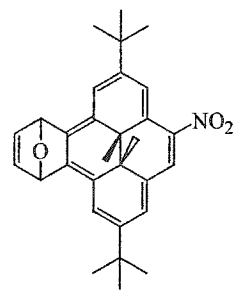

99

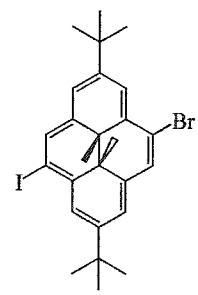

100

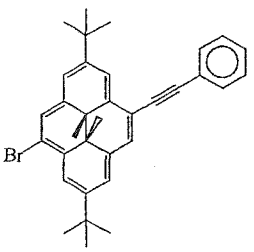

101

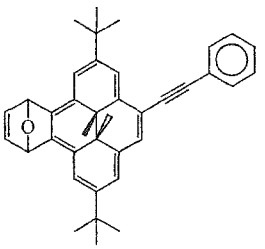

102

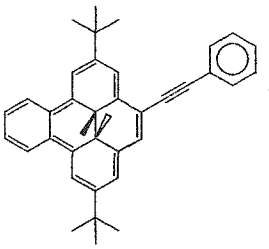

103

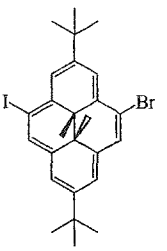

104

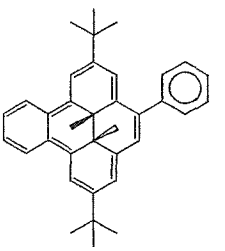

105

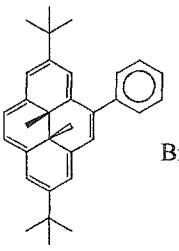

106

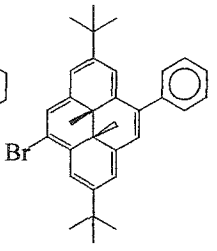

107

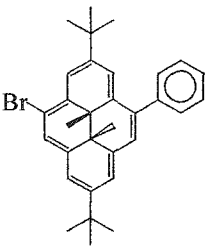

108

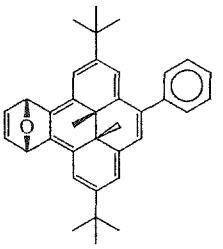

109

110

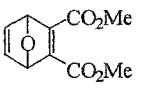

111

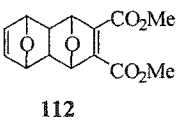

112

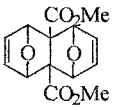

113

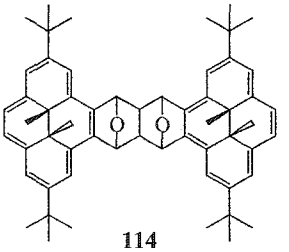

114

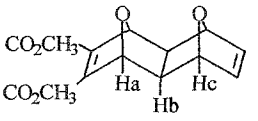

115

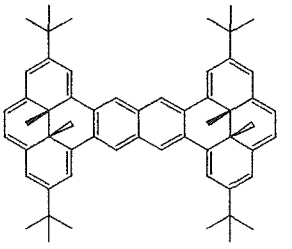

116

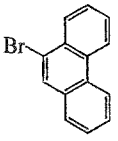

117

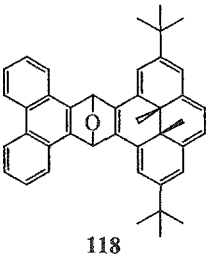

118

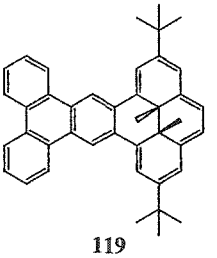

119

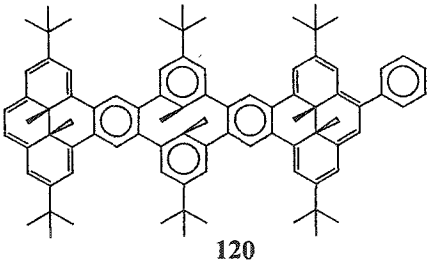

120

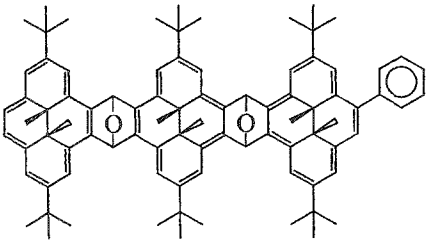

121

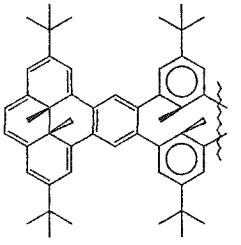

122

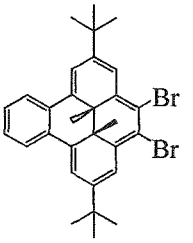

123

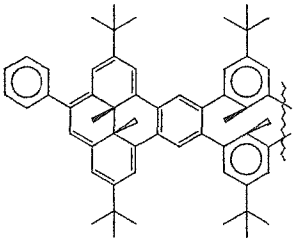

124

List of Abbreviations

Ar	arene
BLE	bond localization energy
CI	chemical ionization
CPD	metacyclophanediene
δ	chemical shift in ppm from standard
dec.	decomposition
DHP	dimethyldihydropyrene
DMF	dimethylformamide
EtOAc	ethyl acetate
EI	electron impact
h	hour
HRMS	high resolution mass spectrum
IR	infrared spectrum
KO^{t}Bu	potassium *t*-butoxide
LSIMS	liquid secondary ion mass spectrometry
Me	methyl
MeOH	methanol
min	minute
mp	melting point
MS	mass spectrum
NBS	N-bromosuccinimide

NMR	nuclear magnetic resonance
bs	broad singlet
s	second, singlet
d	doublet
dd	doublet of doublet
m	multiplet
ppm	parts per million
RE	resonance energy
sd	standard deviation
sub	sublime
t	tertiary group
TBA	tetra-*n*-butylammonium cation
THF	tetrahydrofuran
UV-Vis	ultraviolet and visible spectrum

Acknowledgement

I would like to express my deep gratitude to Dr. R. H. Mitchell for his guidance and constant encouragement during the course of this work. I especially appreciate his patience in the correction of this thesis, both Chemistry and English.

I also thank a previous graduate student, Dr. T. R. Ward for helping me start the lab work, Mrs. Christine Greenwood for recording NMR spectra and Dr. David McGillivary for mass spectrometric analysis.

Finally, financial support from the University of Victoria and from the Natural Sciences and Engineering Research Council of Canada is greatly appreciated.

To my husband, Jian Pu and my sons, Cullen and Gavin

Chapter One Introduction

1.1 Aromaticity

The chemistry of aromatic compounds began with the discovery of benzene by Faraday[1] in 1825. Kekule[2] first suggested the cyclic structure of benzene in 1865 and applied the term aromatic to compounds containing a benzene ring. A year later, Erlenmeyer[3] designated as aromatic compounds, those which had chemical reactivities similar to benzene. At that time, all unsaturated systems with cyclic conjugation were considered to be aromatic, until Willstaetter[4] showed that cyclooctatetraene had no chemical similarity to benzene.

Later, the 19th-century concept of the oscillation of double and single bonds in benzene was replaced by the concept of resonance between canonical structures. Huckel's molecular orbital (HMO) theory made the first successful attempt to account for such stability based on π-electron configurations.[5] Huckel suggested that amongst fully conjugated, planar, monocyclic polyolefins, only those possessing $(4n + 2)$ π-electrons (n is an integer) have special stability.

Although Huckel's work appeared in 1931, it was overlooked by many organic chemists for nearly 20 years until the 1950s, when there was an explosion of work based on the ideas that he presented, and in particular to prepare appropriate compounds to test their validity.

A series of annulenes were prepared. [14]Annulene **1** and [18]annulene **2** were shown to have properties that classified them as aromatic.[6] As well, dehydroannulenes,

such as the cyclopolyenyne **3,** were also prepared and shown to have properties appropriate for a conjugated (4n + 2) π-electron system.

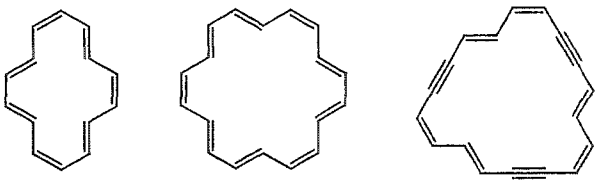

1 **2** **3**

Huckel's rule thus provided a theoretical basis for aromaticity, even though it did not cover all cases, and was still questioned by many chemists. However, it generated interest to find further experimental evidence to describe aromaticity.

1.1.1 Estimation of Aromaticity

Aromaticity is often considered an elusive concept and the choice of criteria is controversial. Different individuals might have different ideas and feelings of exactly what they mean by the term. The one unifying basis for these ideas is that an aromatic compound is "benzene like". But how and in what way?

On looking at the chemical reactivity of benzene, the following properties should be considered.

- Thermal stability.
- Resistance of the ring to oxidation.
- Electrophilic substitution, rather than addition, reactions.

The problem with any criterion based on chemical properties is that it embraces a very wide range of different reactions and types of reactions, and different compounds

may resemble benzene in some way but may differ in others, and thus it is effectively impossible to lay down a precise criterion.

Thermodynamic stability is another possible comparison basis, and it has been proposed that cyclic conjugated systems may be considered to be aromatic if cyclic delocalization makes a negative contribution to their heat of formation.[7] Once again there are problems in providing uniform standards. These include the difficulty often involved in obtaining reliable data and in finding suitable reference compounds with which they may be compared. Furthermore, although delocalization may be an important factor in contributing to the overall stability of a conjugated cyclic polyene, other contributing factors may sometimes nullify or override its effect.

Another criterion is based on physical evidence for delocalization of π-electrons, in particular the equalizing of bond lengths of the aromatic ring. Complete cyclic delocalization of π-electrons in a homocyclic ring should lead to all the bonds being of equal length, as is the case in benzene, where all the bond distances are 1.397Å. In fact, the C-C bond lengths in aromatic compounds should have values that are intermediate between the length of a single C_{sp^2}-C_{sp^2} bond (1.465Å in butadiene) and a C=C double bond (1.337Å in ethylene). However, this criterion obviously does not easily apply to heterocyclic and polycyclic systems because of their lower symmetry. More importantly, X-ray data is needed for this method, and sometimes this is not easy to obtain.

Perhaps the most useful criteria are magnetic criteria, which include diamagnetic anisotropy, diamagnetic susceptibility exaltation and ^{1}H NMR diatropism. The later is currently the most favored one.

The majority of organic molecules do not have permanent magnetic moments and consequently are weakly diamagnetic, having negative magnetic susceptibilities. Most diamagnetic molecules are anisotropic; that is, the magnitudes of the diamagnetic susceptibility along the three perpendicular principle magnetic axes are not equal. The diamagnetic anisotropy is defined as $\Delta\chi_m = \chi_z - \frac{1}{2}(\chi_x + \chi_y)$, where χ_x, χ_y, and χ_z are the three principal components of the diamagnetic susceptibility. Direct measurement of the anisotropy of the molar diamagnetic susceptibilities $\Delta\chi_m$, requires the growth of a monocrystal and an initial determination of the molecular orientation. Analysis shows that only a fraction of $\Delta\chi_m$ for aromatic compounds, about one half for benzene,[8] can be attributed to the ring current, whereas the other fraction is due to local anisotropy. The experimental difficulties and the need to separate the contributions of the local and non-local components limit the widespread use of the anisotropy of diamagnetic susceptibility as a criterion of aromaticity.

A property which is simpler to determine is the difference between the total molar magnetic susceptibility of an aromatic compound and that of an analogous hypothetical compound with localized bonds, $\chi_M - \chi_M^{loc}$, this property is known as the exaltation of diamagnetic susceptibility (Λ)[9] or non-local magnetic susceptibility (χ_M^{nonloc}).[10] The total molar magnetic susceptibility χ_M of the compound under study is measured experimentally by determining the force at which the sample of the substance is repelled by a magnetic field of a given strength. The magnetic susceptibility of the hypothetical compound with localized bonds χ_M^{loc} is calculated as the sum of the contributions of the separate structural elements of the molecule. Table 1 gives some examples of exaltation of diamagnetic susceptibility.

Table 1. Exaltation of diamagnetic susceptibility ($10^{-6}m^3mol^{-1}$).[11]

Compound	Λ
Benzene	13.7
Naphthalene	30.5
Anthracene	48.6
Furan	8.9
1,3-Cyclohexdiene	-0.7
[16]Annulene	-5

Again, the need for hypothetical compounds always provides a chance of obtaining misleading results.

1.1.2 Ring Current and ^{1}H NMR Spectroscopy

NMR spectroscopy is a popular method for the study of diamagnetic compounds. The proton chemical shifts in a NMR spectrum can be related to the diatropicity and paratropicity of the system and hence can serve as a criterion for assessment of their aromatic nature.

Proton chemical shifts for the conjugated π systems drawn in next page are shown in Table 2.

Benzene **4**, which is considered as the "prototype" aromatic molecule, shows a proton chemical shift at δ 7.27, which is about 1.5 ppm downfield from a normal alkene. The additional deshielding can be explained by the induced ring current, which will be discussed later. In [14]annulene **1**, the inner protons are shielded due to the ring current

and appear at δ -0.61. In the isoelectronic bridged annulene **17**, the internal methyl protons appear at δ -4.25. Any deviation from planarity leads to a reduction of ring current. The bridged [10]annulene **12** has a bent geometry, with the internal methylene group pointing away from the π network, the bridge protons appear at δ -0.52 and are less shielded compared to **17**. When an annulene suffers a total lack of planarity, the delocalization is disrupted. As a result, there is no ring current and hence it is atropic.

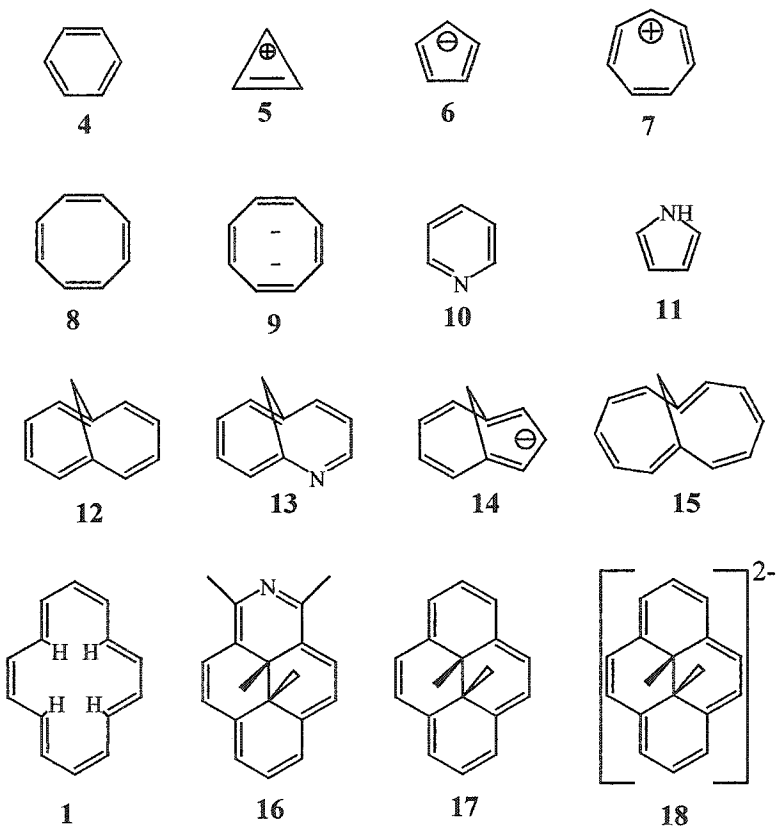

Cyclooctatetraene **8**, is tub shaped and its protons appear at δ 5.7. Since the proton chemical shift falls in the normal alkene range, this suggests there is no special ring current in this molecule. On the other hand, in the near planar [12]annulene **15**, the inner protons are more strongly deshielded than those in normal alkenes. This paratropic

behavior is even more dramatic in the case of dianion **18**, whose internal methyl protons appear at δ 21.

Table 2. ^{1}**H NMR Chemical shifts (δ) of selected π systems.**

Compound	π electrons	δ outer protons	δ inner protons	reference
4	6	7.27		12
5	2	11.10		13
6	6	5.60		14
7	6	9.20		14
8	8	5.70		15
9	10	5.70		15
10	6	8.50 – 7.46		16
11	6	7.70 – 6.05		16
12	10	7.27 – 6.95	-0.52	17
13	10	8.23 – 6.50	0.65 to -0.40	18
14	10	6.80 – 5.40	-0.70 & -1.20	19
15	12	5.50 – 5.20	6.06	20
1	14	7.88	-0.61	21
16	14	9.50 – 8.70	-3.75 & -3.80	22
17	14	8.67 – 7.98	-4.25	23
18	16	-3.19 to -3.96	21.00	24

The protons of cyclopropenium cation **5**, resonate downfield at δ 11.1. In this case, the positive charge also deshields the protons. By the same token, an upfield shift

is experienced by protons in a negatively charged system. This is manifested in the proton chemical shift of the aromatic cyclooctatetraenyl dianion **9**, which is the same as that of the non-aromatic cyclooctatetraene.

In heterocycles, the proton chemical shifts are affected not only by the ring current, which is similar to that in their benzenoid analogs, but also by the charge density on the atom to which the proton is bound. Pyrrole **11,** is more electron-rich than pyridine **10**; the dipole moment of pyrrole points away from the nitrogen, and towards the nitrogen in case of pyridine. The non-ring current factors make the protons in pyridine more deshielded than those in pyrrole.

Vogler[25] has derived an equation relating the observed total shielding effect (σ) to the shielding due to ring current and other factors. This is given in the following equation:

$$\sigma = \sigma^{RC} + \sigma^{LA} + \sigma_{\mu}{}^{0} + \sigma_{v}{}^{q}$$

Where σ^{RC} = Shielding due to ring current

σ^{LA} = Shielding due to the local anisotropy

$\sigma_{\mu}{}^{0}$ = Zero of the chemical shift scale

$\sigma_{v}{}^{q}$ = Shielding due to excess π-electron density

Therefore, interpretation of the chemical shifts has to be carried out with extreme caution, especially in the case of charged systems and heterocycles, where the shielding arising from local anisotropic contributions and excess π-electron density are of equal importance.[26]

The ring current model, although proposed by Pauling[27] in 1936, was first applied to proton chemical shifts by Pople[28] in 1956. According to this model the benzene ring

is looked upon as a conduction loop in which the π-electrons circulate perpendicularly to the direction of the external magnetic field H_0. A secondary magnetic field is induced opposing the external one. This is illustrated in Figure 1.

Figure 1. Induced ring current and proton magnetic deshielding in benzene.

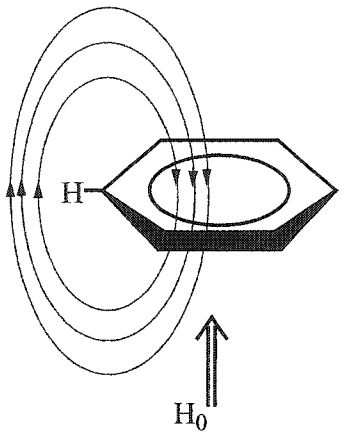

Although there is no proof that ring current exists, the ring current theory does adequately explain the chemical shifts of annulenes, and it has become a widely accepted concept. Haddon's work[29] on the calculation of ring currents for annulenes is quite remarkable. As for the calculation of resonance energy, a reference compound has to be chosen to obtain the model chemical shift (MCS). The reference proton should experience the same magnetic environment as the proton of interest, but without the magnetic contribution from the ring current. Ring current chemical shift (RCCS) = Observed chemical shift (OCS) - Model chemical shift (MCS). Ring current (RC) is calculated by $RCCS_i = RC \times RCGF_i$. (i = 1,..., n). RCGF is the ring current geometric factor; n is the number of distinct chemical shifts in the observed molecule. Because chemical shift is affected by so many factors other than the ring current,[25] the reference

proton chemical shift is almost impossible to estimate for molecules other than annulenes. Haddon's ring current calculation thus mostly applies to annulenes.

A novel comparison was designed by Mitchell[30] using a probe molecule to measure relative aromaticity with respect to benzene. The selected probe is dimethyldihydropyrene (DHP) **17**, in which the internal methyl protons are shielded quite dramatically (δ -4.25). This chemical shift is remarkably affected by fusion of an aromatic ring on the side, but not much by substituents. This phenomenon can be explained by a bond localization effect.

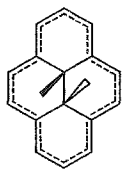

17

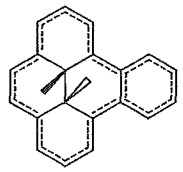

19

When a benzene ring is fused to the [14]annulene **17** to give compound **19**, the ring current in the DHP ring changes profoundly. Because of the π electron delocalization in the benzo moiety, all bonds are partially localized. The complete delocalization in DHP ring is broken; thus, the induced ring current is dramatically reduced. The competition of the ring currents between DHP and benzene depends on their relative resonance energies. The manifestation of the ring current is best shown by the internal proton chemical shifts in such annulenes. An intrinsic relationship exists between proton chemical shift and resonance energy.[29] If different aromatic moieties are fused to DHP, and the internal methyl proton chemical shifts are compared, the resonance energy (or more strictly, the bond localization energy, BLE) of the fused molecule can be determined relative to benzene.

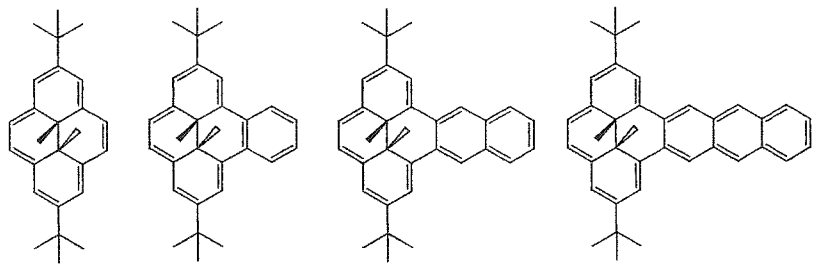

20 **21** **22** **23**

The series with [e]-fused aromatics **20-23** is one of the most recently series studied.[31] There is a near linear relationship between BLE (here Dewar resonance energies are used) and the internal methyl proton chemical shift δ(Me).

$$BLE = [3.39 + \delta(Me)]/2.24$$

Table 3. Comparison of calculated and actual BLE values (benzene units)[a].

Compound	**δ(Me)**	**calculated BLE**	**Actual BLE**
20	-4.06	0.03	0.00
21	-1.58	1.08	1.00
22	-0.54	1.54	1.52
23	0.00	1.78	1.84[a]

[a]Dewar RE (anthracene) = 1.600eV =1.84 benzene units;

1 benzene unit = RE(benzene) = 0.869 eV.

The calculated BLEs in Table 3 are from the above equation. We can see the discrepancies are rather small for all the compounds.

This work gives an experimental determined resonance energy relative to benzene, No reference molecule is needed in calculating the relative resonance energy to benzene.

1.2 Photochromism

Photochromism is a reversible transformation of a chemical species induced in one or both directions by absorption of electromagnetic radiation between two forms, A and B, having different absorption spectra.[32]

$$A \underset{h\nu_2/\text{Thermal}}{\overset{h\nu_1}{\rightleftharpoons}} B$$

There are two types of photochromism. One is when the back reaction occurs thermally, which is called type T; if the back reaction occurs photochemically, it is called type P. Usually the thermodynamically stable form A is colorless or light yellow and form B is colored, and this is then referred to as positive photochromism. When the maximal absorption wavelength of A is longer than B, then the photochromism is negative or inverse. We will see later that our dimethyldihydropyrene (DHP) system is an example of negative photochromism.

In order to be put to practical use, a photochromic compound must have the following properties:[33]

(1) Thermal stability of both isomers;

(2) Low fatigue (can be cycled many times without significant loss of performance);

(3) High sensitivity and rapid response;

(4) Nondestructive readout capability.

Among these requirements, the most important ones are the thermal stability of both isomers and the fatigue resistance.

1.3 Examples of Organic Photochromic Compounds

For photochromic compounds, the chemical processes involved mostly belong to the following five types.

(1) *cis-trans* Isomerization;

(2) Electrocyclic reaction;

(3) Heterolytic cleavage;

(4) Tautomerism;

(5) Homolytic cleavage.

The examples hereafter are followed the five types to illustrate different photochromic compounds.

1.3.1 *cis-trans* Isomerization

(a) Stilbenes

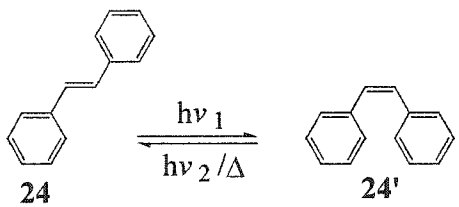

24 **24'**

The *cis-trans* isomerization of stilbene is an early example of a photochromic conversion and now primarily is only of theoretical and historical interest. Henry[34] was the first to delineate with clarity the several processes occurring when stilbenes are irradiated with light.

The ultraviolet absorption spectrum in solution shows that the first absorption maximum of the *trans*-isomer **24** (294 nm) is at lower energy than that of the *cis*-isomer **24'** (272 nm).[35] This implies that the *cis*-isomer is less planar.

Monosubstitution by halogen at the *para* position does not alter the absorption spectra of the stilbenes appreciablly.[36,37] The introduction of groups more polar than halogen, shifts the absorption slightly to the red: *trans*-4-nitro or 4-dimethylaminostilbenes have absorption maxima at ~ 350 nm, whereas the *cis*-isomers have λ_{max} ~ 310 nm.[38]

(b) Azobenzenes

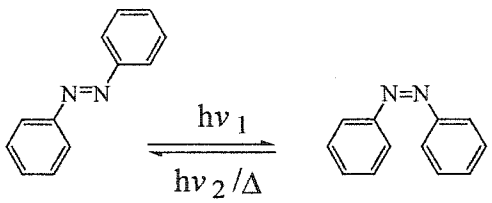

25 **25'**

Azobenzene and nearly all its mono-substituted derivatives have their principal absorption bands (π-π*) in the ultraviolet region and their yellow color is caused by a weak n-π* absorption near 450 nm.[39] On conversion to the *cis*-isomer **25'**, the π-π* band shifts to shorter wavelengths and there is an increase in the strength of the n-π* absorption, often accompanied by a shift in absorption maximum.

Substitution of positions *ortho* or *para* to the azo function with a strongly electron-donating group such as amino or dimethylamino shifts the main absorption band into the visible spectrum, sometimes causing it to overlap the n-π* band.[40]

1.3.2 Electrocyclic Reaction

(a) *cis*-Stilbene to dihydrophenanthrene

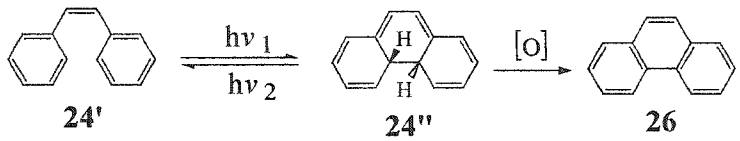

24' **24"** **26**

Two photochromic reactions occur for stilbene: *cis-trans* isomerization and photocyclization.[41,42] They compete with each other. In the presence of air, the dihydrophenanthrene **24"** irreversibly converts to phenanthrene **26** through hydrogen elimination by reaction with oxygen as shown above. When the 2 (or 6) and 2' (or 6') positions of the above phenyl rings were substituted with methyl groups, the elimination reaction was suppressed and the compound underwent a reversible photocyclization reaction, that is, a photochromic reaction, even in the presence of oxygen.[43] However, the lifetime of the colored dihydrophenanthrene was very short; in the dark, the yellow color disappeared in 3 min at 30°C.

(b) Diarylethenes

Diarylethenes are derivatives of stilbenes. For the parent compounds stilbenes, there are several problems which limit their application as switches: the *cis-trans* isomerization competing with the photocyclization, and the oxidation of the photocyclized product to form phenanthrene.

A third problem is the thermal return reaction. The lifetime of the dihydro intermediate of stilbene derivatives is not long enough for practical applications. In the course of searching for thermally irreversible stilbene-like compounds suitable for

photocyclization, Irie[43] has developed a series of diarylethenes involoving heterocycles. The following examples were the first thermally irreversible diarylethenes.

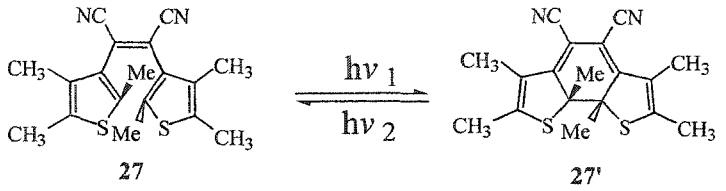

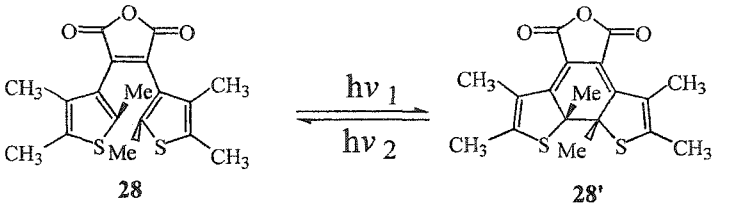

The dicyano and maleic anhydride groups were selected to shift the absorption maxima of the dihydro-type isomers to longer wavelengths. The maleic anhydride group also prohibits the *cis-trans* photoisomerization. The photogenerated dihydro-type isomers of the above two compounds are thermally inert in the dark for more than three months, even at 80°C, but readily regenerated the open ring isomers by irradiation with visible light ($\lambda > 450$ nm).

A theoretical study by Nakamura and Irie[44] produced a guide for the synthesis of thermally irreversible photochromic diarylethenes. This can be summarized as follows:

The activation energy barrier for the forward and reverse reactions correlates with the ground state energy difference between the open- and the closed-ring isomers. The barrier becomes large when the energy difference is small, and vise versa. When the energy barrier is small the cycloreversion reaction readily takes place. On the other hand, the aromatic stabilization energy of the aryl groups correlates well with the ground

state energy difference. For the simple diarylethenes, the highest energy difference was from phenyl group and the lowest was from the thienyl group.

Following the above principle, various diarylethenes with different aryl groups, ethene links and suitable substitutions were synthesized.[33] Most of the closed ring forms are stable with a lifetime over 12 h at 80°C and can undergo ~ 10^4 cycles of opening and closing.

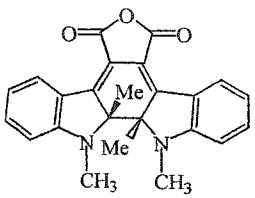

29

620 nm

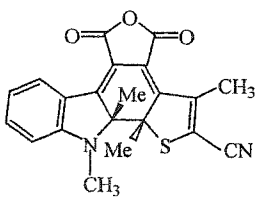

30

628 nm

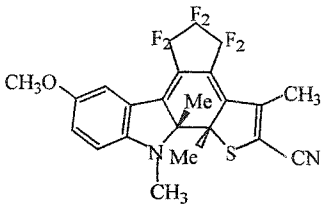

31

665 nm

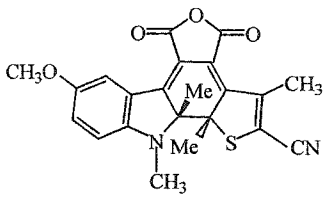

32

680 nm

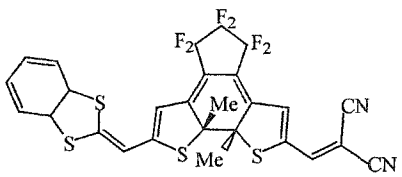

33

828 nm

For application to optical memory, it is desirable to develop photochromic compounds that have sensitivity in the wavelength region 650-830 nm. The absorption spectra of closed ring isomers are affected by substitutents on the aryl groups while the upper cycloalkene structure affects the absorption spectra of open ring isomers. The above picture gives a few successful structures with promising absorption maxima.

Unfortunately, compound **33** with the longest absorption wavelength of the closed ring isomer was thermally unstable, returning to the open isomer in 186 min at 60°C.

Another requirement of photochromic compounds for application, is to have high molar absorption coefficients (ε).

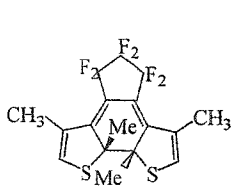

34

5.0×10^3 L mol^{-1} cm^{-1}

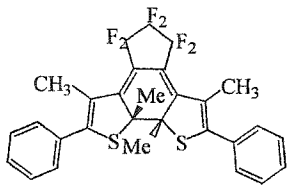

35

1.0×10^4 L mol^{-1} cm^{-1}

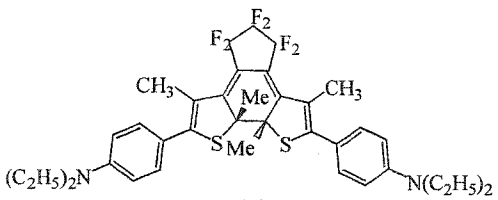

36

1.8×10^4 L mol^{-1} cm^{-1}

The ε value of the parent dithienylperfluorocyclopentene **34** was doubled by introducing phenyl rings at the 5 and 5' positions of the thiophene rings. This further increased to 1.8×10^4 L mol^{-1} cm^{-1} when electron donating *N,N*-diethylamino groups were substituted at the para position of the phenyl rings. Research showed that introduction of electron rich substituents or large π-conjugation systems is effective at increasing ε values. Electron withdrawing substituents did not affect the ε value, although, they increased the absorption maxima.[33]

(c) Dimethyldihydropyrenes

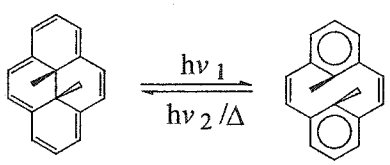

17 **17'**

This is one of the very few negative photochromic systems, where the closed form (DHP) **17**, is the colored stable state, and the open form metacyclophanediene (CPD) **17'**, is the thermally unstable colorless state. Irradiation of DHP with visible light converts it

to the CPD; irradiation with ultraviolet light closes it back to the green DHP. This latter reaction also occurs thermally.

For the following chapters, as for compounds **17** and **17'**, the prime indicates the fully opened photo isomer. The thermal return reaction refers to the reaction in which the open isomer converts to the closed isomer.

Early studies on the parent **17**, and many of its simple substituted derivatives were carried out by Blattmann.[45,46] These results suggested that the quantum yield for the UV closing **17'** to **17**, was close to one, while that for the visible light opening of **17** to **17'**, was only about 0.02. The difference in enthalpy between DHP and CDP is about 3 kcal mol^{-1} regardless of substituents. Electron withdrawing groups at the 2 position, such as, **37** and **38**, increased the photo opening quantum yield for the DHP to CPD reaction to 0.3-0.4, however, they also speeded up the thermal return rate (Table 4).

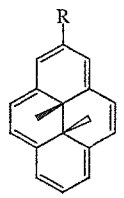

17 R = H
37 R = NO_2
38 R = CHO

Table 4. Rate data (k) at 30°C and activation energies (E_{act}) for thermal return reactions[45]

Compound	k (min^{-1})	E_{act} (kcal mol^{-1})
17	0.001	23.0
37	0.069	20.5
38	0.052	19.7

The substituent effect was also tested at the 4-position of the di-*t*-butyl compound **20**.[45,47] It was found that electron withdrawing groups decreased the thermal return rate. For example, the thermal rates for CPD to DHP conversion of compounds **39** to **42** were 0.0018, 0.0028, 0.0016, 0.0012 min^{-1} at 40°C, respectively, while the parent **20** had a rate of 0.0031 min^{-1} at 40°C.

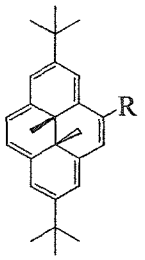

20 R = H
39 R = NO_2
40 R = COC_6H_5
41 R = $COCH_3$
42 R = COC_2H_5

Increasing the size of the internal alkyl group had little effect on the quantum yield, but increased the thermal return rate.[45,47] For example, the thermal return rates of **43'**, **44'**, and **45'** were 0.0044, 0.0047, and 0.012 min^{-1} at 40°C.

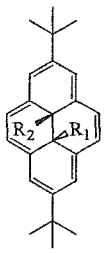

43 $R_1 = CH_3$, $R_2 = C_2H_5$
44 $R_1 = CH_3$, $R_2 = CH_2Br$
45 $R_1 = R_2 = C_2H_5$

Such compounds are also thermally much less stable, due to internal group migration.

Annelation of an aromatic ring had a much larger effect on both quantum yield and thermal return rate.[48,49]

19 **19'**

46 **46'**

Compound **19** readily converts to **19'** quantitatively with projector lamp light. Irradiation with UV light quantitatively converts **19'** back to **19**. This process occurs thermally at a rate of 0.0004 min^{-1} at 30°C, which is much slower than for the parent **17'** to **17** (0.001 min^{-1}) under the same conditions. Photochromic studies were also conducted on the series of **21** to **23**:[50] the thermal return rate of **21'** is 0.0020 min^{-1} at 46°C, which is three times slower than that of **20'**, while the quantum yield of visible light opening reaction increased by 25 times. However, fusion of naphtho- or anthro- groups increases the thermal return rate. The compounds **22'** and **23'** had thermal return rates of 0.0101 and 0.0344 min^{-1} at 46°C, respectively.

It is worth mentioning at this point that when the benzo ring of **21** is replaced by a furan as in **47**, the thermal return rate was found to be the slowest so far, 0.000183 min^{-1} at 46°C.[31,51]

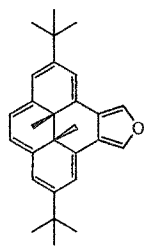

47

Unfortunately, this compound decomposes quickly during the photochromic processes.

One interesting system is the bis benzene annelated **48/48'**.[50,52]

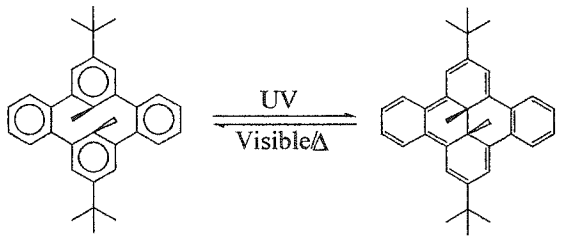

48' **48**

Because of the large resonance stabilization energy of the four benzene rings of **48'**, the thermally stable state is the open CPD form. The thermal return rate of **48** to **48'** is very fast. The half-life of **48** is only 3 min at -10°C. The activation energy of the thermal reaction was determined at low temperature as 20 kcal mol^{-1}.

Fusion of a benzene ring at the [a]- rather than the [e]-position of the parent as in **49/49'** increased the thermal return rate.

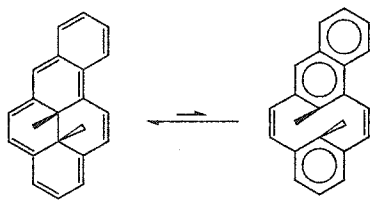

49 **49'**

Visible light irradiation of **49** at room temperature gave no detectable **49'**.[48] Low temperature study has not yet been done to establish the kinetics of this reaction. However, laser flash experiments suggest that the ring opening proceeded.

Photochromic studies on systems with more than one DHP unit were first carried out by Ward.[50,53]

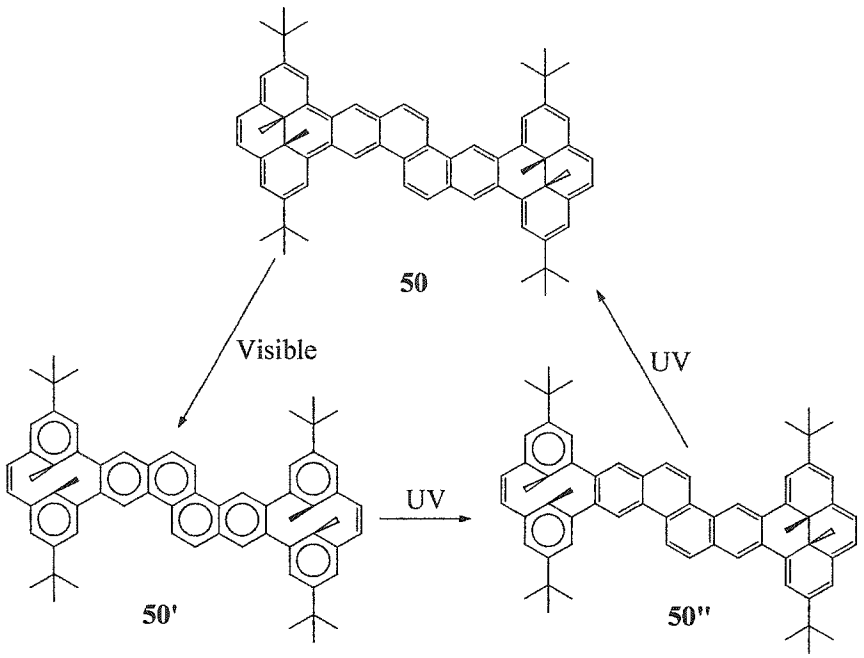

Compound **50** opened quickly to **50'** using visible light. When the latter was irradiated with UV light, the mono closed **50"** was first formed before complete return to the bis-closed **50**. This was determined by both ^{1}H NMR spectroscopy and UV/Vis spectroscopy. The overall kinetics of the thermal reaction of **50'** to **50** was followed by NMR spectroscopy. The thermal return rate at 46°C was determined to be 0.0057 min^{-1} and the activation energy was 24.3 kcal mol^{-1}.

Compound **51** was the first three way photochromic switch in the DHP system,[50,53] in which all three states are clearly separable.

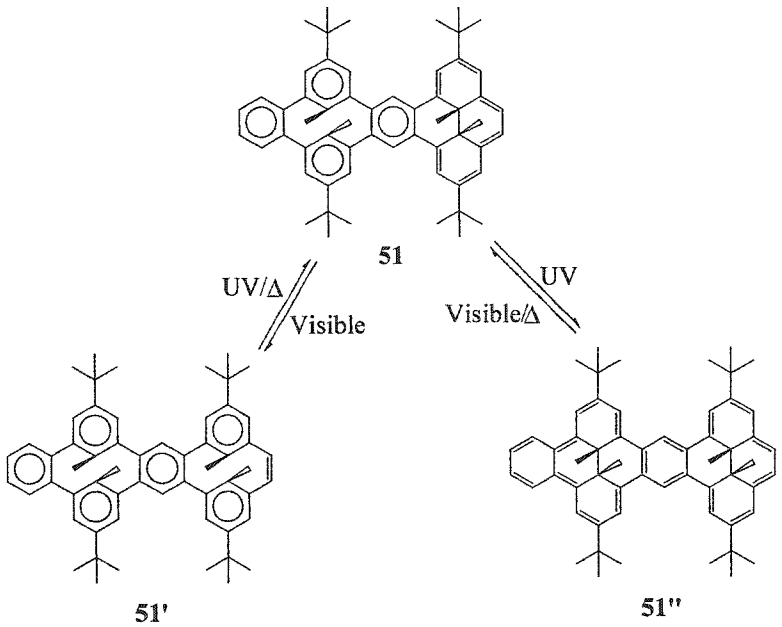

Irradiation of **51** with visible light opened the DHP and gave the colorless **51'**, which on UV irradiation or thermally returned back to **51**. The bis closed system **51"** was obtained using a 355 nm laser flash, and this returned back to **51** very rapidly thermally. The thermal return rate and activation energy of **51'** to **51** was found to be very close to that for the CPD form of benzopyrene **21** to its DHP form: the rate at 46°C for **51'** was 0.00224 min^{-1} and E_{act} was 24.1 kcal mol^{-1}.

It is worth mentioning that an electrically conducting main chain photochromic conjugated polymer incorporating DHP units has been reported recently.[54] It was the first example of electrical conductivity in a backbone photochromic conjugated polymer.

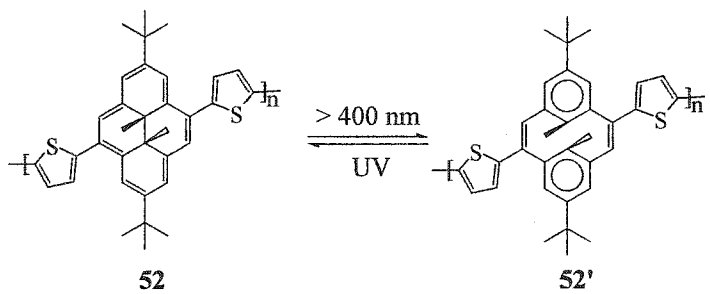

The photochromic process of **52** and **52'** still occurred, but slower than for the monomer. The solution phase of an optoelectronic redox switch was also demonstrated. This study indicates the possibility of making solid state photochromic switches on a molecular level.

(d) Fulgides

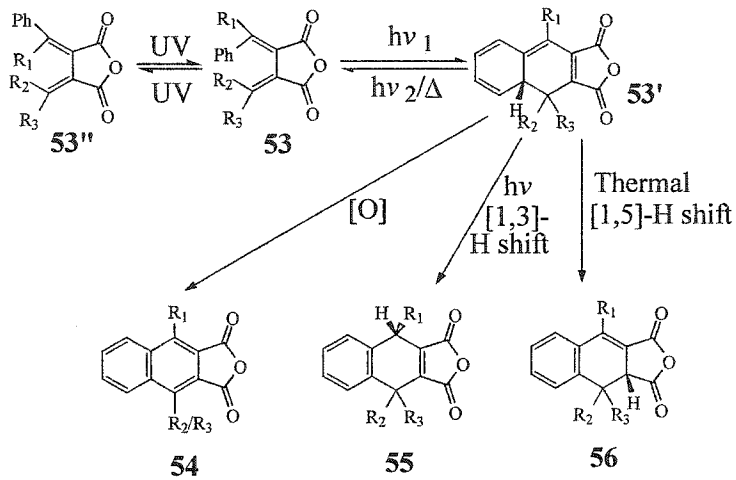

Fulgides were first synthesized and studied early this century[55]. However, the mechanism of the photochromic process remained unclear for a long time. Until the 1960s, the coloration was believed to occur by *cis-trans* isomeration about a double bond.[56] In 1968, Santiago and Becker[57] first recognized that the mechanism was the photochemical 6π-electron cyclization of the hexatriene moiety of **53** to generate **53'**.

Initially fulgides were not very good photochromic compounds because of a number of thermal and side reactions of the colored form **53'**.[55] Besides the thermal ring opening, the major thermal reactions are hydrogen rearrangement and (or followed by) dehydrogenative aromatization.

This changed when the important fulgide **57** was reported by Heller[55,58] in 1981.

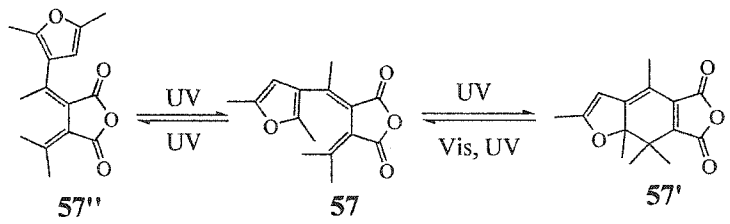

57'' **57** **57'**

Because there are no α-hydrogens on the furan ring, the sigmatropic proton shifts are prevented. In addition, the vicinal methyl groups on the ring closing carbon atoms prevented the thermal ring opening of **57'**. This was thus the first thermally irreversible photochromic molecule in the long history of fulgides. Furthermore, **57'** had a small molar absorption coefficient at 366 nm, where as **57** had a large absorption, and the photochemical back reaction from **57'** to **57** upon irradiation with 366 nm light was negligible. Therefore, the conversion of **57** to **57'** was close to 100%.

Since the discovery of compound **57**, much effort was put into improvement of the photochromism. Replacement of R_1 by a bulkier group, such as, ethyl, *n*-propyl, *iso*-propyl or *tert*-butyl significantly slowed down the *cis-trans* isomeration.[55] Heller[58,59] found that the adamantylidene group, instead of isopropylidene increased the ring-opening quantum yield of visible irradiation. After 1990, the main interest switched to the development of new fulgide derivatives,[60] which include using different aromatic rings, such as, pyrrole, indole, and different substituents onto the aromatic ring as well.

1.3.3 Heterolytic Cleavage

The photochromic reactions of spiropyrans and the closed related spirooxazines are the reversible cleavage of the C-O bond in the spiropyran or spirooxazine rings.[61] Two typical examples are shown below:

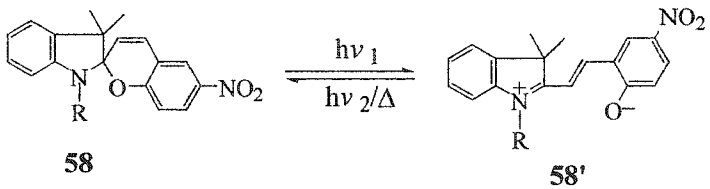

58

(Spiropyran)

58'

(Merocyanine)

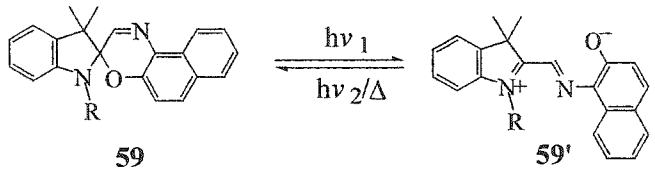

59

(Spirooxazine)

59'

(Merocyanine)

The photochromic properties of spiropyrans were first studied by Fisher and Hirshberg in 1950.[62] The closed forms are usually a nicely crystalline colorless or pale yellow solid. Solutions are colorless or weakly colored, and upon irradiation with ultraviolet light develop color or become more intensely colored. The colored solution fades thermally to their original state.

The open structure is essentially that of a merocyanine dye. Since the thermal fading of the colored forms is relatively fast, it is usually difficult to obtain a UV-Vis spectrum of a pure merocyanine form.[63] However, the merocyanine form has a very strong tendency to associate into aggragates with a stack-like arrangement of the merocyanine molecules.[61] When the molecular dipoles are arranged in a parallel structure, their absorption spectra are shifted to the red. In the case of antiparallel dipole arrangement, the spectra are shifted to the blue. The tendency for merocyanine aggregation is so strong that the aggregates are formed on irradiation of a spiropyran in a methacrylate polymer and even on swelling of the polymer film in a solvent.[61]

1.3.4 Tautomerism

Some anils with structures similar to **60** have been shown to be photochromic. The mechanism was thought to be that a six-membered ring hydrogen transfer to form a colored quinoid structure.[63] The photo generated colors fade with warming.

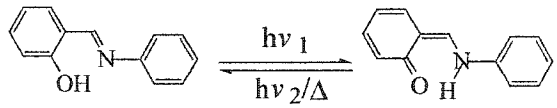

60 **60'**

The thermal return usually is very fast. Thus, photochemical studies have been done mostly at low temperatures.

1.3.5 Homolytic Cleavage

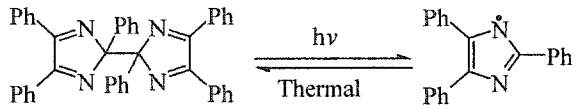

61 **61'**

A yellow benzene solution of compound **61**, upon irradiation with sunlight at 15°C turned to reddish purple.[63] The color disappeared in the dark. This can also be observed in the crystalline state. The structure of **61'** was confirmed by ESR study. However, this type of system is rarely used in modern photochromic studies.

1.4 Thesis Motivations and Objectives

The dimethyldihydropyrene system has proven to be a promising photochromic system. However, with the low quantum yield of visible light opening and fast thermal

return rate, the parent compound **20** does not possess the desired properties to be a molecular photoswitch. The [e]-annelated compound, benzopyrene **21**, made by one previous graduate student in our group, Dr. Ward, shows the best photoswitching properties so far. My research goals were thus as follows:

1. To synthesize more complicated systems with more than one DHP unit (multistate photoswitches).
2. To explore how the photochromic properties of various substituted benzopyrenes change on substitution.
3. As a result of our work above, to attach a substituent on one side of the DHP units in a multistate photoswitch in order to differentiate both ends.
4. To study the thermal kinetics and photoisomerization of the derivatives of benzopyrene **21** so obtained.

Chapter Two Syntheses

2.1 Syntheses of Annelated Dimethyldihydropyrenes with Benzene as a Spacer

The only system known in which the thermally stable form contained two closed DHP units, **50**, was made by Ward.[50,53] In this system, the spacer was the polycyclic chrysene. We were interested to determine whether a simpler spacer such as benzene to give **62** could be made, and whether it would change the photoswitching properties.

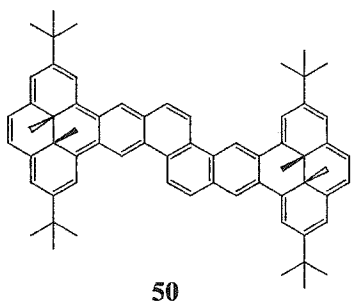

50

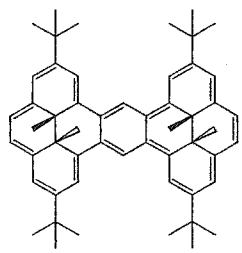

62

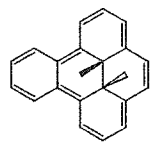

19

Although [e] position annelated dimethyldihydropyrenes have better photoswitching properties than their [a] analogues, the synthesis of the parent **19** was a long process with 9 steps and a 9% overall yield.[64]

Zhou[30,65] found an alternative route to annelate DHPs which did not necessitate going back to a new thiacyclophane synthesis for each new compound.

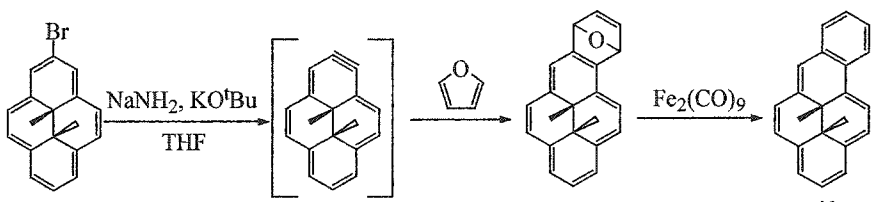

63 **64** **65** **49**

This involved reaction of an intermediate aryne, which was not isolated, with a furan in a Diels-Alder reaction.

To obtain the parent benzopyrene system **19** by this route, the aryne intermediate at the 4,5-positions is required, which in turn requires the bromide **66**.

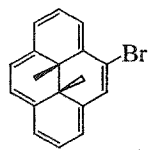

66

However, only the 2,7-positions of the parent **17**, are brominated, so these need to be blocked to introduce a bromine at the 4-position. Thus 2,7-di-*t*-butyl-dimethyldihydropyrene, **20**, was selected as the best starting material, with the bonus that it is much easier to synthesize than the parent **17**.[46,70] Ward[31] showed this route to be successful for benzo[e]pyrene **21**.

2.1.1 A System Containing Two Dimethyldihydropyrene Units

In order to synthesize **62**, the aryne **67**, would need to be trapped by the isofuran **47**[31] which should give the adduct **68** as a mixture of isomers, (for the subsequent use, isomers indicate diastereomers, unless otherwise stated).

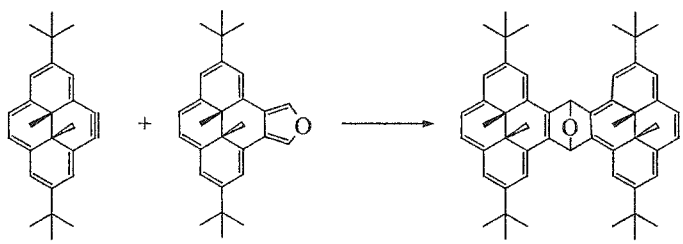

67 **47** **68**

Bromination of **20** with NBS in DMF and CH_2Cl_2 gave bromide **69** in greater than 90% yield.[31]

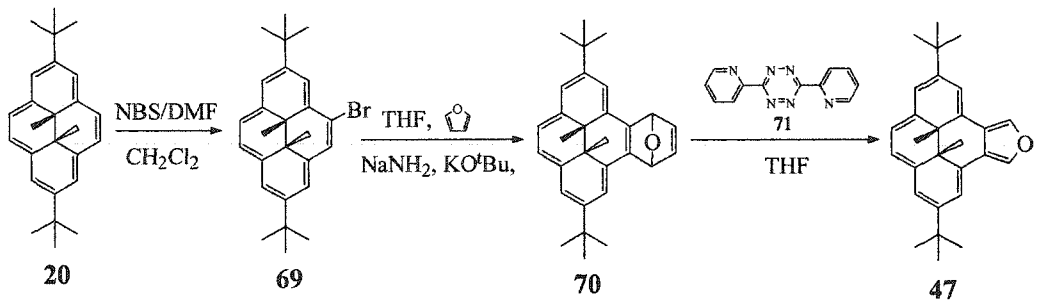

The bromide was first converted to yield the adduct **70**, which on reaction with the tetrazine **71** underwent a retro Diels-Alder reaction to yield the isofuran **47** in 60% overall yield.[31] This was then again reacted with aryne **67**, generated from bromide **69** in dry THF using excess $NaNH_2$, in a Diels-Alder reaction to yield adduct **68**.

This reaction usually finished within a few hours on the milligram scale. However, the compound was difficult to purify because it decomposed during column chromatography on SiGel which was sluggish due to poor solubility. So for synthetic purposes, the crude product was washed several times with a small amount of pentane, to give residual **68** of about 95% purity.

In theory, two diastereomers of **68** could be obtained, one of which is chiral and one is a meso form.

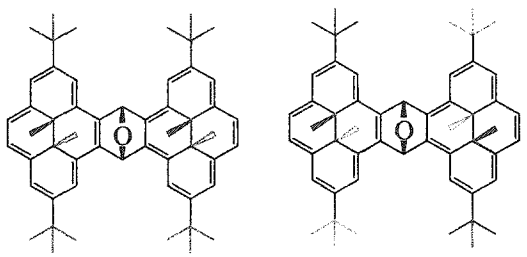

68A **68B**

In **68A**, which has C*s* symmetry, there should be two methyl signals and two *t*-butyl signals (which are illustrated in the same color). Isomer **68B**, also has two methyl signals and two *t*-butyl signals. In fact, both isomers of **68** are obtained in equal amounts and four internal methyl signals could be seen in the ^{1}H NMR spectrum at δ -3.40, -3.44, -4.37, -4.38, as well as four *t*-butyl signals at δ 1.66, 1.70, 1.71, 1.73. The two protons on the oxygen bridge head are identical for the isomer **68B** at δ 7.924 and different for the isomer **68A** at δ 7.976 and 7.918 as two doublets with a small coupling constant of 0.64 Hz. The strong deshielding of these protons is caused by the two DHP rings. Partial ^{1}H NMR spectra of **68** with unequal amount of isomers is shown in Figure 2.

The ^{13}C NMR spectrum confirmed this analysis, i.e. the bridge head carbon signal was a single peak at δ 81.09 for isomer **68B** and two peaks at δ 80.82 and 81.53 for isomer **68A**. The compound gave a correct molecular weight by mass spectrometry (LSIMS) at *m/z* 727.5 (MH+) and a satisfactory elemental analysis.

In our group, furan adducts have normally been deoxygenated with $Fe_2(CO)_9$, and so this was tried first to convert **68** to **62**. After **68** and $Fe_2(CO)_9$ were refluxed in benzene for 1 h, the cooled reaction mixture was filtered through alumina and after the solvent was evaporated, the residual was chromatographed over alumina using benzene/hexanes (1:6). Much green material did not move, but a small amount was eluted and gave a complicated NMR spectrum. There were 3 to 5 peaks in the internal methyl region around δ -1.07 depending upon resolution. Further column chromatography did not reduce the number of peaks. The *t*-butyl region was rather complex and so the mixture was refluxed with Me_3NO in benzene for 1 h to ensure any

iron complex, but the NMR spectrum of the residual was similar in pattern, and the signals were smaller. Either the impurities in the product were not iron metal complexes or Me_3NO did not decomplex them.

Figure 2. Partial ^1H NMR spectra of both isomers of 68 (unequal amount).

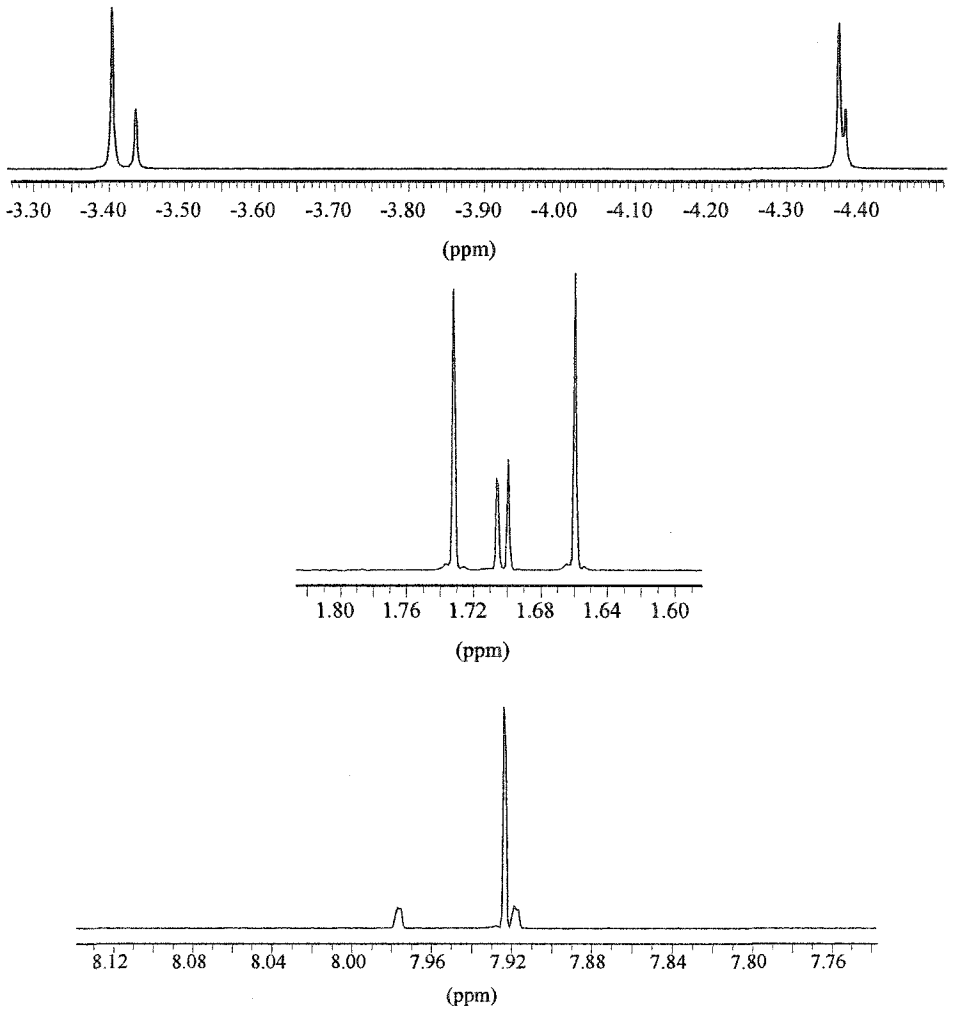

When less than one equivalent of $Fe_2(CO)_9$ was used to deoxygenate the adduct **68**, some starting material **68** was recovered, and the two isomers were present in unequal amounts. This made it possible to assign the ^1H NMR spectra of different isomers, as shown above.

Next, the conversion of **68** to **62** was attempted using sodium in THF.[67] Sodium was added into the solution of **68** in THF under argon, the mixture was stirred in room temperature. Unfortunately, most of the starting material decomposed and remained at the bottom of the plate during TLC. The very small amount that was obtained on chromatography with benzene/hexanes (1:6) gave an internal methyl proton signal at δ -1.07. $(CH_3)_3SiI$[68], which was made in situ from $(CH_3)_3SiCl$ and anhydrous NaI in CH_3CN, and worked well in making benzo[e]pyrene **21,** was also tried, but was not successful. Ti(0)[69], which was generated from $TiCl_4$ and Zn in dry THF, and SmI_2[70] in dry THF under argon, were also attempted, but failed.

On the basis of its chemical shift, the peak at δ -1.07 suggests that **62** was obtained. However, more evidence is required to substantiate this claim.

2.1.2 A system containing three dimethyldihydropyrene units

When a DHP is benzannelated on both sides, the [e,l] positions, then the open CPD form is the thermally stable isomer.[52]

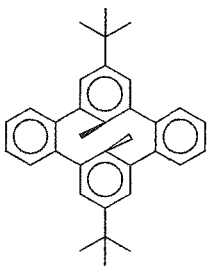

48'

Ward[50,53] made use of this property to prepare a three way switch **51**, in which one DHP is closed, one is open. We thought we could prepare a system with two closed

DHPs utilising the open unit in the center, and thus we thought **72** would be a worthwhile target.

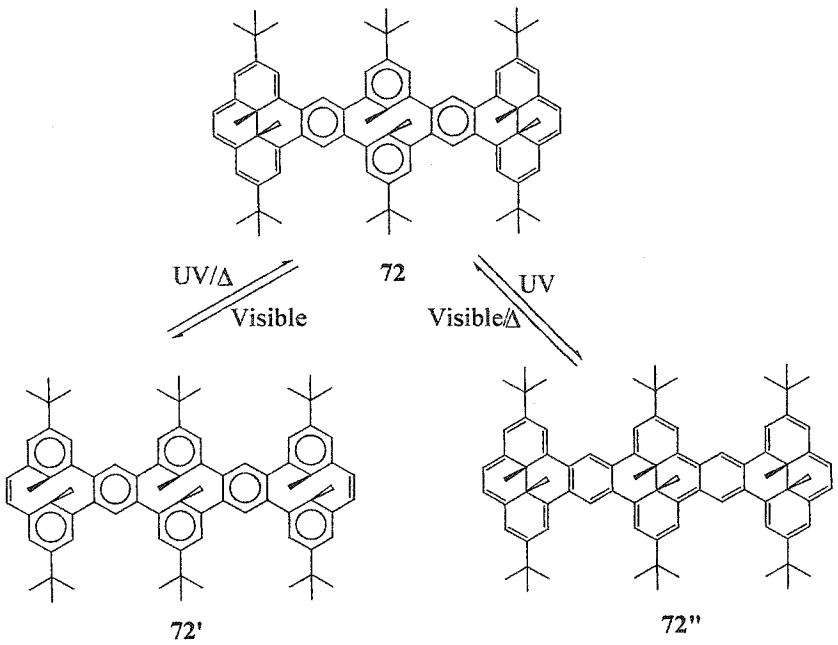

In **72**, irradiation with visible light, should open both terminal DHPs to give **72'**, which should thermally or with UV light return to **72**. Irradiation of **72** with UV light should close the central CPD to give the triple DHP **72"**, which should revert to **72** thermally.

In order to synthesize **72**, we thought we could make use of the *bis*-Diels-Alder reaction that was successful in converting dibromide **73** to bis-adduct **74**.[52]

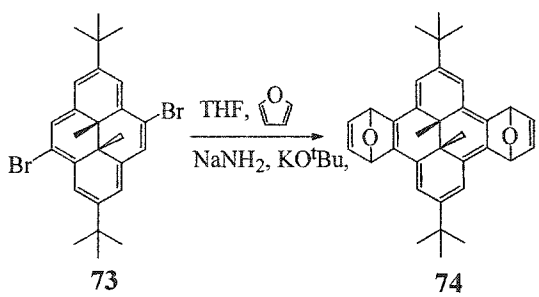

In our case, isofuran **47** would be substituted for the furan. Thus reaction of the dibromide **73** and excess isofuran **47** (3 equivalents) in dry THF with a large excess of $NaNH_2$ and catalytic amount of KO^tBu, resulted in a brown mixture which was filtered through celite and the ^1H NMR spectrum was taken.

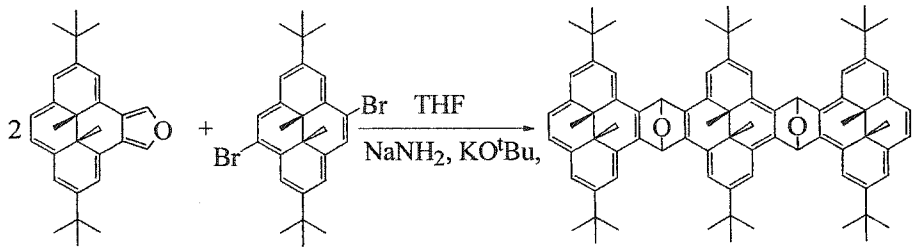

47 **73** **75**

Three groups of new internal methyl signals centered at δ -3.43, -4.58 and -5.28 were found, indicating several isomers of adduct **75** to be present. Because of the poor solubility of the product, further purification was not successful. After the brown mixture was washed with pentane a few times, the residual was greenish and was directly carried on to next step, the deoxygenation.

Crude **75** was refluxed with $Fe_2(CO)_9$ in benzene and the reaction mixture turned dark brown. TLC indicated that a red spot moved in hexanes/benzene (6:1). Column chromatography was used to collect the red portion, which we hoped was **72**.

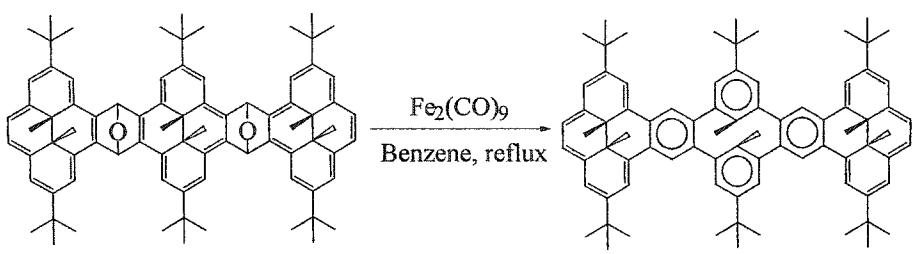

75 **72**

Two major internal methyl proton peaks at δ -1.37 and -1.63 were observed and there were some smaller peaks in this region too, which could not be separated by chromatography.

In the Diels-Alder reaction of the dibromide **73** and furan, there was always some mono adduct **74a** generated.[71]

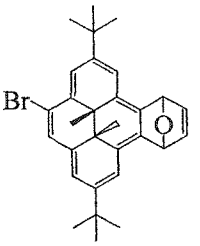

74a

Similarly, the Diels-Alder reaction of **47** and **73** might give a similar product, which on deoxygenation might produce the small peaks.

In an attempt to avoid this, bisfuran **76**[72] was reacted with excess bromide **69** in the presence of $NaNH_2$ and KO^tBu. This should generate **75** without mono adduct.

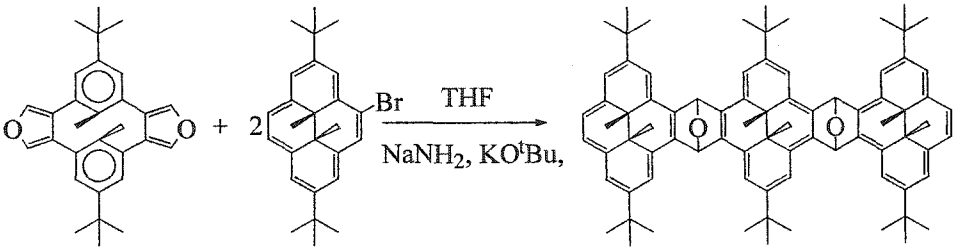

76 **69** **75**

However, surprisingly, after the product from the Diels-Alder reaction was deoxygenated with $Fe_2(CO)_9$, only a small amount of material was obtained which showed the same internal methyl signal pattern as from the reaction of **47** and **73**. As well, there were some peaks around δ -4.0, which could not be identified.

A stepwise route was thus designed.

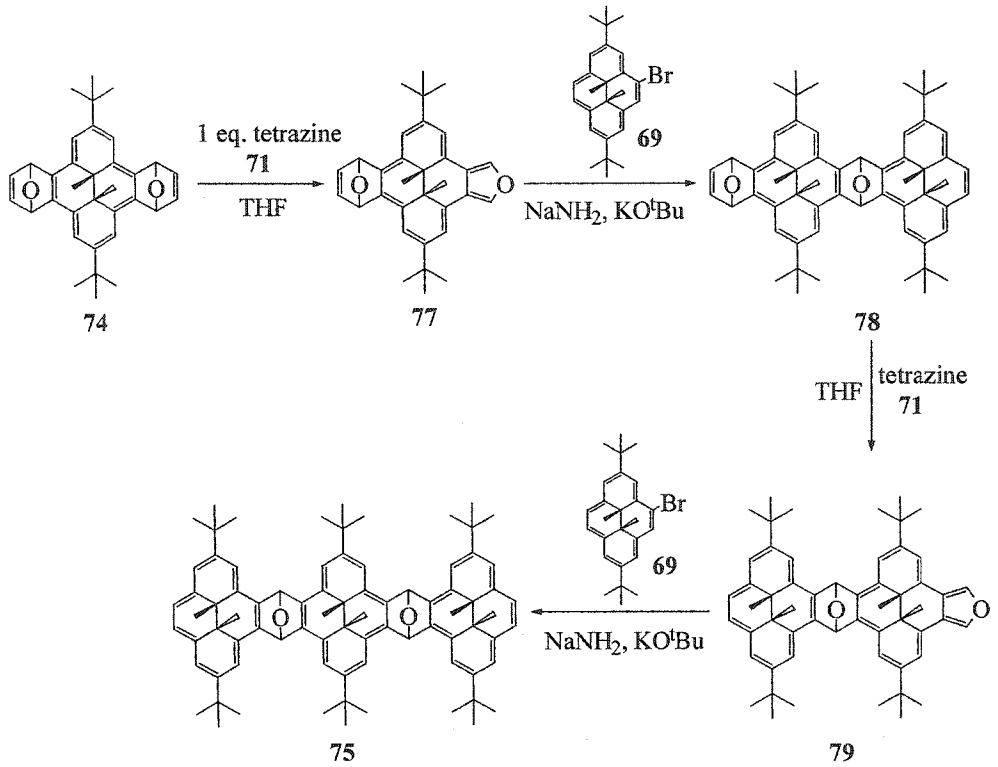

Use of low temperature allowed the monoisofuran **77** to be isolated as the major product from the reaction of **74** and tetrazine[73] **71.** However, the yield of this reaction was generally low at about 30%. The product could be purified by column chromatography over alumina to give a beautiful red-orange solid, mp (dec) 182-183 °C. Some deep purple material remained on top of the column during chromatography, and was suspected to be compound **80.**

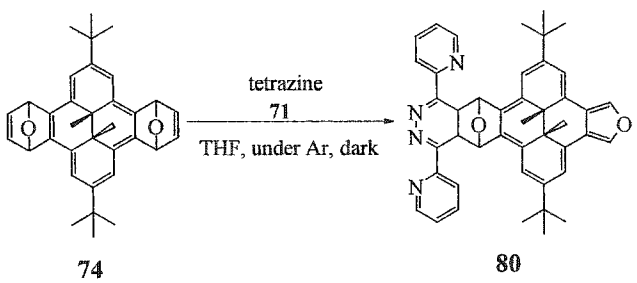

The structure of **77** was indicated by its NMR spectrum. Two signals for the internal methyl protons at δ 0.373 and 0.137 and two *t*-butyl proton signals at δ 1.241 and 1.239 indicate an unsymmetrical structure because of the oxygen bridge.

In comparison of **77** and **81**,[72] the internal methyl proton chemical shifts in **77** are more downfield than in compound **81**, which are at δ -0.98 and -1.20 (d_8-THF).

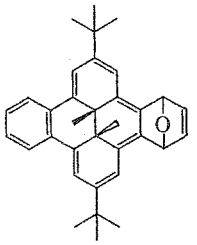

81

This can be explained in terms of the DHP ring current. Because the double bonds in a furan ring are more localized than those in a benzene ring, the ring current in the DHP ring of **77** is much smaller caused by furan fusion than in **81**, due to increased bond fixation.

The ^{13}C NMR spectrum of **77** shows two bridge head carbon peaks at δ 80.22, 80.15. The CI MS gave the appropriate ion for MH+ at *m/z* 451. The HRMS confirmed the formula of $C_{32}H_{34}O_2$ with the exact mass peak at *m/z* 450.2559 (M+); the calculated value is 450.2559.

Compound **77** was used in the next step as soon as possible and reacted with the aryne **67** derived from bromide **69** in a Diels-Alder reaction to give adduct **78** as a mixture of diastereomers in 72% yield. The reaction usually finished within a few hours.

In theory, there could be four isomers. Two have both oxygen bridges up(u) (**78uuA** and **78uuB**) and two have one up one down(d) (**78udA** and **78udB**).

Chromatography was used to separate the isomers into a **78uu** group and a **78ud** group. Further separation of isomers **A** and **B** within each group could not be achieved.

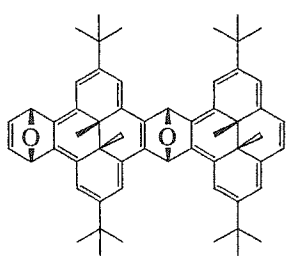

78uuA

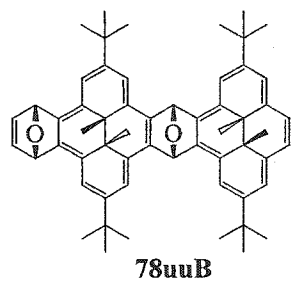

78uuB

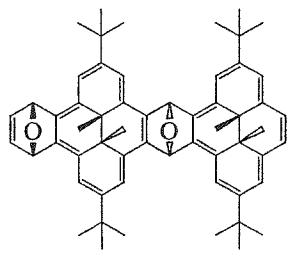

78udA

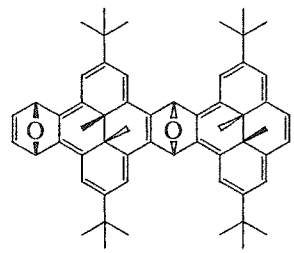

78udB

Because of the difference of the two DHP rings in **78**, there should be four internal methyl signals in the ^{1}H NMR spectrum of each isomer. As determined previously in compound **74**,[52] the **uu** isomer has the largest spread of chemical shift for the internal methyl protons, $\Delta\delta$ = 0.60 ppm, so in **78** the **uu** isomers might be expected to have a larger range in chemical shift than the **ud** isomers. During chromatography, spectra were obtained with unequal amounts of the four isomers, and hence we could determine that the methyl signals for the **uu** group were at δ -4.70, -4.32, -3.47, -3.29 and δ -4.73, 4.31, 3.48, -3.26, while those of the **ud** isomers were at δ -4.43, -4.24, -3.77, -3.25 and -4.41, -4.23, -3.77 and -3.28.

The overall structure is supported by mass spectroscopy (LSIMS) which gave the correct molecular ion of MH+ at *m/z* 793.6 and satisfactory HRMS, found = 793.4987 (MH+), calc = 793.4985.

The Diels-Alder reaction of **78** and tetrazine **71** followed by a spontaneous retro-Diels-Alder reaction readily gave the furan **79** as a mixture of isomers in greater than 90% yield. Compound **79** was not stable on SiGel and slowly decomposed on alumina, with one isomer decomposing faster than the other. After a short alumina column, the less stable isomer in the tail part of the eluant was sometimes only 10% of the more stable isomer. Thus the identification of signals belonging to each isomer was possible.

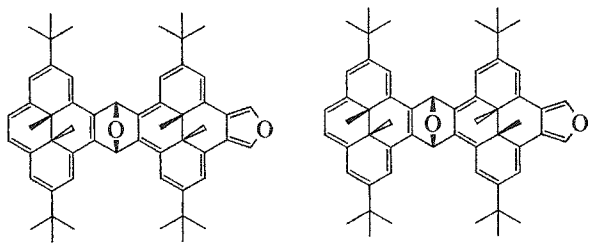

79A **79B**

In **79,** two types of internal methyl proton signals should be present because of the different DHP rings. The internal methyl signals of the DHP attached to the furan should appear further downfield than those in the other DHP ring. In theory, each isomer should give four internal methyl signals. Seven peaks were observed at δ 0.45, -0.52, -0.54 and -3.68, -3.72, -4.02, -4.04, with the one at δ 0.45 being overlapped peaks of two isomers. The correct LSIMS at *m/z* 767.5 (MH+) and HRMS at 766.4737 confirmed that the structural formula of **79** was $C_{56}H_{62}O_2$, (calculated value, 766.4750).

Upon obtaining **79**, the next step, the Diels-Alder reaction with aryne **67** derived from bromide **69** to give **75** should have been straight forward. However, the product **75** could not be properly purified due to its poor solubility.

Thus crude **75** was deoxygenated by refluxing with $Fe_2(CO)_9$ in benzene. Unexpectedly, the resulting deoxygenation product **72** contained the same impurities as before. After column chromatography over SiGel with hexanes/benzene (6:1) as eluant and then recrystallization from toluene, small dark red crystals were obtained, mp (dec) 176-181°C. Unfortunately, upon drying, the crystals broke apart and became a powder. It was thought that solvent was entrained within the crystals. However, crystallization was successful in purifying **72** since the small impurity peaks disappeared from the ^1H NMR spectrum. The overall yield was about 7% from the bis adduct **74**.

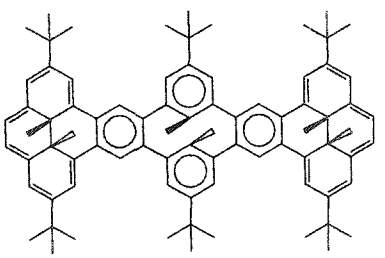

72A

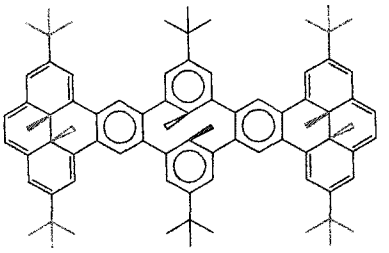

72B

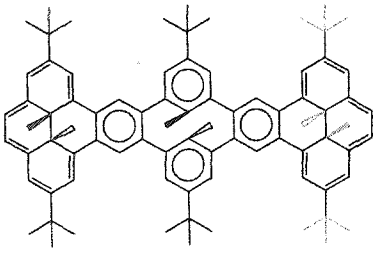

72C

Theoretically, compound **72** could contain three isomers as illustrated above. Diastereomers **72A** and **72B** have *Cs* symmetry, so all the internal DHP methyl proton in each molecule are identical (they are marked in the same colors). Isomer **72C**, however,

due to the CPD ring in the center, the two terminal DHP rings are not identical. There should be one signal for each DHP ring. Overall, four internal methyl proton signals are seen in the ^{1}H NMR spectrum of **72A-C** at δ -1.360, -1.364, -1.622, -1.626. Only one broad peak at δ 1.28 for the internal methyl protons of the central CPD ring is observed.

The structure of **72** was supported by mass spectrometry. An EI MS gave an ion MH_2^+ at *m/z* 1078. The HRMS *m/z* was 1077.7256. Calculated for $C_{82}H_{92}$ (MH+) = 1077.7277. In addition, the elemental analysis is satisfactory.

Although a large number of cyclophanes have been prepared, only a few have heterocycles on the bridges. After obtaining **79**, compound **82** became an interesting target. So, the following reaction was performed.

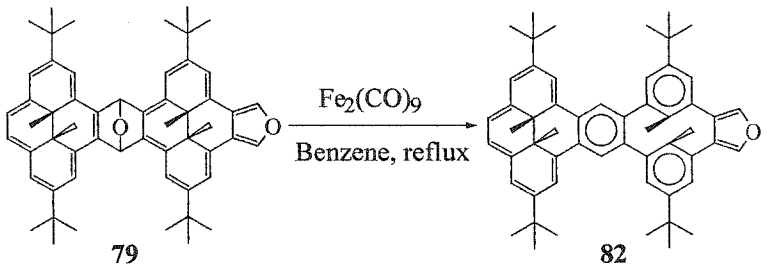

79 **82**

When the reddish brown solid **79** and $Fe_2(CO)_9$ were refluxed in benzene, the reaction mixture gradually turned to red. After chromatography, a red solid **82** was obtained in 80% yield as a mixture of two isomers.

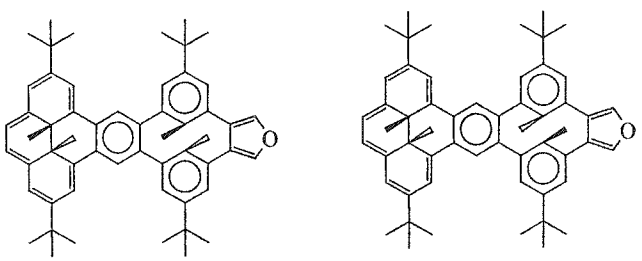

82A **82B**

In theory, there are two internal methyl proton signals and two *t*-butyl signals for the DHP ring, one from **82A**, and one from **82B**, and the same number of signals from the CPD ring. Indeed, the ^{1}H NMR spectrum shows two internal methyl proton signals at δ -1.66 and -1.37, which fall in the region of benzopyrene **21** derivatives. Also two *t*-butyl signals at δ 1.53 and 1.49 indicate the present of a DHP ring. Only one slightly broad signal at δ 1.03 for the internal methyl proton on the CPD is observed, however, two *t*-butyl signals at δ 1.32 and 1.31 could been seen.

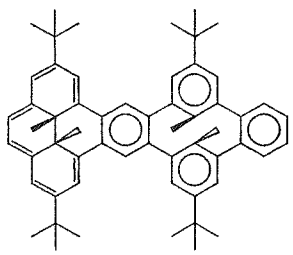

51

The NMR spectra of **82** and its benzo analogue **51**[50] are extremely similar. The two internal methyl signals and two *t*-butyl signals from the DHP ring in **51** are at δ -1.67, -1.37 and δ 1.54, 1.50. The two *t*-butyl signals from the CPD are the same as in **82** at δ 1.32 and 1.31. The greatest difference comes from the internal methyl protons of the CPD ring, which are singlets at δ 1.18 for **51** and δ 1.03 for **82**. Clearly, a furan fused on the CPD ring does not alter the ring current of the DHP ring much.

LSI mass spectra gave the correct molecular ion at *m/z* 750.5 (M+) and HRMS gave an exact mass value of 751.4869 (MH+); $C_{56}H_{62}O$ = 751.4879.

2.2 Derivatives of Benzo[e]dimethyldihydropyrene

Photochemical and photophysical studies have been done of substituent effects on the pyrenes **17** and **20**.[45,46,47] However, photochromic studies on substituted arene annelated dimethyl-dihydropyrenes have not been reported.

In terms of photoswitching properties and stability, benzo[e]pyrene **21** is the best candidate so far. We thus thought that study of substituent effects on compound **21** would be worthwhile. One of our research goals was thus to synthesize **83** with different X and Y groups.

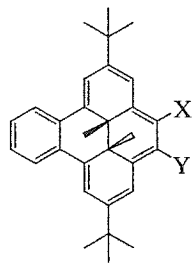

83

Acetyl, nitro and formyl groups have been successfully introduced onto the parent **17**,[74] and acetyl and nitro groups onto the parent benzo system **19**.[75] For **20**, acetyl and nitro groups have also been introduced at the 4- position.[76]

The Friedel-Crafts reaction of **21** with Ac_2O and $BF_3{\cdot}Et_2O$ as Lewis acid went smoothly and the yield of **84** was about 80%.

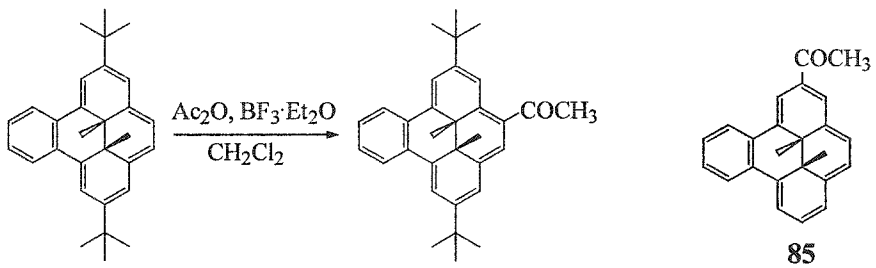

21 **84** **85**

Compound **84** formed nice purple crystals in a mixed solvent of hexanes/CH_2Cl_2 (1:1) by slow evaporation, mp 173-174°C. Both internal methyl and *t*-butyl protons were differentiated by the acetyl group and appeared at δ -1.48, -1.55 and δ 1.51, 1.49, unlike the corresponding 2-acetyl benzopyrene **85**, in which the internal methyl signal appears as a singlet at δ -1.67.[75] The acetyl methyl protons in **84** were a singlet at δ 2.73. In addition, the characteristic carbonyl carbon appeared at δ 201.16 in the ^{13}C NMR spectrum. In the IR spectrum, the conjugated C=O stretching frequency was at 1670 cm^{-1}. The correct CI MS and elemental analysis were also obtained for **84**.

The next target was the nitropyrene **86**. Nitration of DHPs have previously been carried out with $Cu(NO_3)_2 \cdot 2.5H_2O$ in Ac_2O.[76] However, extensive decomposition occurred during the nitration of **21**. The yield of **86** was only 28%, with about 10% of dinitrobenzopyrene **87** as by-product.

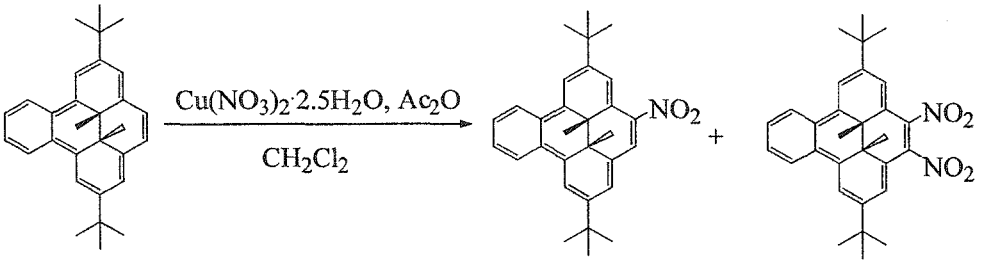

21 **86** **87**

Compounds **86** and **87** were easily separated by column chromatography and both could be further purified by recrystallization in a mixed solvent of hexanes/CH_2Cl_2. **86** Sublimed at 161-162°C, **87** decomposed at 195°C.

The structure of **86** was confirmed by its ^1H NMR spectrum. Due to the strong electron-withdrawing effect of the nitro group, the internal methyl protons were deshielded from δ -1.58 in benzopyrene **21** to δ -1.28 and -1.35 in **86**, with the

differentiation of the two internal methyls indicating the unsymmetrical structure. The two *t*-butyl signals were also differentiated and appeared at δ 1.53 and 1.47. The five aromatic protons on the DHP ring showed five distinct signals.

A correct molecular ion by CI MS at *m/z* 440 (MH+) and satisfactory HRMS confirmed the formula of this compound as $C_{30}H_{33}NO_2$.

The nitro group in compound **88** produces a very different substitution effect for that of **86** on the chemical shifts of internal methyl protons.[68] For **88** a singlet was observed at δ -1.85 for the internal methyl protons, which is the same as in the parent benzopyrene **19**. Why the substituent effects are so different for nitro groups in the 2- and 4-positions remains unclear.

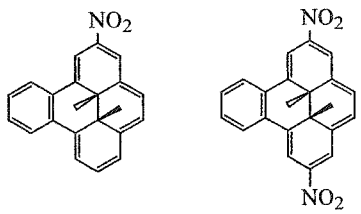

88 **89**

The dinitrobenzo[e]pyrene **87** gave a simple NMR spectrum due to its symmetrical structure. The internal methyl protons were a singlet and were further deshielded to δ -0.70. The *t*-butyl signal appeared a singlet at δ 1.46. Only two DHP proton signals at δ 8.10 and 7.98 were observed.

The experimental value for the exact mass of **87** was 484.2360, consistent with the theoretical value 484.2362. A CI MS also gave correct molecular ion at *m/z* 485 (MH+).

In compound **89**, the internal methyl proton signal appears as a singlet at δ -1.60, which is deshielded by about 0.25 ppm from the parent benzopyrene **19**.[68] It is obvious

that the effect of nitro groups at the 2- or 2,7- positions is not nearly as large as that on 4- or 4,5- positions.

The $TiCl_4$ catalysed formylation reaction[74] to generate compound **90** was not successful. Instead, a mixture of mono- and di-chlorobenzo[e]pyrenes **91** and **92** was obtained.

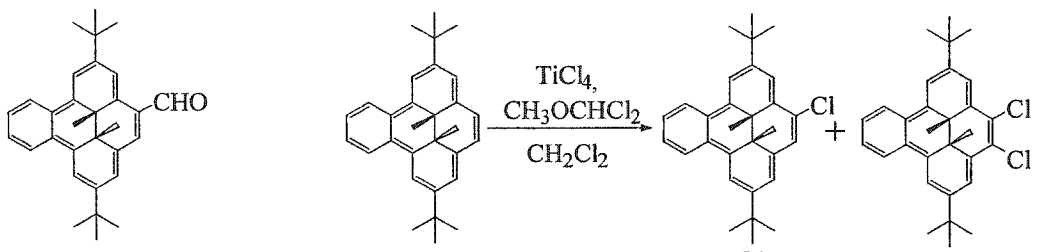

90 **21** **91** **92**

The substituted benzopyrenes obtained above were all by direct substitution of **21**. An alternative approach is first to introduce the substituent on to the more robust parent **20,** and then construct the benzene ring later.

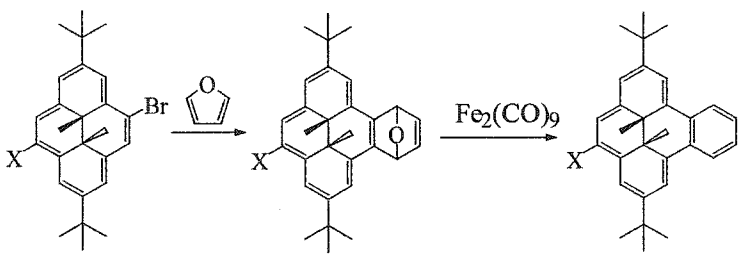

93 **94** **95**

In the case of **93**, generation of the aryne and reaction with furan should form adduct **94**, which on deoxygenation should give the substituted benzopyrene **95**. However, there are limitations to this route:

(1) The functional group X has to be stable under strong basic conditions.

(2) Substituent X should not promote any other reaction than the Diels-Alder reaction between the DHP aryne and furan.

(3) Substituent X should not interfere with the deoxygenation reaction.

Since direct nitration did not work very well for the benzopyrene **21**, it was chosen as the test reaction of the alternate route first.

The same conditions were used for the nitration of bromide **69** as for the parent **20**.[76] The resulting product was a mixture of the three compounds, **96**, **97** and **98**. The green colored **97** could be separated by chromatography on SiGel, mp (sub) 151°C, while the brown mixture of **96** and **98** was not separable.

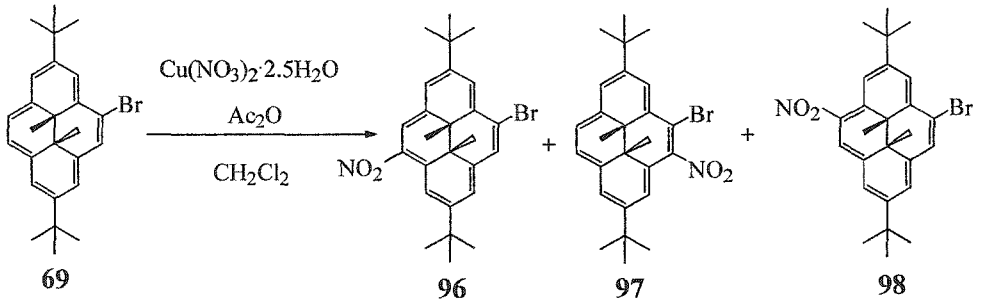

69 **96** **97** **98**

The structure of **97** was easily confirmed from its ^{1}H NMR spectrum. Only **97** showed an AB pattern for H-9,10, which appeared at δ 8.529 and 8.517, while H-1,3,6,8 were doublets with small coupling constants (J = 1.2 Hz). As would be expected for all the isomers, both internal methyl and *t*-butyl groups were differentiated by the unsymmetrical substitution. The internal methyl proton signals for **97** appeared at δ -3.68 and -3.70 and *t*-butyl proton signals were at δ1.69 and 1.63.

Compounds **96** and **98** showed slightly different solubility in pentane. After carefully washing the solid mixture, the residual contained 90% of one isomer. This was only necessary for characterization since in the subsequent Diels-Alder reaction both isomers should yield adduct **99**.

The less soluble isomer, showed a single *t*-butyl peak at δ 1.68 (the methyls were at δ -3.65 and -3.68), and we believe this is isomer **96**, since isomer **98** with both substituents at one end of the molecule should differentiate the *t*-butyl groups most. The *t*-butyl signals of the other isomer were at δ 1.72 and 1.65.

The mass spectrum of **97** showed a characteristic bromine pattern with 1:1 peaks at *m/z* 467 (M+, ^{79}Br) and 469 (M+, ^{81}Br) by CI MS. The HRMS was satisfactory with a *m/z* value 467.1464, calculated value 467.1460 (^{79}Br, MH+).

However, in the subsequent Diels-Alder reaction, **96** and furan in the presence of $NaNH_2$ gave no detectable adduct **99**, and all starting material was consumed.

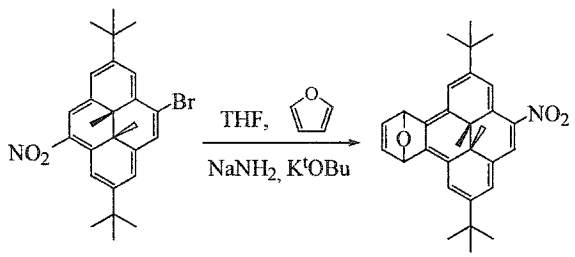

96 **99**

Since the above reaction failed, it suggested that an electron withdrawing group was not a good choice in this stepwise route to generate a substituted benzo[e]pyrene. Instead, we decided that an arylethyne substituent would be a better test of this idea since phenylethynyl has been attached to the parent DHP **20** through bromide **69** by Sheepwash.[77] This reaction required a relatively high temperature, as it was carried out in DMF. In theory, a Sonogashira coupling should be easier with an iodide rather than a bromide. Thus, compound **100** was chosen as the starting material for the sequence to give **103**.

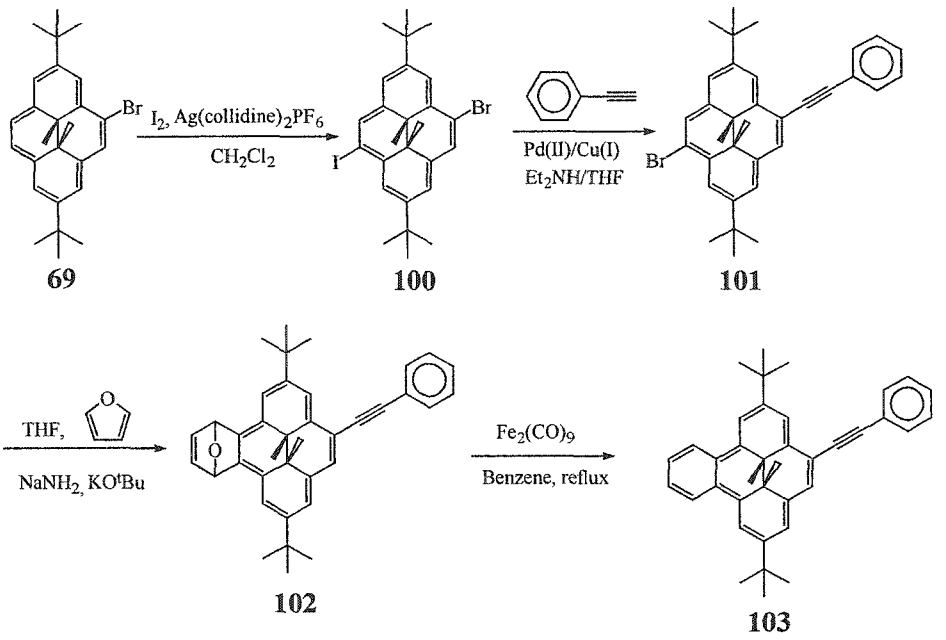

The iodination reagent was generated by reacting I_2 with Ag(collidine)$_2PF_6$ and was used in situ.[78] However, iodination of bromide **69** was very slow at low temperature, and even at room temperature took overnight to complete. Besides the 4,9-isomer **100**, a lesser amount of the 4,10-isomer **104** was also obtained, in about a 3:1 ratio. However, for synthetic purposes, both **100** and **104** should give the same product **102** after the Diels-Alder reaction with furan. Thus, separation of **100** and **104** was only carried out for characterization purposes.

Again, compounds **100** and **104** could not be separated by column chromatogaphy, but their solubilities were slightly different in pentane. After carefully washing of the product mixture a few times with pentane, the ^{1}H NMR spectrum of the residual showed a single internal methyl signal at δ -3.86, the *t*-butyl signals were two slightly separated siglets at δ 1.68 and 1.67, this was believed to be the 4,9-isomer **100**. The signals of the more soluable isomer had a bigger separation of the two *t*-butyl signals, which appeared

at δ 1.70 and 1.66, and the internal methyl showed two peaks at δ -3.93 and -3.95, this isomer was thus believed to be the 4,10-isomer, since with the two substitutents on the same side, both *t*-butyl and internal methyl groups should differentiate more.

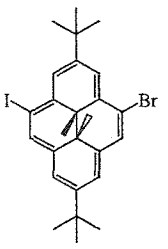

104

The green colored **100** sublimed at 162°C. In the ^{1}H NMR spectrum of **100,** the internal methyl protons showed as a singlet at δ -3.86, the six DHP aromatic protons as six signals at δ 8.90, 8.82, 8.65, 8.64, 8.48, 8.45, but the *t*-butyl groups were two singlets at δ 1.68 and 1.67. The mass spectrum gave correct isotope pattern 1:1 at *m/z* 549 (MH+, ^{79}Br) and 551 (MH+, ^{81}Br), also satisfactory HRMS results. Evidentially, an iodine and bromine do not differentiate the methyls of the DHP proton much.

The Sonogashira coupling of **100** and phenylacetylene went smoothly under mild conditions. $Pd(PPh_3)_2Cl_2$ and CuI were used as catalysts, Et_2NH as the base. The purity of the product depended on the starting material. When a mixture of **100** and **104** was used, the product was also a mixture of 4,10- and 4,9-isomers. However, for synthetic purposes, there was no need to separate the isomers since they would give the same Diels-Alder reaction product after the next step. A small amount of **100,** purified by washing with pentane, was used to make some pure **101** for characterization purposes.

The ^{1}H NMR spectrum of **101** showed two multiplets at δ 7.77-7.73 and δ 7.47-7.38 with integration of 2:3, which was the characteristic pattern of a mono

substituted phenyl group. Both internal methyls and *t*-butyl signals were differentiated by the unsymmetrical structure and their proton signals appeared at δ -3.75, -3.77 and δ 1.71, 1.69, respectively. The ^{13}C NMR spectrum showed the acetylene carbons at δ 95.25 and 89.89. The IR spectrum had a peak at 2196 cm^{-1}, indicating the presence of a triple bond.

The mass spectra showed a correct molecular ion and isotope pattern for one bromine. The HRMS signal found at *m/z* 522.1920 (M+, ^{79}Br), was consistent with the calculated value of 522.1922.

The Diels-Alder reaction of **101** (in fact **101** and the isomer derived from **104** were used), and furan in the presence of the strong base $NaNH_2$ to produce **102** went well. The green product was purified over deactivated SiGel using hexanes/EtOAc (6:1) as eluant to give 73% of **102** as a mixture of two diastereomers. Further separation was not attempted.

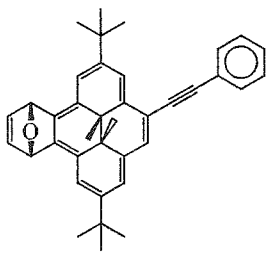

102A

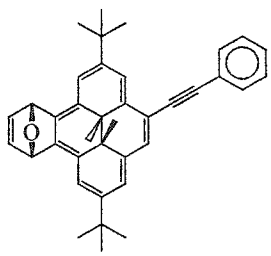

102B

The ^{1}H NMR spectrum showed four signals for the internal methyls at δ -3.158, -3.162, -3.416, -3.424, and four signals for the *t*-butyl groups at δ 1.656, 1.653, 1.608 and 1.604. A weak peak at 2191 cm^{-1} in the IR spectrum showed the presence of a triple bond.

The correct molecular ion at *m/z* 511 (MH+) and satisfactory HRMS analysis confirmed the molecular formula as $C_{38}H_{38}O$.

The deoxygenation of **102** with $Fe_2(CO)_9$ in benzene gave the expected product **103**, together with some unidentified side product. With prolonged reaction time, the NMR signals of the product became smaller. So, TMSI[68] was tested, however, 5 peaks at δ -1.30, -1.40, -1.42, -1.55, -1.60 were present in the DHP region and the products could not be separated by TLC. Searching for clean and effective deoxygenation methods is desireable in the future.

On some occasions, while making the adduct **102**, the phenylethynylbenzopyrene **103** was generated at the same time. In the Diels-Alder reaction of the bromide **101** and furan in two out of five trials, **103** was obtained in a ratio of **103/102** of 20:80 and 50:10 respectively. Different batches of $NaNH_2$ and KO^tBu had been used. Thus, the freshness of the base may affect this reaction.

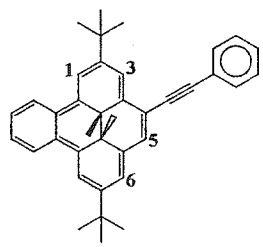

103

The phenylethynyl group further deshielded the internal methyl signals and differentiated them at δ -1.40 and -1.42. Also, there were two signals at δ 1.54 and 1.48 which belong to the *t*-butyl groups. Due to the overlapping of the benzo and phenyl groups, the ^1H NMR spectrum was complicated. The total number of aromatic protons was 14 relative to the 6 internal methyl protons. Four distinct doublets with coupling

constant about 1.0 Hz indicated the 4 protons on the DHP ring, the other proton H-6 was buried in the mutiplet of the phenyl proton signals.

The ^{13}C NMR spectrum had two signals at δ 94.61 and 89.94 for the acetylene carbons, and the IR showed a vibration peak at 2189 cm^{-1}, which indicated the triple bond in the molecule.

The CI MS gave a correct molecular ion at *m/z* 495 (MH+), and a HRMS of 494.2980 is very close to the calculated value of 494.2974.

The successful route to the arene-yne **103** by a coupling reaction suggested that the simple aryl substituted derivative **105** would be a good target.

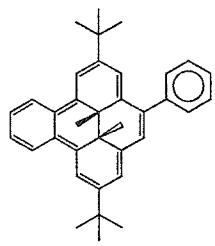

105

Thus the phenyl group was introduced first to the parent **20** by Suzuki coupling of bromide **69** with commercially available phenyl boronic acid[79] using aqueous Na_2CO_3 as base and $Pd(PPh_3)_2Cl_2$ as catalyst. The reaction completed within two hours under reflux in THF, and gave 87% of **106**.

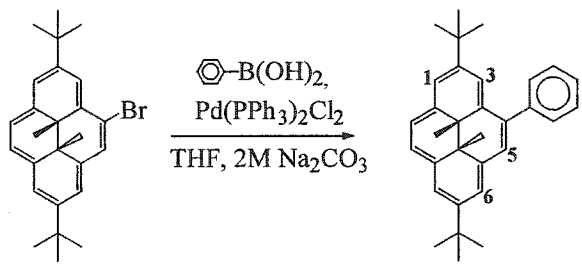

69 **106**

This was purified by column chromatography over SiGel using hexanes/benzene (6:1) as eluant, and gave green crystals, mp 162-163°C. The ^{1}H NMR spectrum showed the unsymmetrical structure of **106** with two internal methyl signals and two *t*-butyl signals at δ -3.84, -3.86 and δ 1.68, 1.59. The phenyl group appeared as three multiplets with integration of 2:2:1. NOESY experiments showed that the protons close to the DHP on the phenyl ring had through space interaction with H-3 and H-5 on the DHP ring.

Mass spectrometry (methane CI) supported the molecular composition with *m/z* 421 (MH+), and the elemental analysis was satisfactory.

The bromination of **106** was carried out at -78°C in dry ice/acetone. By ^{1}H NMR, the product contained a mixture of mostly the 4,9-isomer **107** (85%) and 12% of the 4,10-isomer **108** and 3% of starting material **106**.

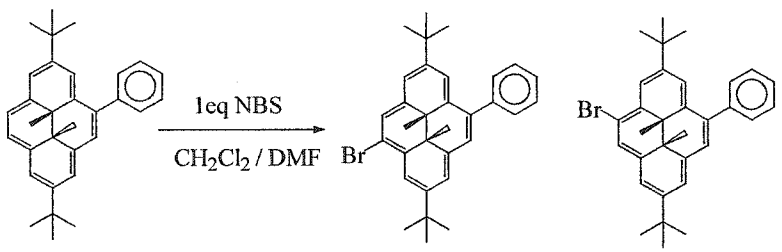

106 **107** **108**

For characterization, the mixture was washed with a small amount of pentane a few times and then the residual contained 95% of the 4,9-isomer **107**. However, for synthetic purposes, both **107** and **108** should give the same Diels-Alder reaction product.

The bromine in **107** deshielded the internal methyl proton signals to δ -3.72, -3.75 from δ -3.84, -3.86 in **106**. The phenyl group showed three multiplets with integration of 2:2:1. The *t*-butyl groups showed two signals at δ 1.69 and 1.56. More importantly, the

mass spectrum displayed a 1:1 bromine pattern at *m/z* 499 (MH+, ^{79}Br) and 501 (MH+, ^{81}Br). The exact mass also confirmed the molecular formula as $C_{32}H_{35}Br$.

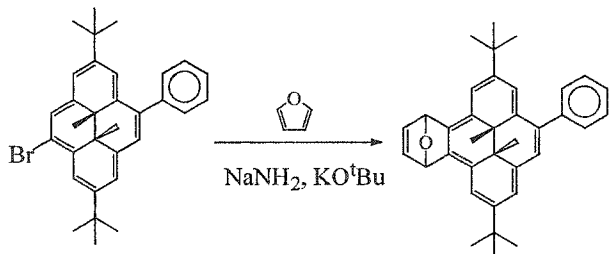

107 **109**

Reaction of **107** with furan and $NaNH_2$ in THF gave the green adduct **109** as a mixture of two equal amount isomers. Like most furan adducts, the product was not stable in halogenated solvents on SiGel, and showed limited solubility in saturated hydrocarbon solvents. Purification of **109** was achieved over deactivated SiGel, and the NMR spectra were taken in $CDCl_3$ which was filtered through alumina before use. For synthetic purposes, **109** was washed with pentane a few times and usually the purity was over 85%, so no column chromatography was needed.

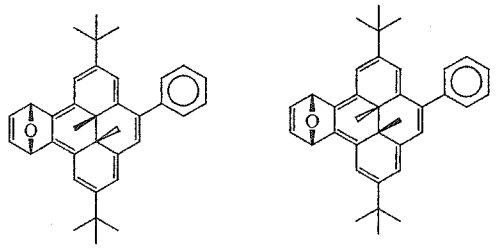

109A **109B**

Four internal methyl and four *t*-butyl signals were expected in the ^{1}H NMR spectrum of **109**. Indeed, four singlets in the internal methyl region at δ -2.88, -2.90, -3.13, -3.17 and four singlets for the *t*-butyl groups at δ 1.602,1.599, 1.502 and 1.496

were observed. The ^{13}C NMR spectrum confirmed the unsymmetrical structures by showing four oxygen bridge head carbon resonances at δ 81.08, 81.06, 80.76 and 80.65.

Mass spectrometry gave the correct molecular ion at *m/z* 486 (M+) by electron impact. Elemental analysis also gave the appropriate percentage of carbon and hydrogen.

The aromatization of adduct **109** was successful with $Fe_2(CO)_9$ in benzene, and gave 81% of **105** as a bright red solid, mp 180-181°C.

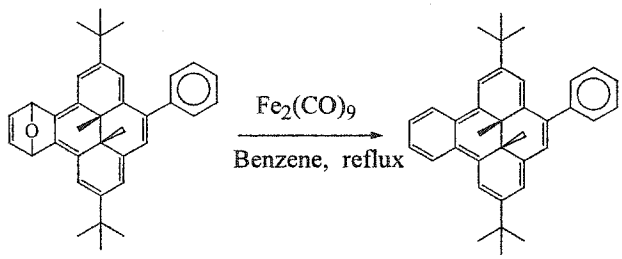

109 **105**

The structure of **105** was confirmed by its ^1H NMR spectrum, which showed the internal methyl groups and the *t*-butyl groups at δ -1.453, -1.456, and δ 1.49, 1.39. Since the methyl protons of parent **21** are at δ -1.58, the effect of substitution of a DHP ring by a phenyl group is much smaller than a fused benzene ring. The protons of the fused benzene moiety still appeared as an approximate AA'XX' pattern. Some of the DHP proton signals were buried under the phenyl proton signals, but the total integration of aromatic protons was in correct ratio to that of the internal methyl protons.

The mass spectrum showed the correct molecular ion at *m/z* 471 (MH+) by methane chemical ionization. A HRMS gave the exact mass as 470.2974; the calculated value was also 470.2974.

2.3 Diels-Alder Reactions of Isopyrofuran 47

Extensive use of isofuran **47** has been made in the synthesis of molecules containing more than one dimethyldihydropyrene unit by way of aryne-furan Diels-Alder reactions. Ward[51] also used **47** with other dienophiles such as, dimethyl acetylenedicarboxylate and fumaronitrile. Both of the reactions worked very well with nearly quantitative yields. However, he was unable to aromatize either adduct to generate useful photoswitching molecules.

The following reactions have been known for many years:[80]

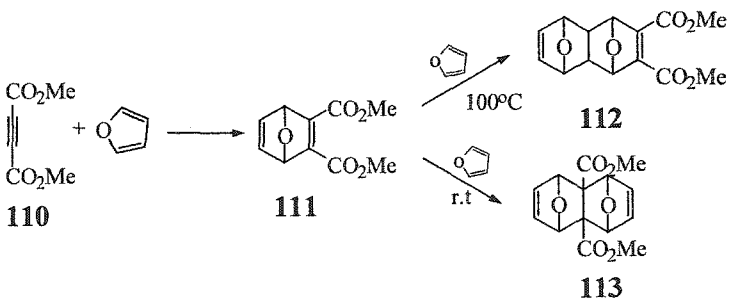

After the first step, the adduct **111** reacts further with excess furan to generate the bis adducts **112** or **113** depending upon reaction temperature. On this basis, we thought that the bis adduct **114** might be generated at high temperature by reacting isofuran **47** and the adduct **70**.

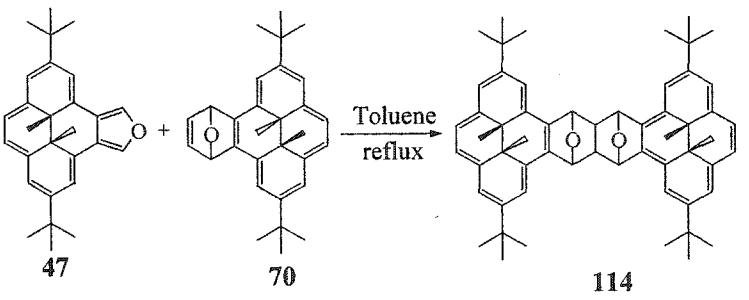

Indeed, when isofuran **47** and adduct **70** were refluxed overnight in toluene, the resultant green product had rather limited solubility in many solvents, including THF, CH_2Cl_2 and EtOAc. The reaction was very moisture and air sensitive. The reaction vessel used must be oven dried and held in a dessicator while cooling. Only a small amount of toluene was required, but 1.2 equivalents of isofuran **47** were used. Excess **47** was used because it had much better solubility in hexanes than **70** and was easily removed afterwards by washing with hexane. The yield of this reaction was then 50% to 75%. Further recrystallization from toluene gave fine green needles of **114**, which decomposed at 219-224°C.

In theory, four cis-fused diastereomers could exist. Two have both oxygen bridges up (u) (**114uuA, 114uuB**) and two have one up and one down (d) (**114udA, 114udB**). Four internal methyl signals and four *t*-butyl signals should be found in the appropriate regions for each pair of isomers.

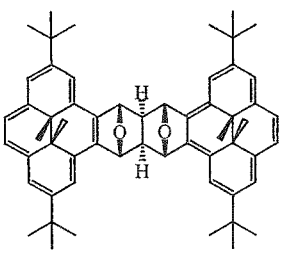

114uuA

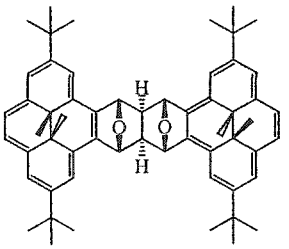

114uuB

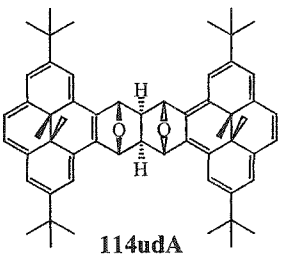

114udA

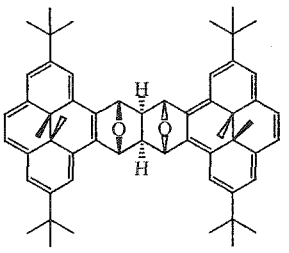

114udB

Due to limited solubility, the NMR spectra were taken at 40°C in $CDCl_3$. However, the ^1H NMR spectrum only showed half the expected number of signals, four internal methyl proton signals at δ -3.861, -3.866, -4.29 and -4.34, and four *t*-butyl signals at δ 1.710, 1.681, 1.679 and 1.659. The proton at the oxygen bridge head showed as four singlets at δ 6.667, 6.651, 6.640, 6.633 and likewise there were four carbon signals at δ 81.53, 81.49, 81.38 and 81.34 in the ^{13}C NMR spectrum. In each of isomers **114uuB** and **114udA**, the two carbons on the CH-CH bridge in the middle of the two oxygen bridges are chemically equivalent and, thus only three signals should be observed in either the group **A** or group **B** isomers. Indeed, three signals appear at δ 54.14, 53.92 and 53.87 from the ^{13}C NMR spectrum, and three signals at δ 2.503, 2.505 and 2.413 in the ^1H NMR spectrum, with the one at δ 2.505 being a singlet, while those at δ 2.503 and 2.413 are doublets each with a coupling constant 6.5 Hz.

From the information above, we deduced that only two isomers either **114uuA** and **114uuB** or **114udA** and **114udB** were obtained experimentally.

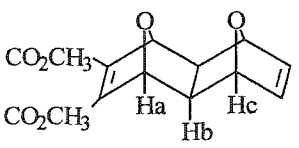

115uu

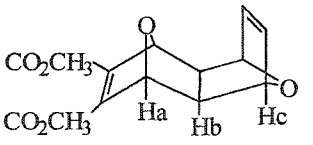

115ud

Compounds **115uu** and **115ud** are known.[80] In the **115uu** isomer with both oxygen bridges up, the coupling constants $J_{ab} \cong 0$ Hz and $J_{bc} \cong 0$ Hz, indicates the dihedral angles between Ha and Hb as well as between Hb and Hc are approximately 90°. In the **115ud** isomer however the coupling constants $J_{ab} \cong 0$ Hz and $J_{bc} \cong 4.5$ Hz indicates the dihedral angles of approximately 90° between Ha and Hb, and 45° between Hb and Hc.

Figure 3. Partial ^{1}H NMR spectra of isomers of 114.

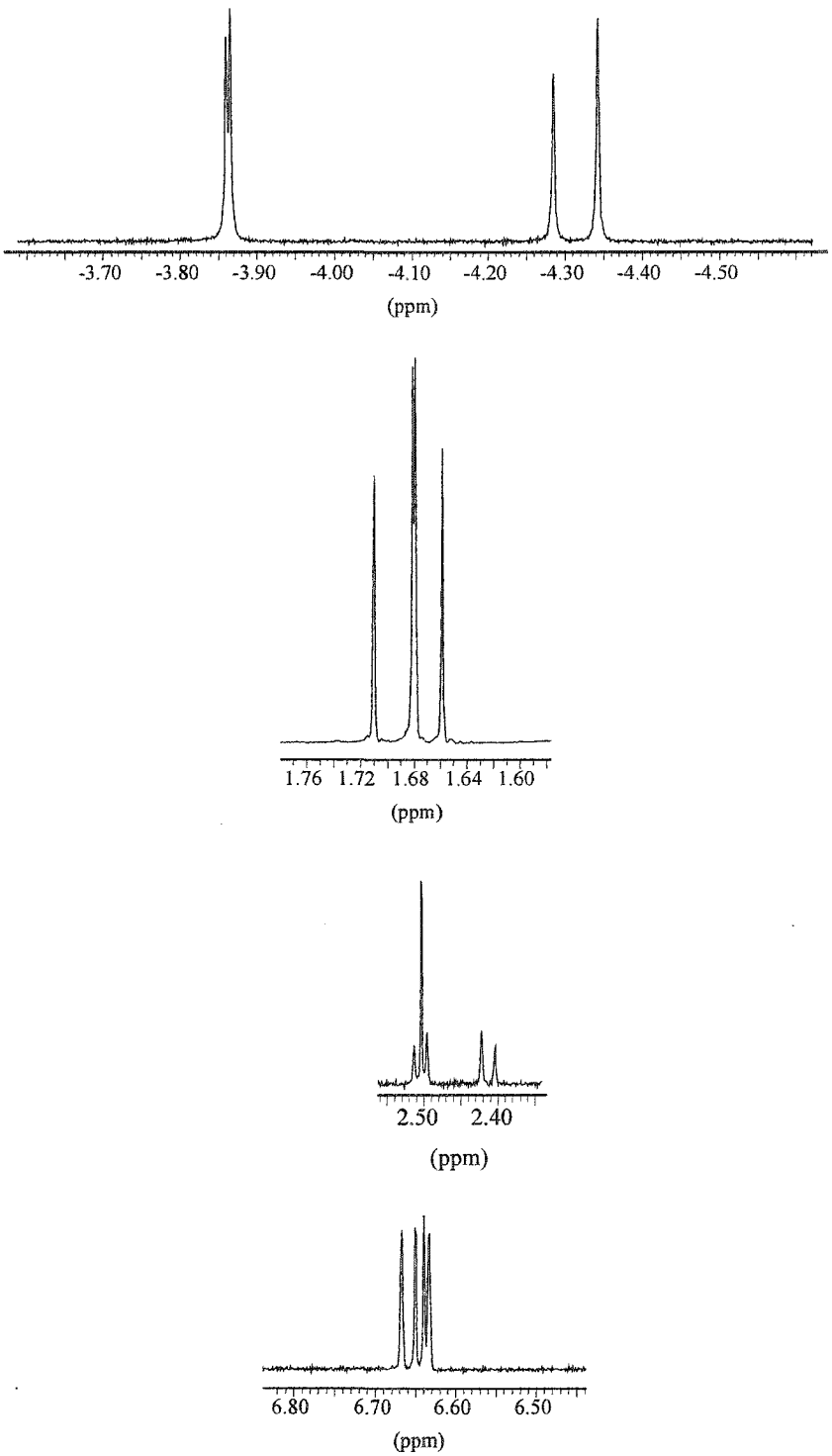

In our case, the bridge head protons appeared as four singlets. The bridge protons on the CH group showed three signals, one singlet, and the other two coupling to each other with a coupling constant of 6.5 Hz. Clearly there is no coupling between the oxygen bridge head protons and the CH-CH bridge protons, which suggest that our isomers have the two oxygen bridges on the same side, i.e., **114uuA** and **114uuB**.

LSIMS gave the correct molecular ion at *m/z* 794.4 (M+) and a HRMS gave 794.5100; calculated as 794.5063.

Deoxygenation and aromatization of **114** was tried with several reagents: BH_3 with $BF_3.Et_2O$, SmI[70], Ti (0)[69], $Fe_2(CO)_9$ with DDQ, and Na in THF, but, only P_2S_5 in CS_2[81] worked.

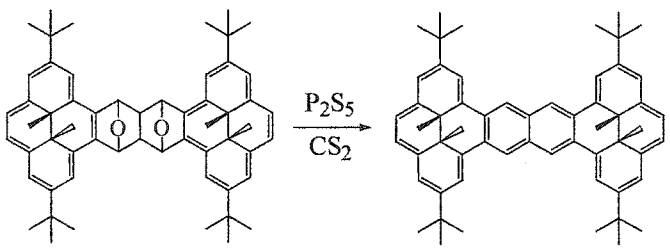

114 **116**

The adduct **114** and P_2S_5 was stirred in CS_2 for a few hours and the solution turned brown. After filtration and evaporation, chromatography was used to purify the product **116**. Surprisingly, the first band which was eluted with hexanes was the red benzopyrene **21**. How **21** was generated in this reaction is not clear. Eluted next was the green product **116** as a mixture of two isomers in about 30% yield.

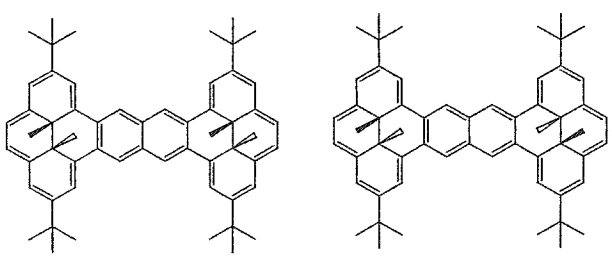

116A **116B**

There were two internal methyl and two *t*-butyl signals present in ^{1}H NMR spectrum at δ -0.325, -0.310 and δ 1.474, 1.470 respectively. Due to the symmetry of the structures, there are only four types of aromatic protons within each isomer, and the most deshielded protons are from the naphtho spacer with chemical shifts at δ 9.196 and 9.190 from each isomer. LSIMS gave a correct *m/z* at 760.6 (M+); the exact mass was found as 761.5064. The calculated value for $C_{58}H_{64}$ (MH+) was 761.5086.

The photochromism study of **116** was done in deaerated THF (due to its low solubility in cyclohexane). Various visible light sources, such as broad spectrum with/without cut-off filters, or monochromic light were used. They all gave the same result that the signal of the UV-Vis absorption spectrum became smaller. This indicated that the sample decomposed under visible light irradiation.

Arynes generated from an aryl bromide and $NaNH_2$ usually react with furan at room temperature, and so they are fairly reactive. Indeed the aryne **67** generated from bromide **69** likewise proved to be a good dienophile, and reacts with furan at room temperature. We hoped the aryne from 9-bromophenanthrene **117** would be reactive enough to undergo the Diels-Alder reaction with isofuran **47**.

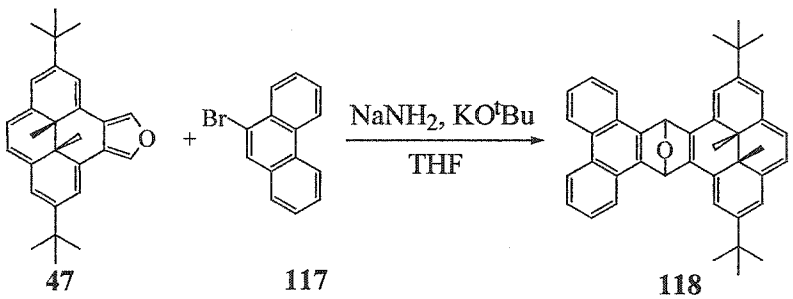

47 **117** **118**

In fact, the above reaction completed overnight and gave 85% of the adduct **118** as green crystals from toluene, mp 221-222°C. The ^{1}H NMR spectrum showed two

singlets for both the internal methyl groups and the *t*-butyl groups at δ -3.14, -4.12 and δ 1.66, 1.63 respectively. The ^{13}C NMR spectrum gave the bridge head carbons at δ 81.72 and 81.14. The CI MS gave a correct molecular ion at *m/z* 561 (MH+) and a correct elemental analysis was also obtained.

The deoxygenation of **118** was carried out with $Fe_2(CO)_9$ and was complete in a few hours. The resulting product **119** was obtained in about 86% yield and had poor solubility in hydrocarbon solvents, such as, hexane and benzene. It was purified by filtration through a short column of deactivated SiGel and crystallization from a mixed solvent of hexane/CH_2Cl_2.

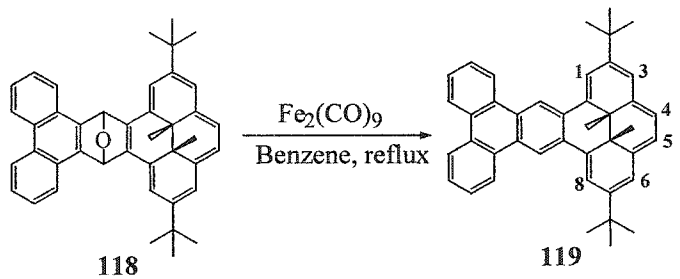

118 **119**

The ^1H NMR spectrum of **119** showed singlets for both the internal methyl and the *t*-butyl protons at δ -1.07 and δ 1.55 respectively. The pattern of the proton spectrum on the DHP ring was similar to benzopyrene **21**, with one sharp singlet for H-4,5, and two doublets each for H-3,6 and H-1,8. All the proton peaks could be assigned by COSY/NOESY spectra. The CI MS gave the correct molecular ion at *m/z* 545 (MH+), and a correct elemental analysis was also obtained.

2.4 An Unsymmetrical System Containing Three Dimethyl-dihydropyrene Units

The successful syntheses of compound **72** and of the substituted derivatives of benzopyrene **21** encouraged us to make a derivative of **72** which was substituted at one end of the DHP rings to differentiate the ends.

We tested first the direct acetylation of **72**, however, as soon as $BF_3{\cdot}Et_2O$ was added, the reaction mixture turned to black and ^1H NMR spectrum showed that all the starting material was consumed. No product traveled on TLC which was DHP like.

We next tried an alternative route in which the central benzene rings were built last. Since a phenyl group had been successfully attached to the benzopyrene **21** by the stepwise route, we decided that the phenyl substituted tris-pyrene **120** was a suitable target through the following reactions.

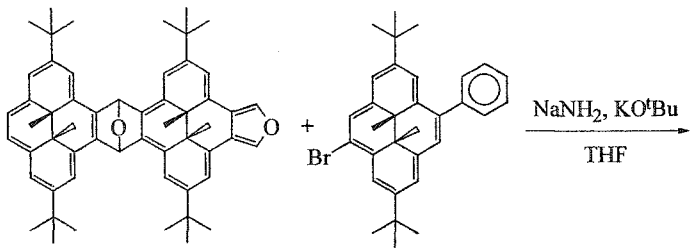

79 **107**

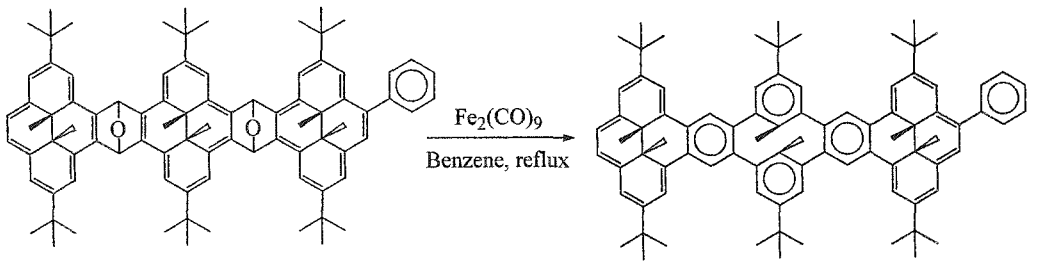

121 **120**

The Diels-Alder reaction of **79** and the aryne derived from **107** was carried out in THF using $NaNH_2$ and gave the adduct **121**. Due to its poor solubility and instability on both SiGel and alumina, the reaction mixture was just filtered through a short alumina column and then used directly in the subsequent deoxygenation reaction. A ^1H NMR spectrum could be taken in C_6D_6, but decomposition occurred very quickly in $CDCl_3$ solution, even when previously filtered through alumina (which worked for other adducts). The crude ^1H NMR spectrum showed three groups of peaks centered at δ -2.8, -4.2 and -5.0 suggested the product contained the correct DHP ring moieties. The crude yield of **121** was 23%.

Deoxygenation of **121** with $Fe_2(CO)_9$ gave product **120** as a mixture of four relatively stable isomers. Chromatography over alumina was used to purify the product.

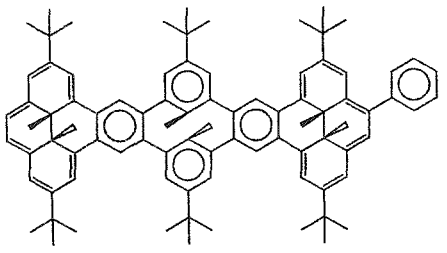

120A

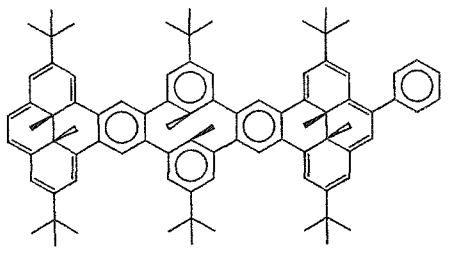

120B

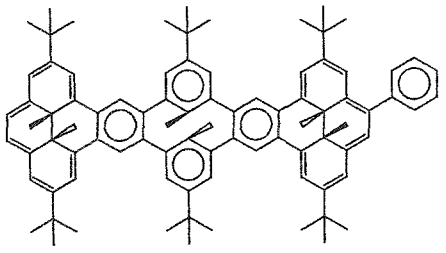

120C

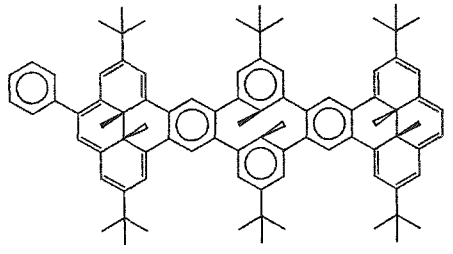

120D

The ^1H NMR spectrum of **120** showed four broad internal methyl proton signals at δ -1.23, -1.36, -1.49 and -1.62. In comparison, the symmetric tris-pyrene **72** showed

only two signals at δ -1.37 and -1.63. The two signals at δ -1.36 and -1.62 of **120** were almost identical to those in **72**, while the two newly generated signals of **120** at δ -1.23 and -1.49 are more deshielded by about 0.14 ppm from δ -1.37 and -1.63 in **72**. As we know, the phenyl group reduces the ring current in the attached DHP ring through partial conjugation. Also, comparing the benzopyrene **21** and the phenyl substituted benzopyrene **105**, the internal methyl protons are more deshielded by about 0.13 ppm from δ -1.58 in **21** to δ -1.45 in **105**. Thus, we can conclude that two new signals of **120** at δ -1.23 and -1.49 were from the phenyl substituted DHP rings. The aromatic proton NMR pattern in **120** is similar to that in **72**, except that more peaks are present consistent with the lower symmetry of **120**.

The LSIMS showed a correct molecular ion at *m/z* 1153.6 (MH+), the HRMS gave the exact mass as 1153.7576, while the calculated value was 1153.7590.

Chapter Three Photochemical and Thermochemical Results and Discussion

3.1 Photochromism

The photochromism of the dimethyldihydropyrene system was first reported in 1965.[46] In section 1.2, we reviewed some of the studies that have shown how substitution and annelation affect the photo opening reaction quantum yield and the rate of the thermal return reaction of the open form to the closed form. Very recently our group has made further reports.[50] As we discussed earlier, arene annelation has the largest effect on photoswitching properties, and the benzene annelated dimethyldihydropyrene **21** is the best photoswitch in the dimethyldihydropyrene series so far.

3.1.1 The Tris-pyrene System 72

Ward studied the photochromic properties of the multistate photoswitches **50** and **51**.[50,51,53] In the case of **50**, two DHP units were connected by means of a planar conjugated arene spacer. In **51**, only one DHP unit is present in the thermally stable isomer, but on irradiation with UV light, two DHP units form. We thought the study of the photochromic property of the tris-pyrene **72** would be worthwhile, since in the thermally stable state, two DHP units are connected by a non-planar spacer, which on irradiation should form three planar DHP units.

In fact, visible light opening of the tris-pyrene **72** to its fully opened photoisomer **72'** could be followed by means of UV-Vis spectroscopy. A deaerated solution of **72** in

cyclohexane, about 0.02 mg/mL, sealed in a quartz UV cell, was irradiated with a monochromic light at 550 nm. A series of spectra were obtained at various time intervals shown in Figure 4.

Figure 4. The sequential UV-Vis spectra of photo openings of 72 at 550 nm.

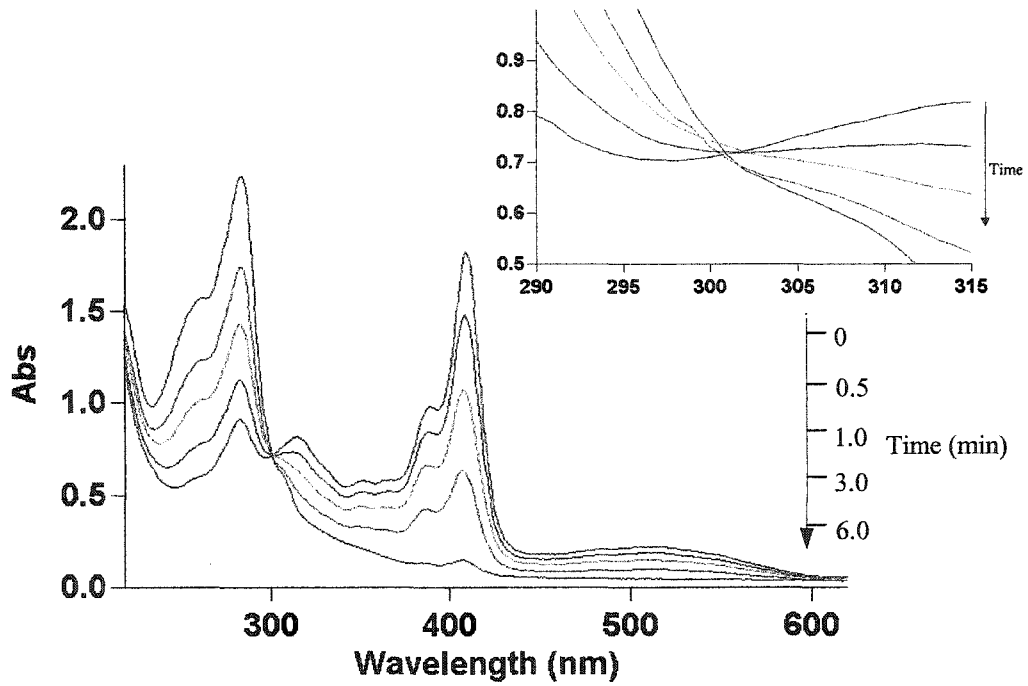

On irradiation at 550 nm, the absorption bands which belonged to the closed isomer **72** at 409 nm and 389 nm decreased, while the 283 nm band increased. The spectrum of the open isomer **72'** essentially consists of partially conjugated benzene rings and the UV-Vis absorption would be expected to be around 280 nm. Careful examination of the spectra, however, showed that an isosbestic point did not exist, suggesting that an intermediate isomer might form, such as **72'''**. In order to confirm our observation, a ^{1}H NMR study was performed. About 5 mg of **72** was dissolved in about 1 mL of $CDCl_3$ (which was filtered through alumina before use) and the solution was filtered

through alumina again to a NMR tube. The dark red solution was bubbled with argon for 30 min and was sealed with parafilm. The NMR tube was chilled in cold water and was irradiated with 500 W tungsten lamp with a 613 nm cut-off filter and monitored by a 300 MHz NMR spectrometer. After 30 min irradiation, the original internal methyl DHP proton signals at δ -1.359, -1.616 decreased, while new peaks at δ -1.373, -1.624 appeared. With longer irradiation, all peaks decreased, but the ratios of new peaks to the original ones were increased (see NMR spectra in Figure 5).

Figure 5. Sequential NMR spectra in the process of visible light opening of 72 at wavelength > 613 nm

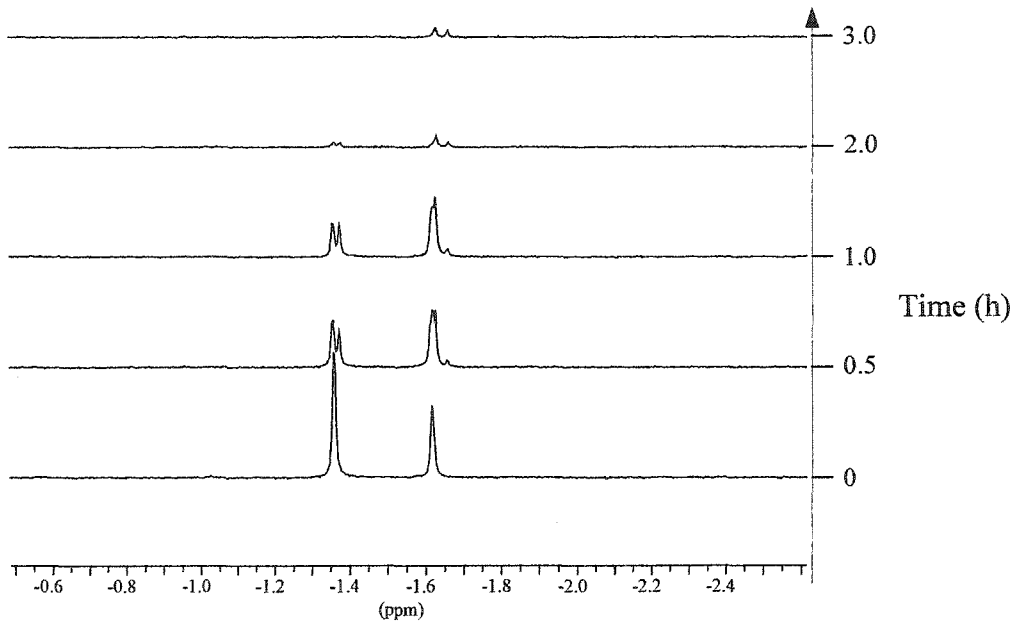

When the conversion was near completion, some white solid started to precipitate out, which was thought to be due to the limited solubility of the fully opened isomer **72'**. Complete disappearance of the peaks in the internal methyl DHP proton region took about 3 h.

Both the UV-Vis spectra and the ^{1}H NMR spectra gave evidence that a third intermediate species, whose structure can only be **72'''**, was generated in the photo opening process, although this could not be isolated pure.

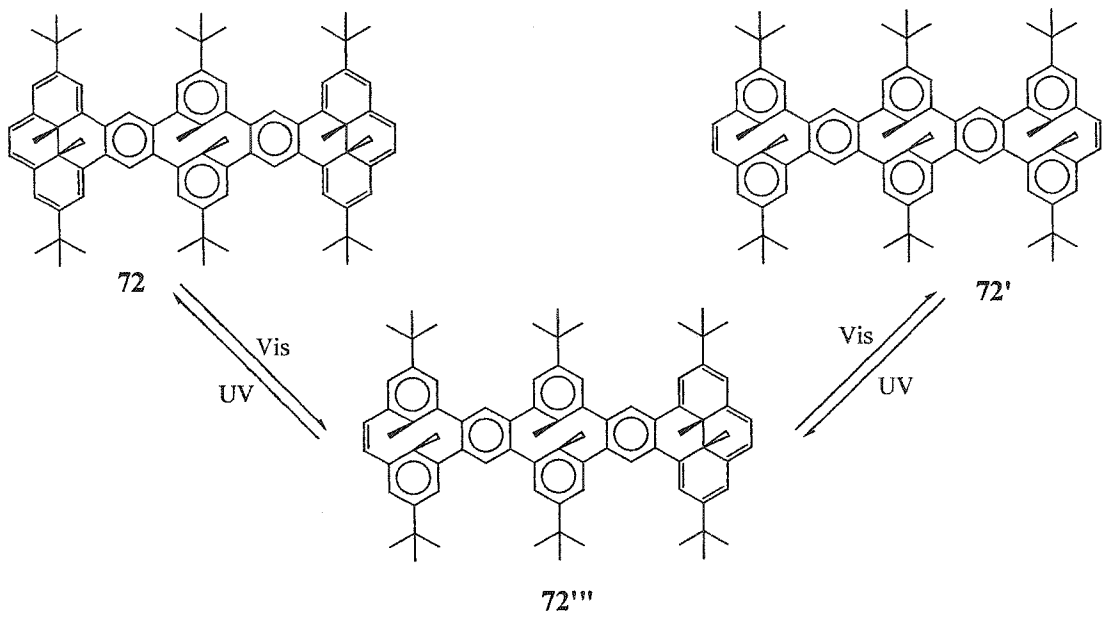

In the case of the bispyrenochrysene **50**, no intermediate could be detected by ^{1}H NMR in the photo opening process, and there was an isosbestic point when the opening was followed by UV-Vis spectroscopy.[53] In **50**, the thermally stable isomer is fully conjugated and planar and so, as the molecule absorbs a photon of energy, a double ring opening may occur.

In the case of **72**, the cyclophane that connects the two DHP rings is not coplanar with the DHP rings, and so sufficient energy probably does not reach both ends of the molecule simultaneously, to open both ends without formation of the intermediate. Figure 6 shows the PCMODEL[82] prediction of the structure of **72**.

Figure 6. The predicted structure of 72 by PCMODEL.

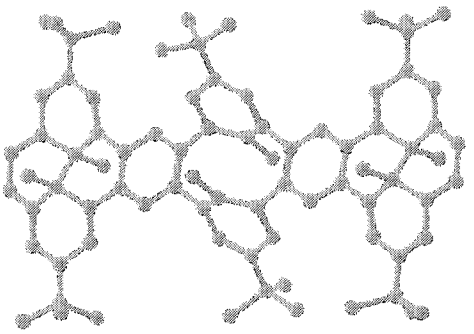

Thus, photo opening of **72** is a two photon process, whereas **50** may be a one photon opening of both DHPs.

Figure 7. Sequential UV-Vis absorption spectra for the UV closing of 72' at different time intervals

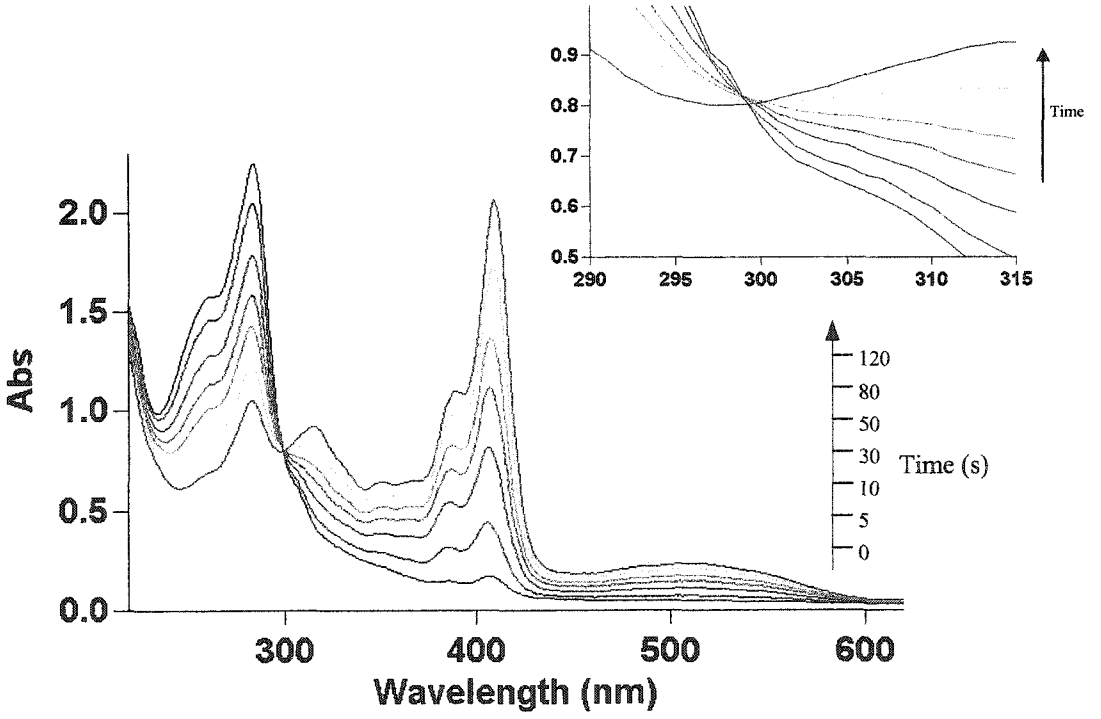

Similarly, after **72** was fully opened to **72'**, the sample was irradiated with 350 nm UV light and this process was followed by both UV-Vis spectroscopy and NMR spectroscopy. The UV-Vis spectra are shown in Figure 7.

The UV closing spectra are very similar to visible opening ones shown in Figure 4, but in the opposite sequence. The colorless solution of **72'** upon irradiation with 350 nm UV light became colored as the band at 283 nm decreased and the bands at 389 nm and 409 nm increased. Again there was no isosbestic point observed.

Figure 8. Sequential NMR spectra in the UV closing reaction of 72' to 72 using 350 nm UV light.

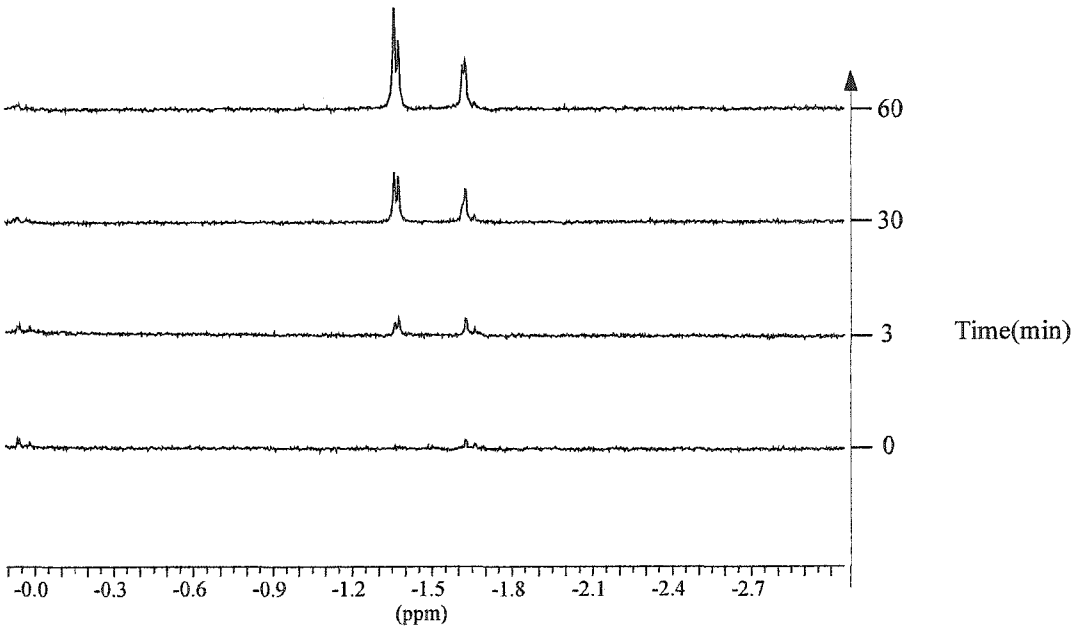

For the NMR study, the same solution used for the above photo opening reaction, after bleaching, was used for the UV closing reaction. The bleached $CDCl_3$ solution with some white precipitate, containing the open form **72'**, (which showed almost no peak in the region expected for internal methyl DHP protons, -1.3 to -1.7 ppm), was irradiated for 3 min at 350 nm, and then the NMR spectrum was repeated. Three peaks in the internal

methyl region were present at δ -1.359, -1.373 and -1.624, with the -1.624 ppm becoming two peaks at -1.616 and -1.624 ppm as time increased (see Figure 8 for NMR spectra). The peaks at δ -1.359 and -1.616 belonged to the thermally stable isomer **72** and grew as the irradiation proceeded. The peaks at δ -1.373 and -1.624 thus belong to the half closed isomer **72'''**. They grew in very fast initially, but the ratio became smaller with continued irradiation as **72'''** closed to **72**. At the same time, the white precipitate dissolved as the UV irradiation progressed.

The changes in both the UV-Vis spectra and the NMR spectra during the photo opening and closing processes between **72** and **72'** suggest strongly that the intermediate **72'''** is involved. This is unlike the case of **50**, in which the intermediate can be seen in the closing reaction, but not in the opening.

3.1.2 The Phenyl Substituted Tris-pyrene System 120

From the photochromic studies of the tris-pyrene system **72** above, we have ascertained that a two photon process is involved in both the photo opening and closing. We thus thought it might be possible to separately open and close the two DHP ends if their UV-Vis absorption spectra were sufficiently different. However, as discussed in the synthesis section above, we had considerable difficulty in functionalising one of the DHP ends of **72**. The only substituted compound which we could make was **120**. The photo opening and closing of this phenyl substituted tris-pyrene system **120** were thus followed by both UV-Vis spectroscopy and ^{1}H NMR spectroscopy.

Figure 9. The sequential UV-Vis absorption spectra in the photo opening of 120 through a monochromator at 550 nm

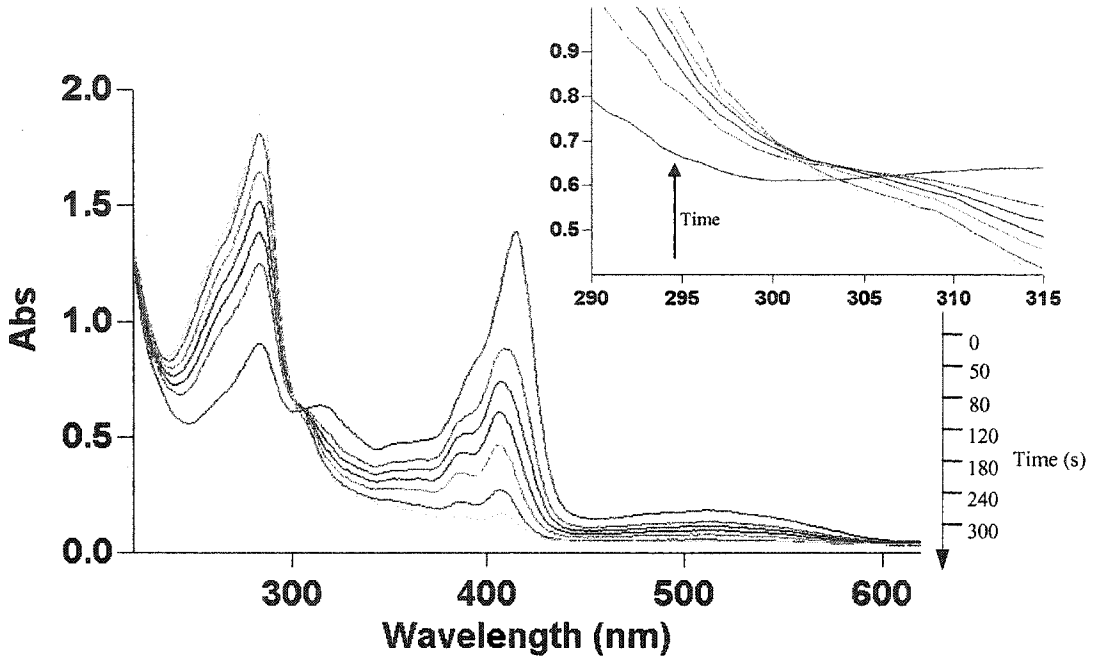

A deaerated cyclohexane solution of **120**, about 0.02 mg/mL, in a quartz UV cell was irradiated through a monochromator at 550 nm. The UV-Vis spectra at various time intervals are shown in Figure 9.

The UV-Vis absorption spectrum of **120** was not very different from that of **72**. The 409 nm band for **72** shifted to 415 nm and was broader in **120**, and the shoulder at 388 nm disappeared.

The solution of **120**, upon irradiation with 550 nm light, the 415 nm band decreased and the 284 nm band increased. The same as in the parent **72'**, the chromophore in the CPD-**120'** is composed of only benzene rings, and thus its UV absorption should be

around 280 nm. The increased intensity of the band at 284 nm indicates the formation of the isomer **120'**.

However, the band at 415 nm also shifted gradually to 407 nm and a shoulder started to appear at 387 nm and shifted to 386 nm with prolonged irradiation. More importantly, there was not an isosbestic point. From this information, we believe a third species is generated in the photo opening of **120** to **120'**, one in which one of the DHP ends has opened, e.g., **120'''**. Because **120** is not symmetric, the question arises, which DHP ring opens first, the one with the phenyl attached or the unsubstituted one?

In fact, when **72** was irradiated with 550 nm light, the band at 409 nm also shifted a little to 407 nm, and the shoulder shifted too, from 389 nm to 386 nm. Comparison of the intermediates **72'''** and the one from the photo opening of **120** to **120'**, suggests that the absorption bands belonging to the DHP at 386 nm and 407 nm were the same. Thus we believe that the intermediate was **120'''** in which the open DHP ring was the phenyl substituted one.

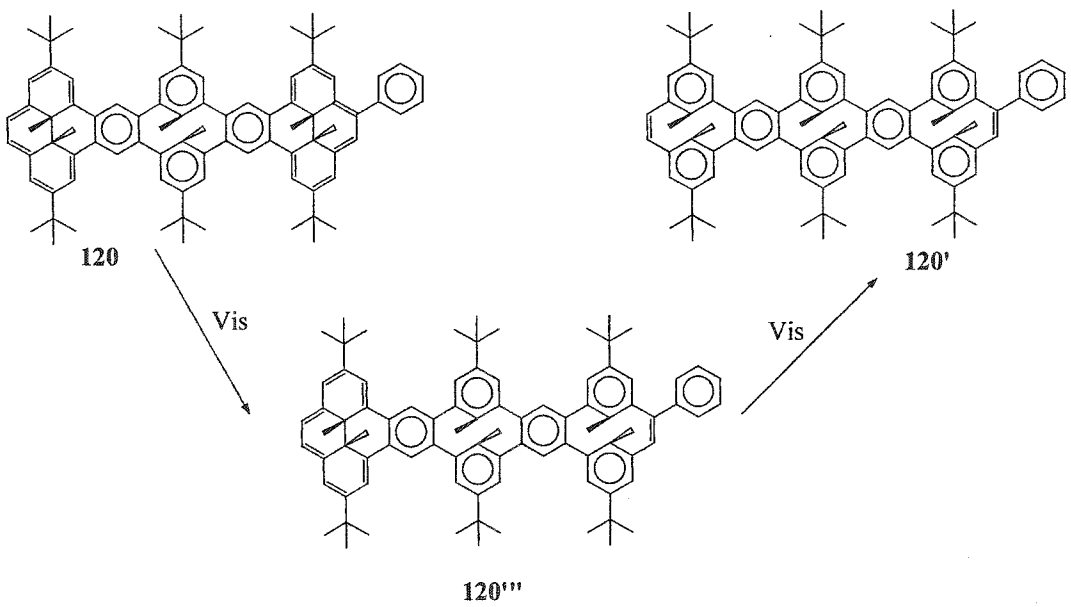

Further experimental evidence which supported the structure of **120'''** was the relative photo opening rate of benzopyrene **21** and phenylbenzopyrene **105**. The details of the experiment will be discussed later. The result is that the photo opening rate of **105** is about three times faster than that of **21**, and thus because it appears from above that both ends open independently, we might thus expect the phenyl substituted end to open faster.

A NMR study was conducted in order to find more evidence of the intermediate. Thus about 2 mg of dark red **120** was dissolved in 1 mL d_8-toluene, and then the solution was filtered through alumina in to an NMR tube. This was then bubbled with argon for 30 min, and then the NMR tube was sealed with parafilm. The sample was cooled with cold water. A 500 W tungsten lamp was used for irradiation through a 590 nm cut-off filter. NMR spectra were taken at various time intervals using a 300 MHz NMR spectrometer.

There are four peaks in the internal methyl region. As we discussed in the synthesis section, two of them, at δ -1.030 and -1.228, belong to the phenyl substituted DHP ring, and the other two, at δ -1.161 and -1.354 belong to the unsubstituted DHP ring. After 15 min irradiation, the two peaks, -1.030 and –1.228, significantly decreased, thus, confirming that the phenyl substituted DHP ring opened first; at the same time two new peaks grew next to the other two peaks, at -1.175 and -1.367, which suggested the intermediate species had a closed unsubstituted DHP ring. With prolonged irradiation, the ratio of the new generated peaks to the original ones became greater. After 55 min irradiation, the peaks at -1.030 and -1.228 had completely disappeared. A further 30 min

irradiation almost fully opened all isomers to form **120'** (see Figure 10 for the NMR spectra).

Figure 10. Sequential ^{1}H NMR spectra of the visible light opening of 120 to 120' using visible light at wavelength > 590 nm.

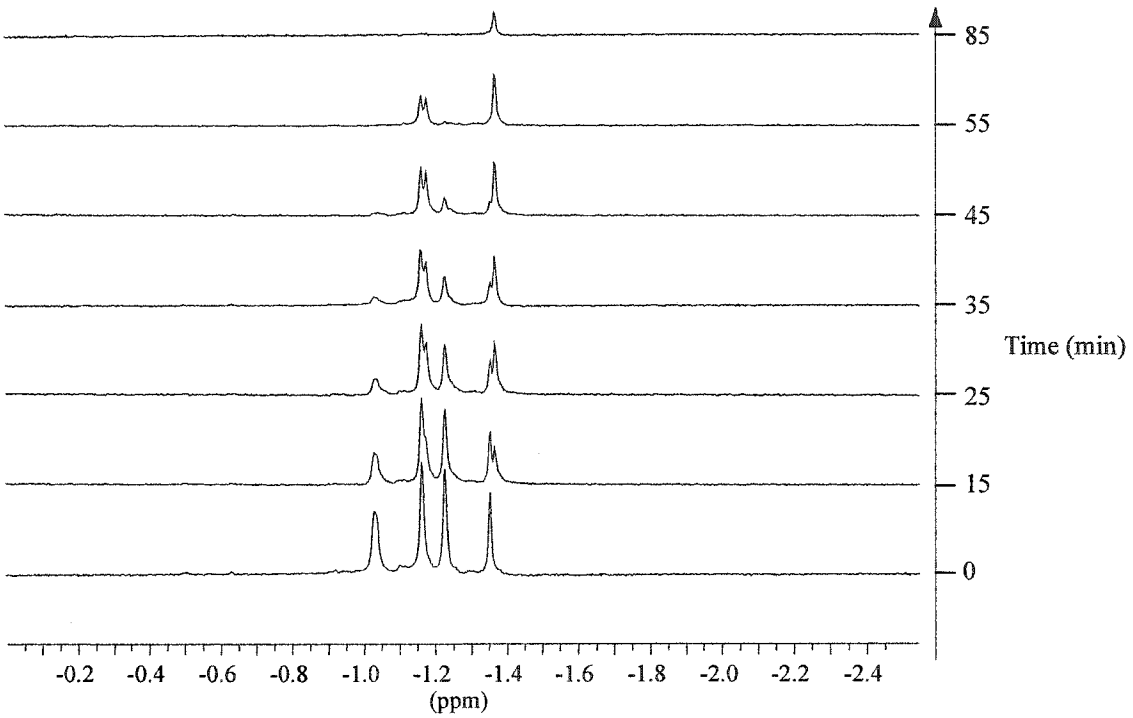

The NMR evidence thus confirms that the intermediate species **120'"** was present during the photo opening of **120** to **120'**.

As with the study of the parent **72'**, the UV closing of **120'** was carried out by sequential irradiation with 350 nm UV light. The spectra are shown in Figure 11.

The spectra obtained during UV closing were not identical to those from the visible opening. In Figure 9, it is easy to see that there is not an isosbestic point. However, in Figure 11, it is not so obvious wherever there is an isosbestic point or not. Careful examination suggests there is not. The shoulder peak at 386 nm in Figure 11 is not so obvious as in Figure 9, though it still can be seen. The shift of the major absorption band

from 407 nm to 415 nm with extended irradiation of UV light still was seen. This evidence suggests that there may be some intermediate species in the UV closing of **120'** to **120**, although it might not be the same as that in the visible opening of **120** to **120'**.

Figure 11. The sequential UV-Vis absorption spectra in the UV closing of 120' via a 350 nm UV light source.

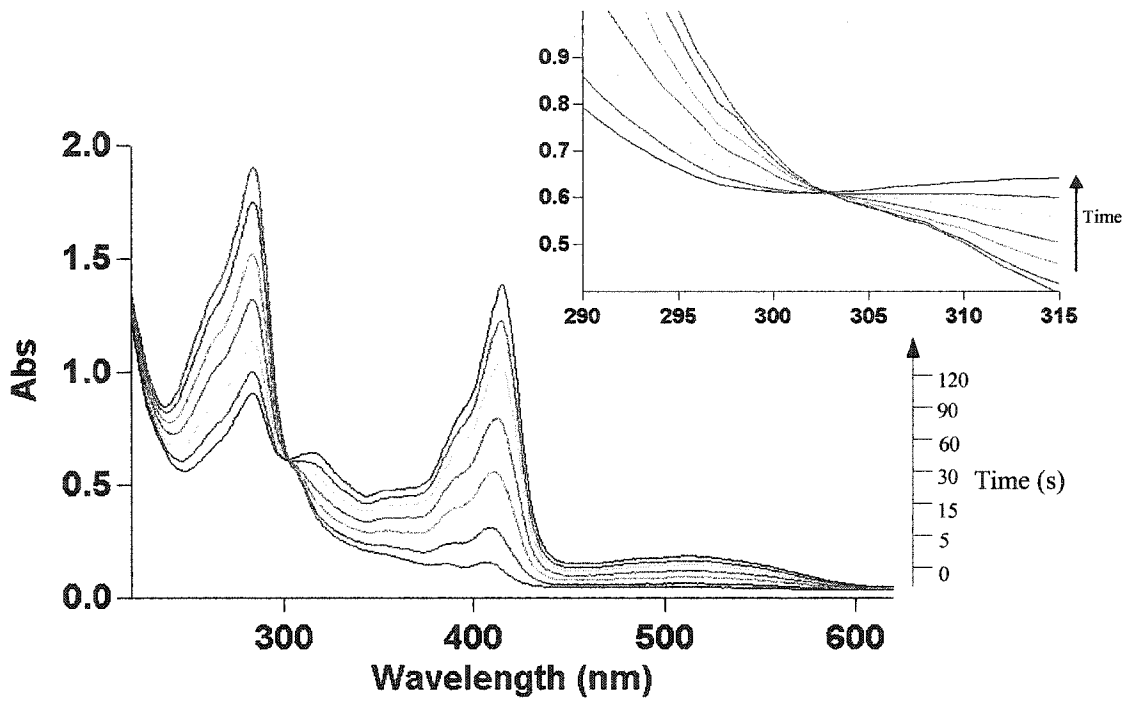

In the study of the UV closing rates of benzopyrene **21** and phenylbenzopyrene **105**, it was found that the UV closing rate of **105'** to **105** was only 1.1 times that of the closing of **21'** to **21**. This suggests that the preference to open the phenyl substituted DHP ring is very small, and that the intermediates in the UV closing process of **120'** to **120** was probably a mixture of **120'''** and **120''''**.

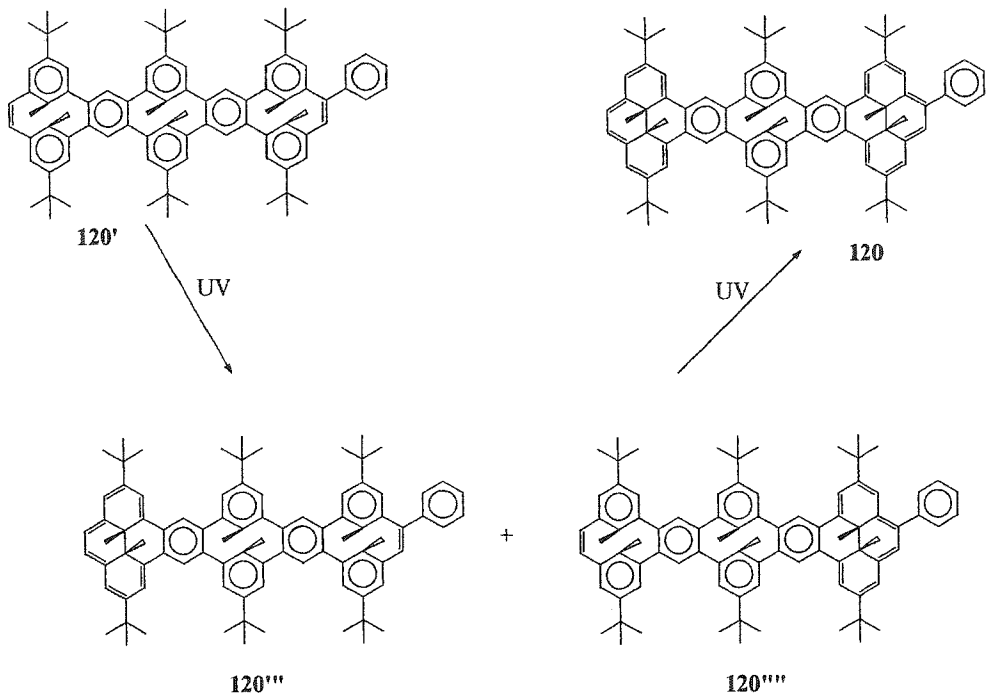

The NMR study was done in d_8-THF. The sample was prepared in the same way as in the photo opening study, but in a quartz NMR tube. The fully closed NMR spectrum in d_8-THF was taken for comparison and the internal methyl region is shown in Figure 12.

Figure 12. The internal methyl region ^{1}H NMR spectrum of phenyltris-pyrene (120) in d_8-THF

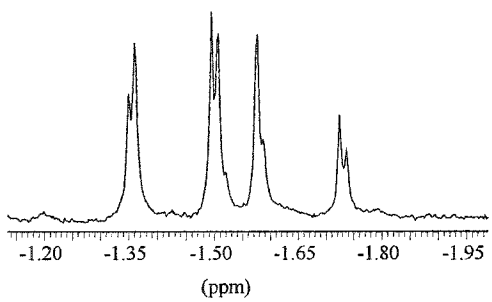

The sample was bleached using visible light and then was irradiated by a 254 nm UV light source with a cold water jacket as cooling system. The sequential UV closing spectra are shown in Figure 13.

Figure 13. Sequential NMR spectra of the UV closing of 120' to 120 using UV light at 254 nm.

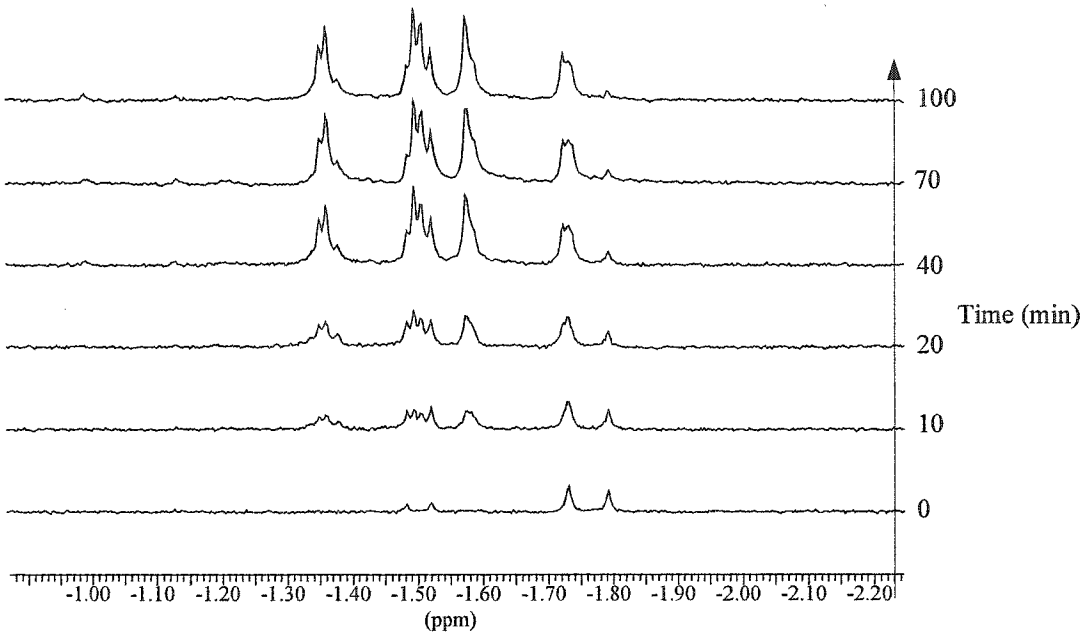

The peak patterns in Figure 12 and 13 are similar, but not identical. In the process of UV closing, all four groups of peaks which belong to the substituted and unsubstituted DHPs grow together. Mono-closed intermediates are probably present but there appears to be little preference in closing the substituted and unsubstituted DHP rings.

3.2 A Photo Opening and Closing Study of the Dimethyldihydro-pyrenes Using Excess Light

It is important for photochromic materials to have a short photo response time. For this purpose, a pico- or femtosecond laser photolysis experiment is needed. However, instruments are not always available to perform such experiments.

As we stated previously, benzopyrene **21** is one of the best photochromic compounds amongst simple arene annelated DHPs. Thus, we use **21** as a reference to compare photo openings and closings of the photo switch molecules in this thesis.

3.2.1 General Conditions

The photo openings and closings were followed by means of a UV-Vis spectrometer. The solution of benzopyrene **21** and the compound to be compared were prepared in equal molarity in quartz UV cells using cyclohexane as solvent (unless otherwise stated). The prepared solutions were bubbled with argon for 30 min and the UV cells were sealed with parafilm.

For photo-openings, a 500 W tungsten lamp served as a visible light source. Two cells, one containing the reference **21** and the other containing the compound to be compared, were placed side by side and irradiated with visible light using a 590 nm cut-off filter. An electrical fan was used to cool the samples. UV-Vis spectra were taken at various time intervals.

For photo-closings, a mercury pen light which emitted at 254 nm was used as the UV light source. The cells were put side by side in front of the UV light. An electrical fan was used as the cooling system. UV-Vis spectra were taken at various time intervals.

Both photo opening and closing processes were analyzed according to 0^{th} order and 1^{st} order kinetics, and it was found the experimental data fitted 1^{st} order kinetics best. Thus the results reported here were analyzed using 1^{st} order kinetics. Linear curve fitting was done in an MS Excel spreadsheet.

3.2.2 Molecules Containing a Single Pyrene Unit

The relative visible light opening rates of several simple substituted benzopyrenes and the annelated triphenyleno-DHP **119,** and the UV closing of their photoisomers were studied first. Compound **119** had to be studied in THF because of low solubility in hydrocarbon solvents. The results are shown in Table 5 (the original plots are shown in the experimental section).

Table 5. Ratios of relative photo opening rates (Vis-open) of some simple DHP systems relative to benzopyrene 21 at room temperature and relative photo closing rates (UV-close) of their photoisomers relative to 21'.

Compound	Vis-open	Compound	UV-close
21	1.0	**21'**	1.0
84	22.0	**84'**	1.1
103	6.4	**103'**	1.3
105	4.2	**105'**	1.1
119	2.8	**119'**	1.7

All the substituted benzopyrenes and the triphenylene annelated DHP **119** open faster than benzopyrene **21** itself. The acetyl substituted **84** opens the fastest. However, the UV closing rates of all compounds are not much different from that of **21'**. Photophysical studies[47,77,83] show that the quantum yields for the UV closing of all the DHP systems studied are high, e.g., **21'** to **21** is about 0.4. Thus, it appears that the UV closing rates for all DHP systems are close and relatively fast. Although the photo opening rate determined here and the quantum yield can not be directly compared, a fast

photo opening rate certainly indicates usefulness as a switch even in the absence of a detailed quantum yield study.

3.2.3 The Tris-pyrene System 72

The photo opening of the tris-pyrene **72** and photo closing of **72'** were studied in THF. The results are shown in Figure 14 and Figure 15. As we discussed before, the photo opening process goes through the half opened intermediate state **72'''** before becoming the fully opened **72'**, unfortunately, the UV-Vis spectra of **72** and **72'''** overlap each other. In section 3.1.1, we concluded that in our tris-pyrene system, two photons open the molecule, and the two benzopyrene moieties of **72** behave independently.

Figure 14. Plots for visible light opening of 72 (trisdhp) and 21 (bdhp)

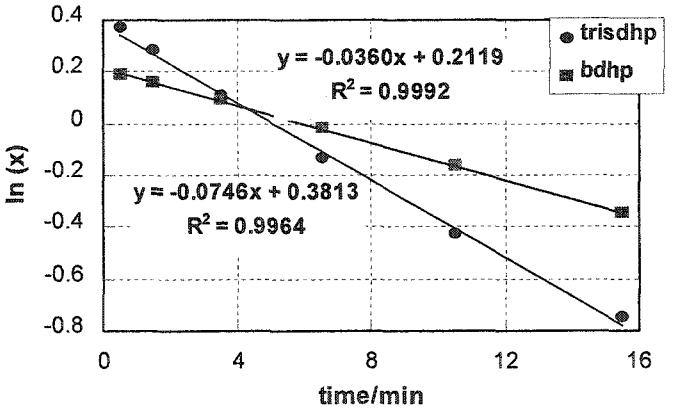

Figure 14 shows the photo opening results. The linear curve fits the experimental data points well, thus, we infer that the photo opening rates of **72** → **72'''** and **72'''** → **72'** were very close. We can imagine the closed form **72** as two substituted benzopyrene molecules and **72'''** as one substituted benzopyrene molecule. The photo opening rate

we measured here could be translated to the reaction of the opening of a substituted benzopyrene structure **122**.

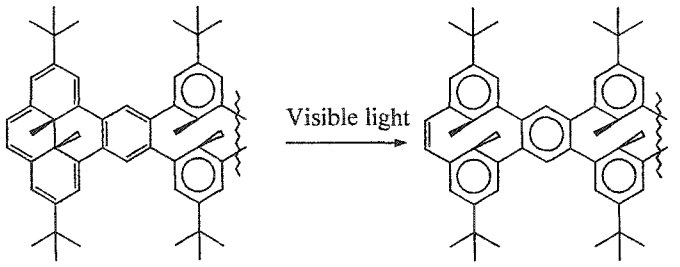

122 **122'**

The experiment showed that the photo opening rate of **72** was 2.1 times as that of **21**, which is fairly close to the result for triphenyleno-DHP **119**. This is not surprising because both **119** and **72** can be viewed as a benzopyrene with ortho substituted phenyl rings on the benzene side.

Figure 15. Plots for UV closing of 72'(triscpd) and 21'(bcpd)

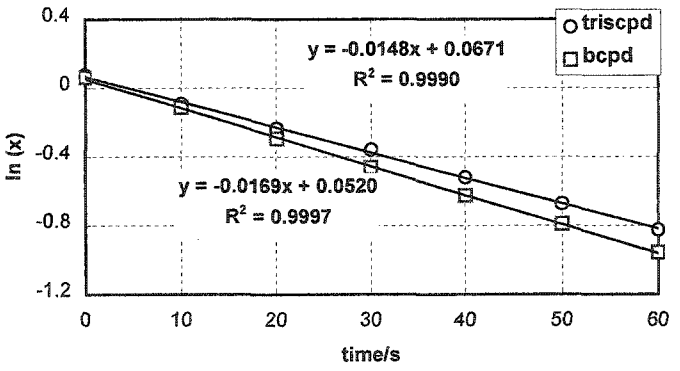

The same as in the photo opening reaction, the UV closing of **72'** → **72** that we measure by UV-Vis method is essentially that of the open form structure **122'** to its closed form **122.** Here, we assume that the two benzopyrene moieties close independently and with a similar closing rate (see Figure 15).

The UV closing rate of **72'** → **72** is 0.9 times as that of **21'**→ **21**. Like all other simple systems studied earlier, the UV closing rate does not vary much from that of **21'**.

3.2.4 The Phenyl Substituted Tris-pyrene System 120

The study of the photo opening process of the symmetrical compound **72** indicates that the opening rates of the stepwise reactions are almost the same. It would be interesting to see if a system could be obtained where the stepwise reactions have different opening rates. Thus, the phenyl substituted tris-pyrene **120** was studied and the results are presented here.

Figure 16. Plots for visible light opening of 120 (ptrisdhp) and 21(bdhp)

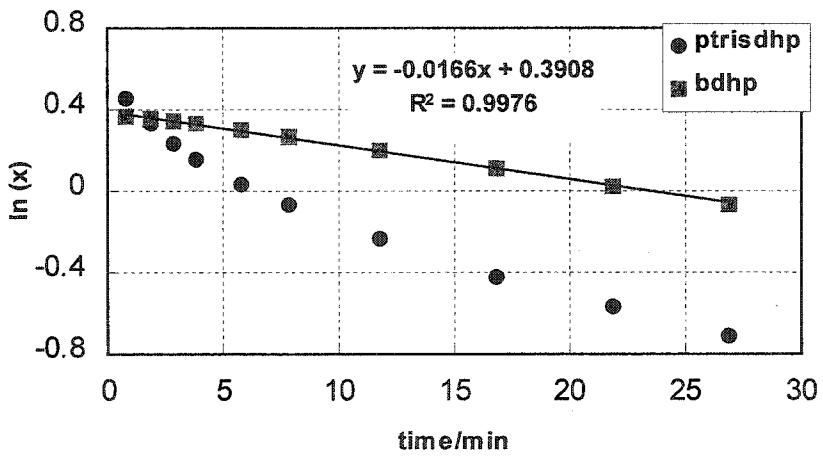

Figure 16 shows the photo opening results of compound **120** and **21** under the same conditions. The photo opening data of **120** can not be fitted into a linear curve. This is expected since the photochromic study showed that the photo opening of **120** went through the intermediate **120'"**, and then formed the fully opened **120'**. The photo

opening process of **120** can be separated into three stages which are expressed by the following equations:

Stage 1: **120 → 120'''**

Stage 2: **120 → 120'''** & **120''' → 120'**

Stage 3: **120''' → 120'**

The initial stage of the photo opening process was almost exclusively the opening of the phenyl substituted DHP ring. The opening rate should be relatively large and early data points should show to a relatively straight line fit. This is shown in Figure 17.

Figure 17. Plot for visible light opening of 120 (ptrisdhp) in stage 1

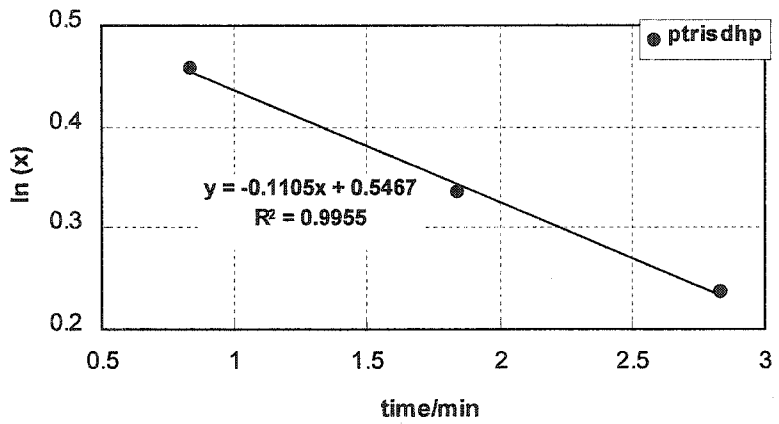

In this manner, the initial photo opening rate of **120** is determined to be 6.7 times that of **21**. Compared to the model compound phenylbenzopyrene **105**, which opens 4.2 times as fast as **21**, the substituents at the benzo side further increase the opening rate about two times. This is consistent with the data from the parent **72**, which opens 2.1 times as fast as benzopyrene **21**. After the initial opening of **120**, the fully opened **120'** is produced slowly. Thus, the second stage consists of two processes and the average opening rate should decrease. Figure 18 gives the experimental results.

Figure 18. Plot for visible light opening of 120 (ptrisdhp) in stage 2

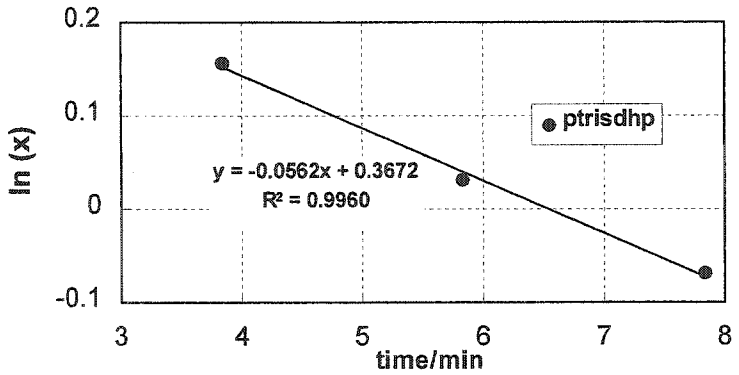

The linear curve fitting gives a qualitative idea on the overall opening rate, which is about 3.4 times as fast as benzopyrene **21**. Although the apparent opening rate is slowed down, it is still larger than that of the parent **72**, which is as it should be.

The final stage of the opening process of **120** is the opening of the benzopyrene structure **122**. Theoretically, we would predict that opening rate of the final stage should be very similar to that of the parent **72**. The experiment results are shown in Figure 19.

Figure 19. Plot for visible light opening of 120 (ptrisdhp) in stage 3

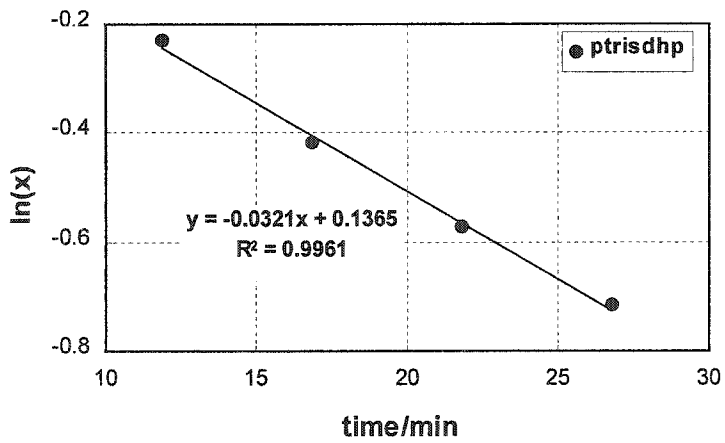

The relative photo opening rate of **120** in the final stage is 1.9 times that of **21**, which is very close to that for the parent **72**. The fact that the absorption wavelength

during the final stage stays unchanged at 404 nm supports the idea that there is a single final species with a closed DHP ring.

3.3 The Thermal Closing Reactions

So far all photochromic dimethyldihydropyrenes also show a thermochromic reaction as well.[31,46,50] The ultimate goal of shutting off the thermal reaction between the photoisomers has not yet been achieved. However, there are some systems where the thermal reaction rate is sufficiently slow ($\tau_{1/2}$ is about 1 week at room temperature), for example **21**, which could thus potentially be put to practical applications.

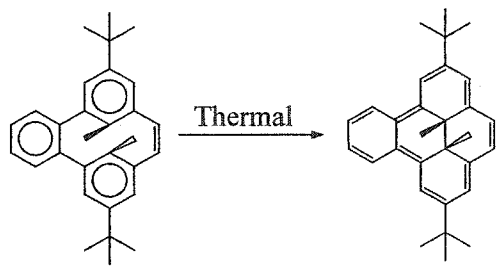

21' **21**

Thus, knowledge of the thermal closing data is also important to the photochromic properties of dimethyldihydropyrenes.

The thermal reaction was studied using UV-Vis spectroscopy. The photo bleached sample in toluene was held at a fixed temperature and its absorption monitored at the maximum absorption in the wavelength range of 380 nm to 420 nm at various time intervals. Nine compounds were studied and their thermal closing rates were determined at various temperatures.

For easy tracking of the compounds studied, their DHP structures are shown below.

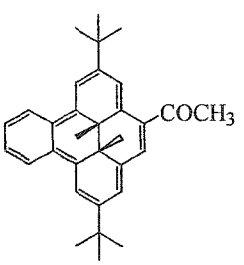

84

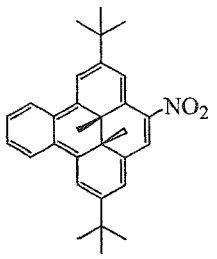

86

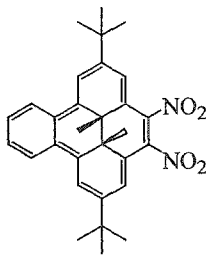

87

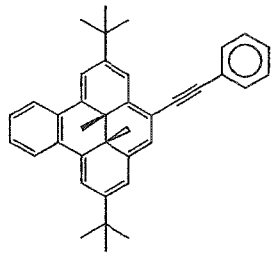

103

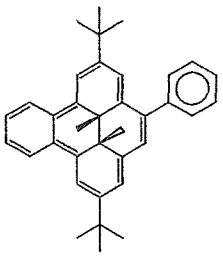

105

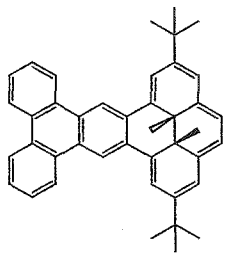

119

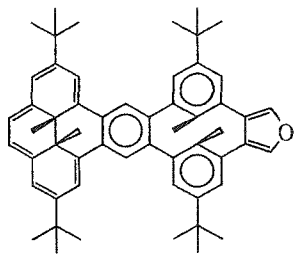

82

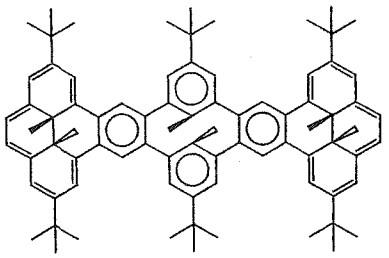

72

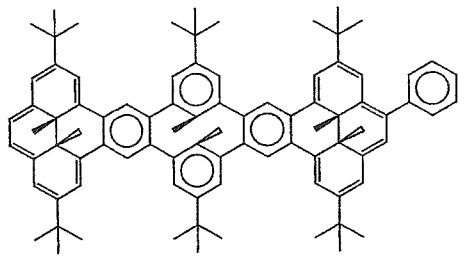

120

Each thermal reaction was followed at least at three temperatures, 46°C, 60°C and 70°C. The plots and all other thermal data are given in experimental section. The kinetic data at 46°C are presented in Table 6.

Triphenyleno-DHP, which has a medium thermal return reaction rate, was chosen to estimate standard deviation. Three runs were done for each temperature 46°C, 60°C, 70°C. The standard deviation was calculated for each temperature, the largest value (3.8%) was chosen to apply to all kinetic data. Similarly, E_{act}, $\Delta H^{\neq}$ and $\Delta S^{\neq}$ were

calculated for each run, standard deviations were thus calculated as 2.8%, 2.9% and 44%, respectively to apply to dynamic data.

Table 6. Thermal return rates and half lives $\tau_{1/2}$ at 46°C.

Reactions	**rate (min^{-1})**	**$\tau_{1/2}$ (h)**
21' to 21^{50}	0.00200 ± 0.00008	5.75 ± 0.23
84' to 84	0.00141 ± 0.00006	8.19 ± 0.33
86' to 86	0.00123 ± 0.00005	9.39 ± 0.38
87' to 87	0.00216 ± 0.00009	5.35 ± 0.21
103' to 103	0.00820 ± 0.00033	1.41 ± 0.06
105' to 105	0.00214 ± 0.00009	5.40 ± 0.22
119' to 119	0.00307 ± 0.00012	3.76 ± 0.15
82' to 82	0.00242 ± 0.00010	4.77 ± 0.19
72' to 72	0.00204 ± 0.00008	5.66 ± 0.23
120' to 120	0.00197 ± 0.00008	5.86 ± 0.23

After obtaining the kinetic data, the Arrhenius and Eyring equations were used to determine the activation energies, enthalpies and entropies.

Table 7. Thermal dynamic data derived from the kinetic results.

Reaction	E_{act} (kcal mol^{-1})	$\Delta H^{\neq}$ (kcal mol^{-1})	$\Delta S^{\neq}$ (cal deg^{-1} mol^{-1})
21' to 21[50]	24.5 ± 0.7	23.9 ± 0.7	3.8 ± 1.7
84' to 84	24.4 ± 0.7	23.6 ± 0.7	2.2 ± 1.0
86' to 86	23.6 ± 0.6	22.9 ± 0.6	-0.2 ± 0.1
87' to 87	23.2 ± 0.6	22.5 ± 0.6	-0.3 ± 0.1
103' to 103	22.7 ± 0.6	22.0 ± 0.6	0.9 ± 0.4
105' to 105	23.9 ± 0.6	23.2 ± 0.6	1.9 ± 0.9
119' to 119	23.9 ± 0.6	23.3 ± 0.7	2.7 ± 1.2
82' to 82	24.0 ± 0.6	23.4 ± 0.7	2.6 ± 1.2
72' to 72	24.1 ± 0.7	23.5 ± 0.7	2.6 ± 1.2
120' to 120	24.2 ± 0.7	23.6 ± 0.7	2.8 ± 1.3

3.3.1 Substituted Benzo-CPD Systems

Although activation energies and enthalpies do not change dramatically on substitution, their effect on the thermal return rate is significant. The presence of the electron withdrawing, nitro and acetyl groups in **84'** and **86'** reduce the thermal return rates. At 46°C, the thermal decay half lives ($\tau_{1/2}$) of **84'** and **86'** were 8.19 h and 9.39 h, which are considerably slower than for the parent **21'**(5.75 h). We expected that two nitro groups on the DHP ring would slow down the thermal return reaction further. However, in the ortho-dinitro compound **87**, the thermal return rate increased from that in **86** such that, $\tau_{1/2}$ was 5.35 h, much the same as the unsubstituted parent **21**.

This is different from the dibromo derivative **123'**.[50] Ward found that **123'** had a slower thermal return rate ($\tau_{1/2}$ = 9.50 h) than the parent **21'**. He proposed that the two large bromine atoms would sterically hinder each other in the more planar DHP form.

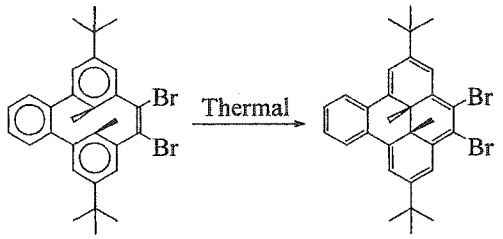

123' **123**

In our case, the second nitro group did not slow down the thermal return rate. A nitrogen atom is not as large as a bromine atom, and so steric hinderence may not have such large an effect as in the case of **123'**. However, the nitro group has a much greater electronic effect than bromine, but how this affects the thermal return rate is not clear. Dr. R. V. Williams (University of Idaho) has now been able to locate a calculated transition state for the closing reaction. He finds that it has considerable (50%) radical character. Different electronic groups would thus be expected to affect this transition state, and work is needed to determine just how.

3.3.2 The Triphenyleno-CPD System 119

Triphenylene behaves more like isolated benzene rings than a polycyclic hydrocarbon. Thus the structure of **119** can be drawn as two independent benzene rings connected to a benzopyrene through a six membered ring. Thus, the thermal return reaction of **119'** to **119** should theoretically be similar to that of **21'** to **21.**

Experimentally, the E_{act} of the reaction of **119'** to **119** is 23.9 kcal mol^{-1}, which although not significantly different from that of the reaction **21'** to **21,** does show up in a

rate difference: the half life of its thermal return reaction $\tau_{1/2}$ is 3.76 h, which is slightly faster than that of the reaction **21'** to **21**, 5.75 h.

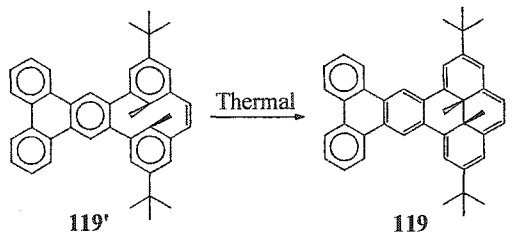

119' **119**

Certainly triphenylene annelation would not change strain or bond lengths much from that of benzene annelation, but would stablize an intermediate radical more and increase the thermal reaction rate.

3.3.3 The Furano System 82'

The thermal return reaction of the furano system **82'** to **82** is similar to that of **21'** to **21**. The furanocyclophane does not affect the thermal return reaction much, except the thermal return rate is slightly faster. The results found here also are consistent with the analogous system **51'** to **51**, in which the furan is replaced by a benzene.[50]

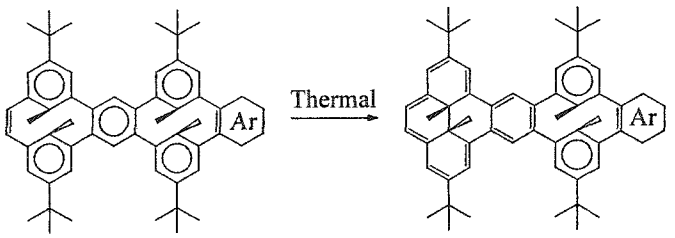

82' **Ar** =  **82**

51' **Ar** =  **51**

In the visible opening process, the benzopyrene **21** opens either in the presence or absence of oxygen, however, the furano-system **82** only opens when no oxygen is

present. In the presence of oxygen, the UV-Vis absorption spectrum did not change under visible irradiation.

3.3.4 The Tris-CPD System 72'

The thermal return reaction of **72'** to **72** was first followed by ^1H NMR spectroscopy. The sample was prepared as that for the photochromic studies. The NMR tube containing **72** in a solution of $CDCl_3$, cooled with cold water, was irradiated under visible light using a 590 nm cut-off filter to bleach the solution. After ca. 1 h, the solution was almost colorless with some white precipitate, which was believed to be the open form **72'**. The bleached sample was stored at 40°C in a water bath in the dark and the thermal return reaction was followed by NMR spectroscopy.

Figure 20. Sequential NMR spectra of thermally closing 72' to 72.

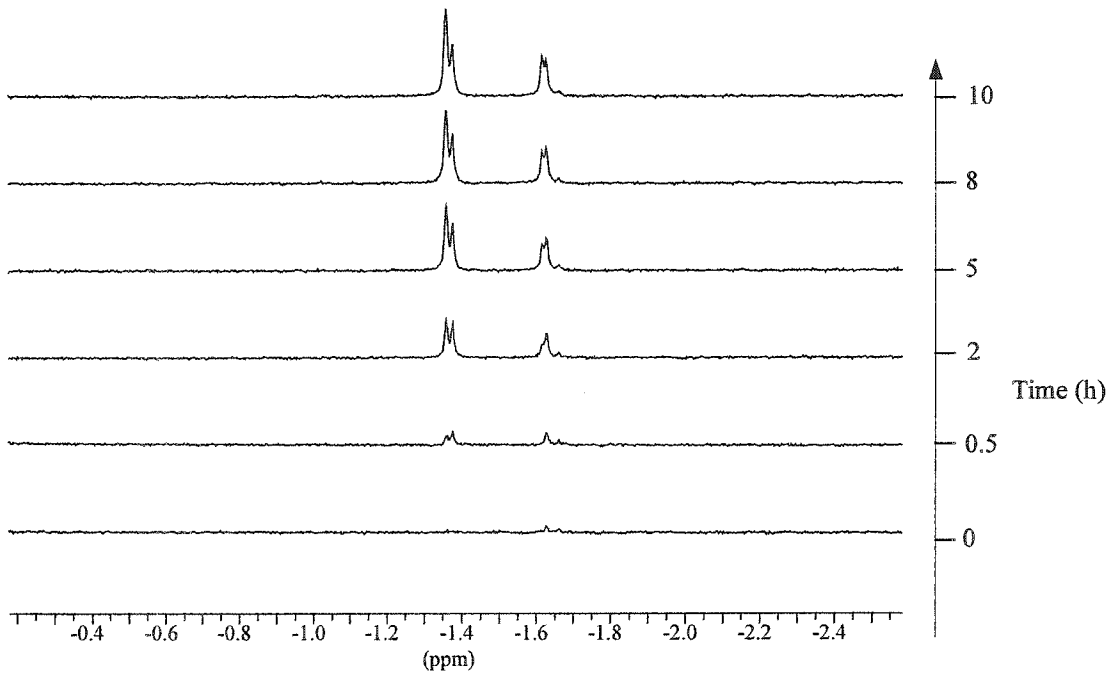

After 30 min, very small peaks at δ -1.359, -1.373 and -1.624 appeared. After 5 h, the peak at -1.359 was significantly larger than that at -1.373, and the peak at -1.624 became two peaks at -1.624 and -1.616. As we discussed previously, the peaks at -1.359 and -1.616 belong to the closed form **72**, the peaks at -1.373 and -1.624 belong to the intermediate **72'''**. The sequential ^{1}H NMR spectra are shown in Figure 20.

The NMR spectra clearly show that the thermal return reaction, just like the UV induced closing reaction, goes through intermediate **72'''** to form the closed form **72**.

$$72' \xrightarrow{k_1} 72''' \xrightarrow{k_2} 72$$

The rates of the two consecutive reactions, k_1 and k_2, should be very similar since each step contains the closing of one benzo-CPD ring. However, the concentration of the intermediate **72'''** can not be measured by either NMR or UV-Vis spectroscopy, thus, it is not possible to measure k_1 and k_2 separately. The kinetics that can be determined thus use one or the other of the following two equations.

$$72' \longrightarrow 72 \qquad (1)$$

$$72' \longrightarrow 72''' + 72 \qquad (2)$$

In the first, a distinct signal for fully closed **72** is needed. This is not easily achieved, due to the partial overlap of the NMR signals of **72** and **72'''**.

In this thesis, the kinetic studies of thermal return reactions were followed using UV-Vis spectroscopy. In this specific study, the chromophores of **72** and **72'''** are both benzene and benzopyrene, and thus their UV-Vis absorption spectra should be very similar. In fact, in the studies we have done on both the photo opening and closing processes, the intermediate species **72'''** was present and the major absorption peak shifted only from 409 nm to 407 nm in cyclohexane or the other way around.

The thermal return reaction was carried out in toluene, and it was found the major absorption peak which was used for kinetic study shifted from 409 nm to 413 nm. As for the UV closing, we assumed that the absorption band measured was the overlap of absorption of **72** and **72'''**. Thus, the kinetic study performed in this thesis is derived from the second equation.

From the photochromic and thermochromic studies we have made, the conclusion can be drawn that the two benzopyrene ends in **72** act independently. In fact, the absorption coefficient (ε) of **72** is about double the value of benzopyrene **21**. Thus, the kinetics of **72** that we measured in the second way should be very similar to **21**. Our experimental results prove this point. The activation energy and enthalpy were very close to those determined for benzopyrene **21'** to **21**. The thermal return half lives for **72'** and **21'** were 5.66 h and 5.75 h respectively.

3.3.5 The Phenyl Tris-CPD System 120'

Sequential ^{1}H NMR spectra were taken in d_8-toluene to study the thermal return process. Sample was prepared the same as in the photochromic study and the reaction was performed in 65°C. The dark red solution was irradiated with visible light to form the open isomer **120'** such that there was no ^{1}H NMR signal in the internal methyl DHP region (δ -1 to -2). The bleached sample was then put in a water bath at 65°C and the appearance of internal methyl signals in this region were observed. As we discussed in the synthesis chapter, there are four isomers of the closed form **120**. Unlike the symmetric parent **72**, all the DHP internal methyls in **120** are different due to the substituent. There could thus be up to 16 signals around the δ -1 region. Fortunately,

not every methyl proton is different enough to generate a distinct signal, as we only observe 4 broad peaks. We assign the two peaks at δ -1.030 and -1.228 to the phenyl substituted DHP ring, and the two at δ -1.161 and -1.354 to the unsubstituted DHP ring.

Figure 21. Sequential NMR spectra of thermally closing 120' to 120.

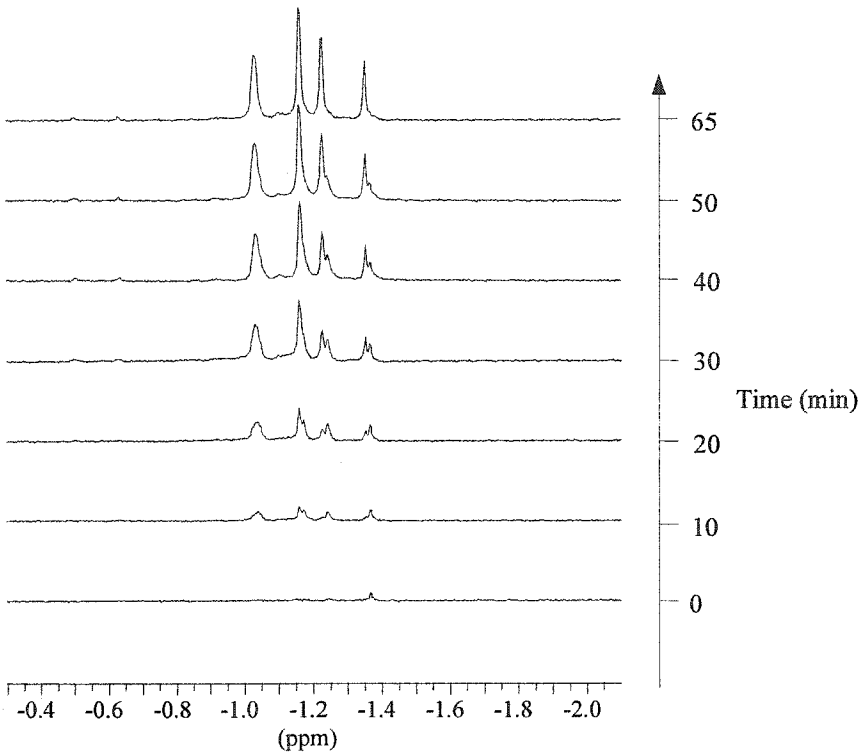

The sample was placed in the water bath, and after 10 min the NMR spectrum was measured. The signals that belonged to the closed isomer **120** were already present. There were also additional peaks: δ -1.024, -1.041 beside the signal at δ -1.030, and peaks at δ -1.175, -1.244 and -1.367 beside the signals at δ -1.161, -1.228 and -1.354 respectively. With prolonged irradiation, all peaks grow, and the ratio of the signals belonging to the closed form **120** become relatively greater. After about 65 min, the other peaks disappeared and only those peaks that belonged to isomer **120** remain.

The NMR study thus clearly shows that intermediates are formed during the thermal return process. By comparison with the photochromic studies, we believe that these intermediates are the two species **120'"** and **120""**.

Kinetic studies of **120'** were carried out as for the parent compound **72'** in toluene using a UV-Vis spectrometer. As for **72'→72**, the kinetics of **120'→120** that we measure here are for the overall reaction **120' → 120"' +120"" +120.** The NMR study implies that the two DHP rings close stepwise independently, and thus we convert the thermal closing of **120'→120** as the combined results of closing structures of **122'→122** and **124'→124.**

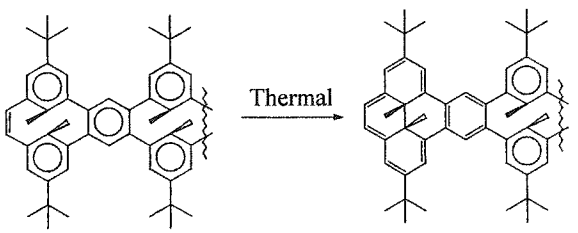

122' **122**

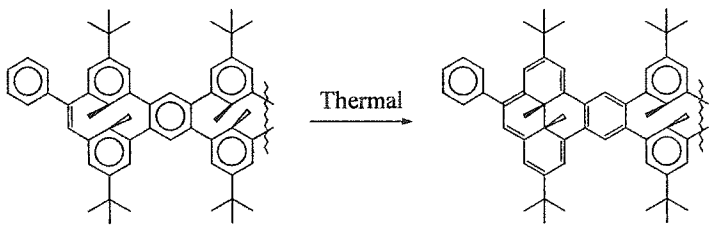

124' **124**

Since in **105**, the phenyl substitution does not alter the thermal return reaction much, we assume the closing reaction rates of **122'** and **124'** are the same. Thus, the thermal reaction **120' → 120** is finally converted to the reaction **122' → 122.**

Our experimental results for the thermal return reaction half life $\tau_{1/2}$ at 46°C of **120'** is 5.86 h, and 5.66 h for the parent **72'**. Activation energies and enthalpies are almost identical.

3.4 Electrochemical Readout of the Photoisomers of 72

We recently have shown[50] that electrochemical readout of the state of the benzo switch **21/21'** is possible. The closed form **21** is essentially an 18π planar system, while the open form **21'** contains only isolated 6π systems. Electrochemically, 6π benzenoid systems are rather inert, while an 18π system should be easy to oxidize. Indeed, **21** in dry degassed CH_2Cl_2 containing $TBAPF_6$ does show oxidation at $E_{p,a}$ = 0.75 V (peak anodic current, relative to Ag° reference electrode). When the electrochemical cell was irradiated, **21'** formed and then across the same potential window (0 to 1 V), the open state was redox silent.

Similarly, the open isomer **72'** has essentially isolated benzene rings, whereas, the closed form **72,** consists of two benzopyrenes connected via a benzenoid cyclophane spacer. The large π system of **72** should be considerably easier to oxidize electrochemically than the isolated 6π systems of **72'**.

A solution of tris-pyrene **72** in dry degassed CH_2Cl_2 (0.1 mol L^{-1}) containing $TBAPF_6$ was placed in a quartz cell using Pt button electrodes and Ag^0 reference electrode, using a scan rate of 100 mV/sec over a potential window from 0 to 1.00 V (ferrocene $E_{p,a}$ = 0.55 V). Two peak anodic current were found centered at 0.45 V and 0.69 V. The cell was then irradiated with a 500 W household tungsten lamp affixed with a 400 nm cut-off filter for a few seconds, which opened **72** to **72'**, and then across the

same potential window, the opened form was relatively redox silent. The voltammogram is shown in Figure 22.

Figure 22. Voltammogram of tris-pyrene 72 (red line) and photoisomer 72' (blue line)

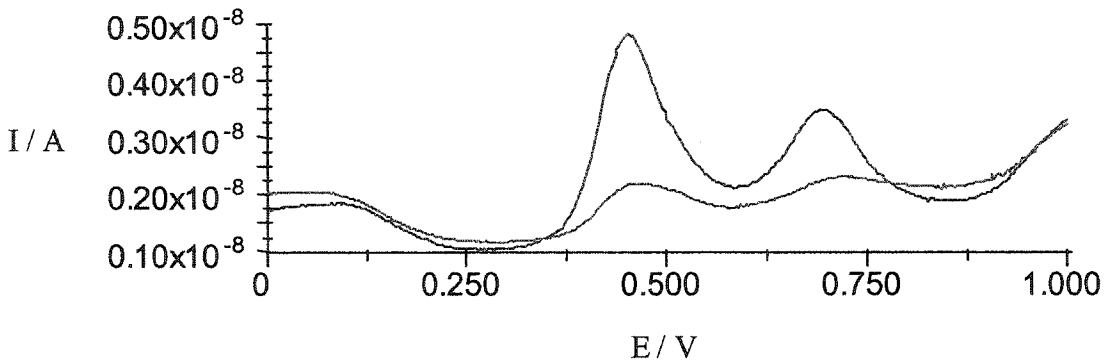

The voltammogram clearly demonstrates that **72** is electrochemically very different from **72'**. It would appear that there are two oxidation peaks for **72**, one of which is at a similar potential to that of **21**, and one which is at a lower potential. Further work is required to determine exactly why this is.

Chapter Four Conclusions

Two useful intermediates, the furan **77** and **79** were synthesized from the bis-furan adduct **74**. These two furans ultimately led to the successful syntheses of tris-pyrene system **72**, the furanocyclophanedhp **82**, and the phenyl substituted tris-pyrene **120**. These are the most highly condensed DHP containing systems so far known.

A number of new benzopyrene systems have also been synthesized for comparison to the above condensed systems. The acetyl and nitro benzopyrene **84** and **86** were obtained by direct substitution. The phenyl derivative **105** and the phenylethynyl benzopyrene **103** were obtained by Suzuki and Sonogashiracouplings.

The naphtho fused tetracene analogue, **116** was obtained from isofuran **47** and adduct **70**.

The photochromism of all these systems was studied. The multistate systems appear to open each DHP end separately rather than synchronously. Photo opening and closing rates were obtained relative to the benzopyrene **21**. We have found that the substituents, phenyl, phenylethynyl, acetyl increase the relative photo opening rate by 4, 5 and 21 times, respectively. This is important for generation of faster switches.

The phenyl substituted DHP end of **120** was also found to open faster than the unsubstituted end. UV closing rates are not much affected in these systems.

Thermal closing rates were also studied. Although activation energies do not change dramatically from that of **21** (unlike non-benzo[e]pyrene system), reaction rates do change with substitution. A nitro group slows the thermal return rate the most, with an acetyl group close behind. Since the acetyl group speeds the photo opening the most,

the combination of increased photo opening rate and decreased thermal closing rate makes the acetyl derivative **84** now the best switch so far. This may be very important if the switch is to be incorporated into a functional unit, eg, a conducting circuit.

In multistate switches, we have shown that the ends can act independently, even with the relative poor differentiation, such as phenyl group. If an acetyl group shows the same properties to a multiswitch that it does to the benzopyrene system **21**, then a true three way switch operating in the visible region may be possible.

Chapter Five Experimental Section

5.1 General Experimental Conditions and Instrumentation

Melting points were determined on a Reichert 7905 melting point apparatus intergrated to an Omega Engineering Model 199 Chromel-alumel thermocouple. Infrared spectra were recorded on a Bruker IFS25 FT-IR spectrometer as KBr discs, calibrated with polystyrene and only the major peaks are reported. UV-Vis spectra were recorded on a Cary 5 UV-VIS-NIR spectrometer in the stated solvents. Proton NMR spectra were recorded at 360 MHz on a Bruker AMX 360 spectrometer, or at 300 MHz on a Bruker AC 300 spectrometer in $CDCl_3$ using the solvent residual peak (7.240 ppm for $CHCl_3$) for calibration. Carbon NMR spectra were recorded on a Bruker AMX 360 (90.6 MHz), using the solvent peak at 77.0 ppm for calibration. Where peaks within the same sample are very close in chemical shift, a third decimal place is given. Mass spectra were recorded on a Finnigan 3300 gas chromatography-mass spectroscopy system using methane as a carrier gas for chemical ionization or electron impact (EI) at 70 eV. FAB or LSI mass spectra and exact mass measurements were done on a Kratos Concept-H instrument using perfluorokerosene as the standard. Elemental analyses were performed by Canadian Microanalytical services Ltd., Vancouver, B.C. All evaporations were carried out under reduced pressure on a rotary evaporator, and all organic extracts were washed with water and dried over anhydrous $MgSO_4$ or K_2CO_3 as appropriate. Silica gel (SiGel) refers to Merck silica gel, 60-200 mesh. Alumina refers to Aldrich aluminum oxide, activated, neutral, Brockmann I, standard grade, ~150 mesh. All alumina and deactivated silica gel were deactivated with 4% (by weight) aqueous

ammonia solution (28-30% by weight). Where NMR assignments are made, these were on the basis of 2D COSY/NOESY experiments for 1H and HETCORR/HMQCB experiments for ^{13}C.

5.2 Syntheses

9,18-Epoxy-2,7,11,16-tetra-*t*-butyl-*trans*-17b,17c,18c,18d-tetramethyl-17b,17c,18c,18d-tetrahydrotetrabenzo[de,uv,jk,op]pentacene (68)

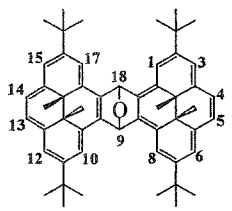

68

The isofuran **47**[31] (80.0 mg, 0.208 mmol) and the bromide **69**[31] (132.0 mg, 0.312 mmol) were added to an oven dried two neck round bottom flask. Dry THF (20 mL) was added via syringe and then $NaNH_2$ (400 mg, 10 mmol) and KO^tBu (~ 5 mg). The mixture was then stirred over night under argon. The solvent was evaporated and the residue was dissolved in benzene (40 mL) and was filtered through alumina with a thin layer of celite on top, using benzene as eluant. The green filtrate was collected and evaporated. The residue was carefully washed with hexanes (about 1 mL each time) until hexane was almost colorless. The solid was then air dried to give 118 mg (78%) of the adduct **68** as a mixture of two isomers in an approximate 1:1 ratio, (in later cases, when more than one isomers were obtained, no preference was observed with any particular isomer, unless otherwise stated). After the next step, the deoxygenation, some of these isomers were returned, but now in unequal amounts (approximate 2:1 ratio of isomer I and II below),

the NMR spectra of this sample enabled us to identify the signals from both isomers, mp (dec) 207-213 °C; ^{1}H NMR, Isomer I, (360 MHz) δ 8.77 (d, J = 1.2 Hz, 2H, H-1,8 or 10,17), 8.61 (d, J = 1.3 Hz, 2H, H-1,8 or 10,17), 8.28 (unresolved doublets, 2H, H-3,6, or 12,15), 8.22 (d, J = 0.9 Hz, 2H, H-3,6, or 12,15), 8.186 & 8.166 (AB, J = 8.3 Hz, 4H, H-4,5,13,14), 7.92 (s, 2H, H-9,18), 1.73 (s, 18H, $C(CH_3)_3$), 1.66 (s, 18H, $C(CH_3)_3$), -3.40 (s, 6H, CH_3), -4.37 (s, 6H, CH_3). Isomer II, δ 8.80 (d, J = 1.3 Hz, 2H, H-1,8 or 10,17), 8.66 (d, J = 1.2 Hz, 2H, H-1,8 or 10,17), 8.26-8.25 (overlapping unresolved doublets, 4H, H-3,6,12,15), 8.18 (s, 4H, H-4,5,13,14), 7.98 (d, J = 0.63 Hz, 1H, H-9 or 18),), 7.92 (d, J = 0.64 Hz, 1H, H-9 or 18), 1.71 (s, 18H, $C(CH_3)_3$), 1.70 (s, 18H, $C(CH_3)_3$), -3.44 (s, 6H, CH_3), -4.38 (s, 6H, CH_3). ^{13}C NMR (90.6 MHz) (isomer assigned referred only to peak labeled) δ 145.44, 145.36, 145.20, 137.39, 137.35, 137.09, 137.00, 136.93, 136.86, 136.78, 127.20, 127.09, 126.74, 126.54, 124.17 (I), 124.09 (II), 124.02 (I), 121.24 (I), 121.05 (I), 120.93 (II), 116.19 (II), 115.74 (I), 115.39 (I), 115.23 (II), 81.53 (II), 81.09 (I), 80.82 (II), 35.90, 35.81, 32.76, (I), 32.55 (II), 31.79, 31.72, 30.60 (I), 30.38 (II), 30.32 (II), 16.00 (II), 15.91 (I), 14.13 (I), 13.97 (II); IR (KBr) 1616, 1456, 1360, 1346, 1262, 1212, 1045, 886, 869, 649 cm^{-1}; LSIMS *m/z* 727.5 (MH+) ; Anal. Calc'd for $C_{54}H_{62}O$: C, 89.66; H, 7.34. Found: C, 89.96; H, 7.19.

Tris-pyrene (72)

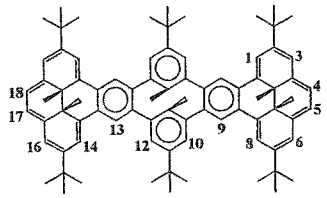

72

TrisDHP precursor **75** (crude 21 mg, 0.019 mmol) and $Fe_2(CO)_9$ (10 mg, 0.027 mmol) were refluxed in benzene under argon for 1 hr and the mixture was slowly cooled to room temperature. The solvent was evaporated and the residual was chromatographed on deactivated SiGel using hexanes/benzene (6:1) as eluant and gave 9 mg (44%) of the product **72** as a mixture of three isomers. Further purification of **72** was carried out by recrystalization from toluene, mp (dec) 176-181°C. These peaks of the NMR spectrum then appeared in two groups in unequal amount due to the different solubilities of the various isomers.

^{1}H NMR (360 MHz), group I: δ 9.00 (s, 4H total, H-9,13,22,26), 8.37 (br. s, 4H, H-1,8,14,21), 7.40 (d, J = 0.9 Hz, 4H, H-3,6,16,19), 7.17 (s, 8H, H-4,5,17,18,10,12,23,25), 1.53 (s, 36H, $C(CH_3)_3$ from DHPs), 1.365, 1.360 (s, 36H total, $C(CH_3)_3$ from cyclophane), 1.28 (br. s, 6H, CH_3 from cyclophane), -1.37 (br. s, 12H, CH_3 from DHPs).

^{1}H NMR (360 MHz), group II: δ 9.142 & 9.136 (s, 4H, H-9,13,22,26), 8.55 (br. s, 4H, H-1,8,14,21), 7.52 (br. s, 4H, H-3,6,16,19), 7.31 (s, 4H, H-4,5,17,18), 7.17 (s, 4H, H-10,12,23,25), 1.56 (s, 36H, $C(CH_3)_3$ from DHPs), 1.365, 1.360 (s, 36H total, $C(CH_3)_3$ from cyclophane), 1.28 (br. s, 6H, CH_3 from cyclophane), -1.63 (br. s, 12H, CH_3 from DHPs).

^{13}C NMR (90.6 MHz) δ 150.28, 144.74, 144.50, 141.93, 141.49, 140.10, 139.95, 138.63, 138.48, 137.93, 134.92, 134.48, 129.46, 129.25, 129.07, 124.38, 123.42, 121.25, 120.99, 119.87, 117.35, 116.77, 35.62, 35.56, 35.49, 34.99, 34.37, 31.53, 30.91, 30.76, 30.46, 29.71, 18.84, 17.96, 17.46; UV (chloroform) λ_{max} (ε_{max}) nm 287 (53,400), 310 (47,700), 394 (43,600), 413 (74,200), 513 (9,600), 628 (1,100); EI MS *m/z*, 1078 (MH_2+); HRMS. Calc'd for $C_{82}H_{92}$ (MH+): 1077.7277. Found: 1077.7256. Anal. Calc'd for $C_{82}H_{92}$: C, 91.39; H, 8.61. Found: C, 90.32; H, 8.79.

Tris-pyrene precursor (75)

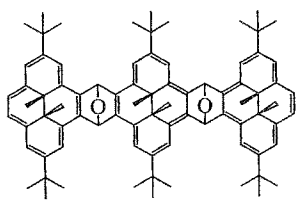

75

$NaNH_2$ (400 mg, 10 mmol) and KO^{t}Bu (2 mg) were added to a solution of the furanodihydropyreneadduct **79** (20 mg, 0.026 mmol) and the bromide **69** (18 mg, 0.043 mmol) in dry THF (15 mL) under N_2, and the mixture was stirred for 5 hr and filtered through a short alumina column (2 cm). Usually, the solvent was evaporated and the residual was used directly for the next reaction step. Since the product **75** had poor solubility and was not very stable in solution, purification tried at this step was not very successful. Benzene and hexanes/CH_2Cl_2 (1:1) were used, but not polar enough to elute **75** effectively. With increasing polarity of the eluant, much brownish material eluted with **75**. The crude product which contained 6 isomers was used for ^1H NMR (300 MHz), The chemical shift regions were as follows: δ 8.86-8.44, 8.08-7.87 (ring protons), 1.87-1.76

(*t*-Bu on the middle ring), 1.64-1.55 (*t*-Bu on the side rings), -3.36, -3.37, -3.39, -3.50, -4.54, -4.57, -4.58, -4.62, -5.25, -5.28, -5.30 (internal methyls).

Isofuran-furan adduct (77)

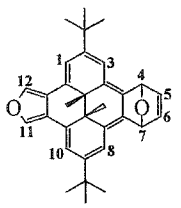

77

Tetrazine[73] **71** (51.3 mg, 0.217 mmol) was added to a cooled (0°C) solution of the bis adduct[52] **77** (103.4 mg, 0.217 mmol) in dry THF (50 mL) under N_2 and was stirred for 3 hr. The solvent was evaporated and the residual was chromatographed on alumina using hexanes/benzene (1:1) as eluant and gave 28.3 mg (29%) of the product **77** as a red-orange solid, mp (dec) 182-183°C; ^{1}H NMR (360 MHz) δ 8.017 & 8.012 (d each, J = 1.7 Hz, 2H, H-11,12), 6.836 & 6.830 (d each, J = 1.4 Hz, 2H, H-1,10), 6.675 & 6.570 (dd each, J = 5.6, 1.8 Hz, 2H, H-5,6), 6.409 & 6.381 (d each, J = 1.4 Hz, 2H, H-3,8), 5.737 & 5.701 (dd each, J = 1.8, 1.4 Hz, 2H, H-4,7), 1.241 (s, 9H, $C(CH_3)_3$), 1.239 (s, 9H, $C(CH_3)_3$), 0.373 (s, 3H, CH_3), 0.137 (2, 3H, CH_3); ^{13}C NMR (90.6 MHz) δ 144.56, 144.28, 137.01 & 136.99 (C-11,12), 136.69 & 135.45 (C-5,6), 132.12, 131.67, 131.10, 131.04, 128.75, 128.60, 120.72, 120.61, 116.79 & 116.74 (C-1,10), 113.76 & 113.71 (C-3,8), 78.83 & 78.81 (C-4,7), 42.37, 41.64, 34.67, 34.65, 29.56 ($C(\underline{C}H_3)_3$), 22.04, 19.76; IR (KBr) 1617, 1366, 1251, 1163, 1050, 1030, 874, 854, 822, 771, 643 cm^{-1}; CI MS *m/z*, 451 (MH+); HRMS. Calc'd for $C_{32}H_{34}O_2$: 450.2559. Found: 450.2559.

Isofuran adduct (78)

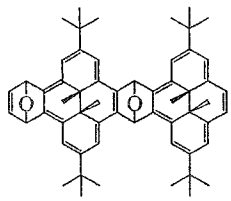

78

$NaNH_2$ (400 mg, 10 mmol) and KO^tBu (2 mg) were added to a solution of the isofuran-furan adduct **77** (45.9 mg, 0.102 mmol) and the bromide **69** (56.1 mg, 0.133 mmol) in dry THF (40 mL) under N_2, and the mixture was stirred for 5 hr. The solvent was evaporated and the residual was filtered through alumina and hexanes/benzene (1:1) as eluant and gave 58 mg (72%) of the product **78** as a green solid as a mixture of four isomers, LSIMS *m/z* 793.6 (MH+); HRMS. Calc'd for $C_{58}H_{64}O_2$ (MH+): 793.4985. Found: 793.4987. These four isomers on further chromatography over aluminum oxide using hexanes/benzene (1:1) as eluant, were separated into two portions which were oxygen bridge *syn-* and *anti-* isomers, each containing two methyl isomers.

anti-Isomers (ud), mp (dec) 183-188°C; ^{1}H NMR (360 MHz) isomer I: δ 8.85 (d, J = 1.3 Hz, 1H), 8.67 (d, J = 1.3 Hz, 1H), 8.66 (d, J = 1.2 Hz, 1H), 8.57 (d, J = 1.3 Hz, 1H), 8.22 (m, 2H), 8.161-8.152 (m, 2H), 8.084 (s, 2H), 7.97 (d, J = 0.72 Hz, 1H), 7.88 (d, J = 0.70 Hz, 1H), 7.23-7.20 (m, 1H), 7.09 (dd, J = 5.54, 1.74 Hz, 1H), 6.57-6.52 (m, 2H), 1.75, 1.72, 1.71, 1.69, 1.68, 1.67, 1.63 (s(I +II), 72H, $C(CH_3)_3$), -3.28, -3.77, -4.23, -4.41 (s, 3H each, CH_3). Isomer II: δ 8.79 (d, J = 1.2 Hz, 1H), 8.70 (d, J = 1.2 Hz, 1H), 8.65 (d, J = 1.2 Hz, 1H), 8.53 (d, J = 1.4 Hz, 1H), 8.25 (d, J = 1.0 Hz, 1H), 8.20 (d, J = 1.3 Hz, 1H), 8.17 (d, J = 1.2 Hz, 1H), 8.13 (d, J = 1.2 Hz, 1H), 8.080 (2H), 7.93 (d, J = 0.70 Hz, 1H), 7.90 (d, J = 0.72 Hz, 1H), 7.23-7.20 (m, 1H), 7.10 (dd, J = 5.47, 1.80 Hz, 1H), 6.57-6.52 (m, 2H), 1.75, 1.72, 1.71, 1.69, 1.68, 1.67, 1.63 (s (I +II), 72H, $C(CH_3)_3$),

-3.25, -3.77, -4.24, -4.43 (s, 3H each, CH_3). ^{13}C NMR (90.6 MHz) δ 145.50, 145.41, 145.21, 144.98, 141.04, 140.95, 140.68, 140.41, 140.27, 137.92, 137.76, 137.35, 137.23, 137.08, 136.98, 136.91, 136.67, 128.56, 128.24, 128.10, 127.88, 127.59, 127.46, 127.20, 126.88, 124.29, 124.26, 121.34, 121.20, 121.08, 117.63, 117.31, 116.53, 116.40, 115.72, 115.30, 115.15, 115.02, 114.83 (aromatic & alkene carbons), 81.90, 81.70, 81.62, 81.52, 81.38, 81.19 (carbons attached to oxygen bridge), 35.98, 35.89, 35.83, 35.77, 33.06, 32.91, 32.81, 32.71, 32.28, 32.15, 31.25, 31.07, 30.32 (aliphatic carbons), 31.94, 31.91, 31.65, 31.62 ($C(CH_3)_3$), 16.39, 16.29, 15.07, 15.00, 14.44, 14.28, 14.14 (CH_3).

syn-Isomers (uu), mp (dec) 179-182°C; IR (KBr): 1614, 1463, 1392, 1362, 1346, 1260, 1035, 871, 646 cm^{-1}; ^{1}H NMR (360 MHz) isomer III: δ 8.84 (d, J = 1.2 Hz, 1H), 8.687-8.684 (m, 1H), 8.66-8.65 (m, 1H), 8.55 (d, J = 1.3 Hz, 1H), 8.16 (d, J = 1.1 Hz, 1H), 8.14 (d, J = 1.3 Hz, 1H), 8.13 (d, J = 1.3 Hz, 1H), 8.11 (d, J = 1.2 Hz, 1H), 8.068 (s, 2H), 7.97 (d, J = 0.6 Hz, 1H), 7.89 (d, J = 0.54 Hz, 1H), 7.07 (dd, J = 5.5, 1.9 Hz, 1H), 6.93 (dd, J = 5.5, 1.8 Hz, 1H), 6.58 (dd, J = 1.8, 0.7 Hz, 1H), 6.56 (dd, J = 1.8, 0.8 Hz, 1H), 1.76, 1.722, 1.719, 1.685, 1.677, 1.65, 1.61 (s (III +IV), 72H, $C(CH_3)_3$), -3.29, -3.47, -4.32, -4.70 (s, 3H each, CH_3). Isomer IV: δ 8.82 (d, J = 1.1 Hz, 1H), 8.687-8.684 (m, 1H), 8.66-8.65 (m, 1H), 8.51 (d, J = 1.2 Hz, 1H), 8.27 (d, J = 1.1 Hz, 1H), 8.21 (d, J = 1.2 Hz, 2H), 8.20 (d, J = 1.1 Hz, 1H), 8.063 (s, 2H), 7.93 (d, J = 0.5 Hz, 1H), 7.90 (d, J = 0.6 Hz, 1H), 7.09 (dd, J = 5.5, 1.8 Hz, 1H), 6.94 (dd, J = 5.5, 1.8 Hz, 1H), 6.53 (dd, J = 1.9, 0.8 Hz, 1H), 1.76, 1.722, 1.719, 1.685, 1.677, 1.65, 1.61 (s (III +IV), 72H, $C(CH_3)_3$), -3.26, -3.48, -4.31, -4.73 (s, 3H each, CH_3).

^{13}C NMR (90.6 MHz) δ 145.47, 145.44, 145.39, 145.32, 145.23, 145.00, 144.82, 141.05, 140.92, 140.84, 140.74, 140.52, 140.45, 140.27, 137.72, 137.62, 137.59, 137.46,

137.13, 137.08, 136.95, 136.88, 136.79, 128.75, 128.16, 127.99, 127.87, 127.83, 127.71, 127.63, 127.43, 127.21, 127.07, 126.76, 124.25, 124.21, 121.32, 121.28, 121.16, 121.07, 117.66, 117.31, 116.57, 116.46, 115.77, 115.32, 115.08, 114.82, 114.77, 114.65 (aromatic & alkene carbons), 81.92, 81.69, 81.62, 81.50, 81.39, 81.24 (carbons attached to oxygen bridge), 35.98, 35.91, 35.82, 35.79, 35.74, 34.66, 33.84, 33.77, 33.03, 32.89, 31.41, 31.26, 31.21, 31.01 (aliphatic carbons), 31.96, 31.91, 31.65, 31.60 ($C(CH_3)_3$), 16.58, 16.45, 16.40, 16.28, 14.22, 14.11, 12.86 (CH_3).

Furanodihydropyreneadduct (79)

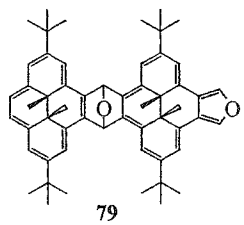

79

Tetrazine[73] **71** (18.3 mg, 0.078 mmol) was added to a solution of the isofuran adduct **78** (56 mg, 0.071 mmol) in dry THF (20 mL) under N_2 and was stirred for 1 hr. The solvent was evaporated and the residual was filtered through alumina using hexanes/benzene (1:1) as eluant and gave 51 mg (93%) of the product **79** as a reddish-brown solid as a mixture of unequal amounts of two isomers, mp (dec) 190°C; ^1H NMR (300 MHz), Isomer I, δ 8.54 (s, 1H), 8.43 (s, 1H), 8.40 (s, 1H), 8.36 (s, 1H), 8.324 (s, 1H), 8.316 (s, 1H), 7.98 (s, 1H), 7.97 (s, 1H), 7.07 (s, 1H), 7.05 (s, 1H), 7.00 (d, J = 1.6Hz, 1H), 6.84 (d, J = 1.6Hz, 1H), 6.81 (d, J = 1.6Hz, 1H), 6.76 (d, J = 1.6Hz, 1H), 1.694, 1.66, 1.35, 1.28 (s, 9H each, $C(CH_3)_3$), 0.45, -0.54, -3.68, -4.02 (s, 3H each, CH_3).), Isomer II, δ 8.58 (s, 1H), 8.48 (s, 1H), 8.40 (2H), 8.33 (2H), 7.96-7.99 (2H), 7.09 (s,

1H), 7.06 (s, 1H), 6.95 (1H), 6.88 (1H), 6.83(d, 1H), 6.81 (1H), 1.685, 1.33, 1.31 (s, 9H each, $C(CH_3)_3$), 0.45, -0.52, -3.72, -4.04 (s, 3H each, CH_3). LSIMS *m/z* 767.5 (MH+); HRMS. Calc'd for $C_{56}H_{62}O_2$ (M+): 766.4750. Found: 766.4737.

Dihydropyrenofuranobenzocyclophanes (82)

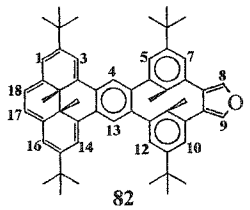

82

The unequal amount of a mixture of isomers of furan **79** (31 mg, 0.040 mmol) and $Fe_2(CO)_9$ (17.6 mg, 0.048 mmol) were refluxed in benzene (20 mL) for 1 hr. The solvent was evaporated and the residual was chromatographed on alumina using hexanes/benzene (6:1) as eluant and gave 24.3 mg (80%) of cyclophane **82** as a mixture of unequal amount of two isomers, red crystals, mp (dec) 172°C. ^{1}H NMR (360 MHz), isomer I: δ 9.10 (s, 2H, H-4,13), 8.51 (d, J = 1.2 Hz, 2H, H-3,14), 7.79 (s, 2H, H-8,9), 7.50 (d, J = 1.1 Hz, 2H, H-1,16), 7.30 (s, 2H, H-17,18), 7.12 (d, J = 2.2 Hz, 2H, H-5,12), 7.06 (d, J = 2.2 Hz, 2H, H-7,10), 1.53 (s, 18H, $C(CH_3)_3$ from DHP), 1.32 (s, 18H, $C(CH_3)_3$ from cyclophane), 1.03 (s, 6H, CH_3 on cyclophane), -1.66 (s, 6H, CH_3 on DHP). ^{13}C NMR (90.6 MHz) δ137.97 (C-8,9), 129.20 (C-5,12), 127.67 (C-7,10), 123.62 (C-4,13), 121.23 (C-17,18), 119.86 (C-1,16), 116.74 (C-3,14), 35.52, 34.88, 34.20, 31.44 ($C(\underline{C}H_3)_3$ from DHP), 30.84 ($C(\underline{C}H_3)_3$ from cyclophane), 18.21 (CH_3 on cyclophane), 17.36 (CH_3 on DHP), + see below.

^{1}H NMR (360 MHz), isomer II: δ 8.95 (s, 2H, H-4,13), 8.31 (d, J = 1.2 Hz, 2H, H-3,14), 7.78 (s, 2H, H-8,9), 7.37 (d, J = 1.1 Hz, 2H, H-1,16), 7.15 (s, 2H, H-17,18), 7.12 (d, J =

2.2 Hz, 2H, H-5,12), 7.05 (d, J = 2.2 Hz, 2H, H-7,10), 1.49 (s, 18H, $C(CH_3)_3$ from DHP), 1.31 (s, 18H, $C(CH_3)_3$ from cyclophane), 1.03 (s, 6H, CH_3 on cyclophane), -1.37 (s, 6H, CH_3 on DHP). ^{13}C NMR (90.6 MHz) δ137.97 (C-8,9), 128.99 (C-5,12), 127.67 (C-7,10), 124.68 (C-4,13), 120.96 (C-17,18), 119.86 (C-1,16), 117.40 (C-3,14), 35.59, 35.44, 34.30, 30.67 ($C(\underline{C}H_3)_3$ from DHP), 30.29 ($C(\underline{C}H_3)_3$ from cyclophane), 18.21 (CH_3 on cyclophane), 17.96 (CH_3 on DHP), + see below. The following18 quaternary ^{13}C NMR peaks could not be assigned to a particular isomer: 150.09, 144.72, 144.43, 141.12, 140.65, 140.48, 140.36, 138.56, 138.42, 137.63, 137.49, 135.73, 134.83, 134.33, 131.73, 130.07, 129.38, 128.97; UV (cyclohexane) λ_{max} (ε_{max}) nm 280 (25,700), 303 (21,300), 354 (17,200), 385 (24,200), 405 (35,100), 455 (4,000), 481 (4,000), 509 (4,200), 627 (500); IR (KBr) 1593, 1465, 1361, 1264, 1225, 1043, 872, 790, 748, 669 cm^{-1}; LSIMS *m/z,* 750.5 (M+); HRMS Calc'd for $C_{56}H_{62}O$ (MH+): 751.4879. Found: 751.4869.

4-Acetyl-2,7-di-*t*-butyl-*trans*-12c,12d-dimethyl-12c,12d-dihydrobenzo[e]pyrene (84)

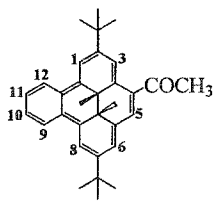

84

Ac_2O (1 mL) was added to a solution of the benzo[e]pyrene **21**[31] (25.0 mg, 0.0635 mmol) in CH_2Cl_2 (20 mL) under argon. After stirring for 10 min, ten drops of $BF_3{\cdot}Et_2O$ were added and the mixture was stirred for another 30 min. Saturated $NaHCO_3$ solution was then added to quench excess Ac_2O and $BF_3{\cdot}Et_2O$. The organic phase was then washed, dried and evaporated. The residual was chromatographed over SiGel, using hexanes/CH_2Cl_2 (1:1) to give 21 mg (77%) of the product **84** as purple crystals, mp 173-

174 °C; ^{1}H NMR (360 MHz) δ 9.76-8.72 (m, 2H, H-9,12), 8.65 (d, J = 1.2 Hz, 1H, H-3), 8.33 (d, J = 1.3 Hz, 1H, H-1), 8.27 (d, J = 1.3 Hz, 1H, H-8), 7.67-7.60 (m, 2H, H-10,11), 7.48 (d, J = 0.71 Hz, 1H, H-5), 7.377-7.375 (m, 1H, H-6), 2.73 (s, 3H, $COCH_3$), 1.51 (s, 9H, $C(CH_3)_3$), 1.49 (s, 9H, $C(CH_3)_3$), -1.48 (s, 3H, CH_3), -1.55 (s, 3H, CH_3); ^{13}C NMR (90.6 MHz) δ 201.16, 151.32, 145.27, 141.95, 137.97, 137.01, 134.63, 129.61, 129.11, 127.99, 126.59, 126.12, 124.79, 124.39, 120.56, 120.21, 117.81, 117.59, 116.95, 36.92, 36.25, 35.38, 34.74, 30.78, 30.54, 18.03, 17.40; UV (cyclohexane) λ_{max} (ε_{max}) nm 228 (23,600), 256 (13,200), 311 (16,200), 328 (17,900), 342 (20,200), 385 (24,000), 518 (5,000), 636 (1,000); IR (KBr) 1670, 1475, 1360, 1252, 1222, 1203, 878, 753, 641 cm^{-1}; CI MS *m/z*, 437(MH+); HRMS. Calc'd for $C_{32}H_{36}O$: 436.2766. Found: 436.2768. Anal. Calc'd for $C_{32}H_{36}O$: C, 88.02; H, 8.31. Found: C, 87.66; H, 8.60.

2,7-Di-*t*-butyl-4-nitro-*trans*-12c,12d-dimethyl-12c,12d-dihydrobenzo[e]pyrene (86), and 2,7-Di-*t*-butyl-4,5-di-nitro -*trans*-12c,12d-dimethyl-12c,12d-dihydrobenzo-[e]pyrene (87)

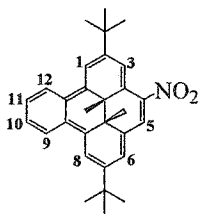

86

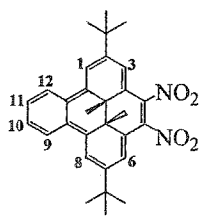

87

A solution of the benzopyrene **21** (50 mg, 0.127 mmol) in CH_2Cl_2 (4 mL) was added to a previously stirred mixture of Ac_2O (0.5 mL) and $Cu(NO_3)_2{\cdot}2.5H_2O$ (44.2 mg, 0.190 mmol) under argon. The mixture was stirred at room temperature and was monitored by TLC until the starting material had disappeared in about 20 min. The

reaction mixture was washed with saturated $NaHCO_3$ solution and then H_2O and dried and evaporated. The residual was chromatographed over SiGel using first hexanes/CH_2Cl_2 (2:1) to elute the mononitrobenzopyrene to give 16 mg (28%) of **86**, mp (sublimes) 161-162°C; second hexanes/CH_2Cl_2 (3:2) to elute the dinitrobenzopyrene to give 7 mg (11%) of **87**, mp (dec) 195°C;

Mononitro **86** : ^{1}H NMR (360 MHz) δ 8.73-8.69 (m, 2H, H-9,12), 8.63 (d, J = 1.3 Hz, 1H, H-3), 8.34 (d, J = 1.3 Hz, 1H, H-1), 8.25 (d, J = 1.3 Hz, 1H, H-8), 7.74 (d, J = 0.92 Hz, 1H, H-5), 7.64-7.71 (m, 2H, H-10,11), 7.380-7.386 (m, 1H, H-6), 1.53 (s, 9H, $C(CH_3)_3$), 1.47 (s, 9H, $C(CH_3)_3$), -1.28 (s, 3H, CH_3), -1.35 (s, 3H, CH_3); ^{13}C NMR (90.6 MHz) δ 155.13, 146.89, 139.46, 139.05, 137.82, 137.51, 134.97, 129.98, 128.82, 127.54, 126.69, 125.07, 124.49, 120.42, 118.47, 116.98, 115.58, 115.05, 38.81, 36.72, 35.48, 35.43, 30.44, 30.39, 18.18, 17.91; IR (KBr) 1490, 1310, 1287, 1259, 874, 753, 639 cm^{-1}; CI MS *m/z*, 440 (MH+); HRMS. Calc'd for $C_{30}H_{33}NO_2$: 439.2511. Found: 439.2508.

Dinitro **87** : ^{1}H NMR (360 MHz) δ 8.53-8.55 (m, 2H, H-9,12), 8.10 (d, J = 1.2 Hz, 2H, H-1,8), 7.98 (d, J = 1.3 Hz, 1H, H-3,6), 7.68-7.71 (m, 2H, H-10,11), 1.46 (s, 18H, $C(CH_3)_3$), -0.70 (s, 6H, CH_3); ^{13}C NMR (90.6 MHz) δ 156.23, 139.11, 136.02, 129.43, 128.46, 125.01, 118.34, 113.00, 39.80, 36.57, 30.37, 29.90, 19.14;
UV (cyclohexane) λ_{max} (ε_{max}) nm 221 (31,100), 234 (29,700), 251 (21,200), 401 (13,300), 417 (11,500), 503 (2,200), 619 (300); CI MS *m/z*, 485 (MH+); HRMS. Calc'd for $C_{30}H_{32}N_2O_4$: 484.2362 . Found: 484.2360.

4-Bromo-2,7-di-*t*-butyl-9-nitro-*trans*-10b,10c-dimethyl-10b,10c-dihydropyrene (96) &

4-Bromo-2,7-di-*t*-butyl-5-nitro-*trans*-10b,10c-dimethyl-10b,10c-dihydropyrene (97)

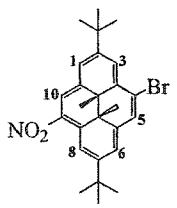

96

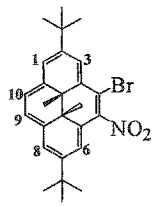

97

A solution of the bromide **69** (145 mg, 0.342 mmol) in CH_2Cl_2 (10 mL) was added to a homogenized mixture of Ac_2O (10 ml) and $Cu(NO_3)_2 2.5H_2O$ (120 mg, 0.516 mmol) under argon. The mixture was stirred under room temperature for 1 hr and washed with saturated $NaHCO_3$ solution and then H_2O and dried and evaporated. The residual was chromatographed over SiGel using hexanes/CH_2Cl_2 (1:1) as eluant. The first green band was collected to give 14 mg (9%) of the first product **97**, mp (sublimes) 151°C; The second brownish band was a mixture of the 2nd product **96** and the 4,10-*cis*-bromonitro-DHP **98**. The total brownish mixture weighed 105 mg. These two compounds could not be separated by chromatography, however, their solubilities are slightly different. By carefully washing a few times with small amount of pentane, the residual, **96** turned out to be pure enough for characterization, mp 224-226°C;

4-bromo-5-nitro-dihydropyrene **97**: ^{1}H NMR (360 MHz) δ 8.91 (d, J = 1.3 Hz, 1H, H-6), 8.57 (d, J = 1.2 Hz, 1H, H-8), 8.56 (d, J = 1.1 Hz, 1H, H-1), 8.529 (AB, J = 8.3 Hz, 1H, H-9 or 10), 8.517 (AB, 1H, H-9 or 10), 8.41 (d, J = 1.2 Hz, 1H, H-3), 1.69 (s, 9H, $C(CH_3)_3$), 1.63 (s, 9H, $C(CH_3)_3$), -3.68 (s, 3H, CH_3), -3.70 (s, 3H, CH_3); ^{13}C NMR (90.6 MHz) δ 150.82, 149.68, 143.07, 138.21, 137.92, 135.79, 131.78, 126.82, 125.93,

125.17, 123.83, 123.09, 122.59, 114.99, 36.53, 36.45, 32.34, 31.68, 31.60, 30.02, 14.49, 14.47; IR (KBr) 1540, 1358, 1347, 1263, 1234, 668 cm^{-1};

4-bromo-9-nitro-dihydropyrene **96**: ^1H NMR (360 MHz) δ 9.669-9.667 (m, 1H, H-10), 9.171-9.169 (m, 1H, H-8), 8.922-8.918 (m, 1H, H-1), 8.744-8.743 (m, 1H, H-3), 8.703-8.697 (m, 1H, H-6),), 8.539-8.546 (m, 1H, H-5), 1.68 (s, 18H, $C(CH_3)_3$), -3.65 (s, 3H, CH_3), -3.68 (s, 3H, CH_3); ^{13}C NMR (90.6 MHz) δ 154.25, 148.58, 140.02, 138.76, 134.67, 132.63, 130.45, 128.03, 125.84, 125.65, 121.90, 120.32, 119.12, 118.77, 36.98, 36.29, 32.03, 31.83, 31.72, 31.67, 15.37, 14.57; IR (KBr) 1592, 1527, 1304, 1243, 1143, 949, 857, 769, 673 cm^{-1}; CI MS *m/z*, 467 (MH+, ^{79}Br); HRMS. Calc'd for $C_{26}H_{30}BrNO_2$: 467.1460 (^{79}Br). Found: 467.1464.

4-Bromo-2,7-di-*t*-butyl-9-iodo-*trans*-10b,10c-dimethyl-10b,10c-dihydropyrene (100)

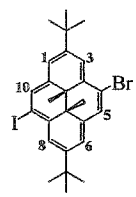

100

I_2 (150 mg, 0.591 mmol) was added to a solution of $Ag(collidine)_2PF_6$[78] (292 mg, 0.590 mmol) in CH_2Cl_2 (50 mL). The mixture was stirred for 5 min to dissolve as much I_2 as possible and then the bromide **69** (100 mg, 0.236 mmol) was added to the turbid mixture, which was then stirred under argon at room temperature overnight. Aqueous $NaHSO_3$ (~10%, 20 mL) was added and the reaction mixture was stirred vigorously for 5 min and hexanes (50 mL) was then added. The whole mixture was filtered through celite to a separatory funnel. More Aqueous $NaHSO_3$ (~10%) was used to wash the organic

phase and then followed by water. The organic phase was dried over $MgSO_4$ and solvent was evaporated. The green residual was chromatographed over SiGel using hexanes/CH_2Cl_2 (6:1) as eluent to give 118 mg crystalline solid, which contained 4-bromo-9-iodo-dihydropyrene **100** (67%), 4-bromo-10-iodo-dihydropyrene **104** (33%) by NMR spectral integration. The mixture was used directly in the next reaction. Some of the product was carefully washed with a small amount of pentane a few times. The solid which remained mainly 4-bromo-9-iodo-dihydropyrene **100** (over 92% by NMR), mp (sublimes) 162°C; ^{1}H NMR (360 MHz) δ 8.90 (s, 1H, H-5), 8.82 (d, J = 1.2 Hz, 1H, H-8), 8.65 (d, J = 1.2 Hz, 1H, H-3), 8.64 (s, 1H, H-10), 8.48 (br. s, 1H, H-1), 8.45 (br. s, 1H, H-6), 1.68 (s, 9H, $C(CH_3)_3$), 1.67 (s, 9H, $C(CH_3)_3$), -3.86 (s, 6H, CH_3); ^{13}C NMR (90.6 MHz) δ 148.89, 147.97, 138.04, 137.70, 136.00, 133.50, 132.30, 126.97, 126.72, 122.15, 121.65, 121.38, 116.72, 93.13, 36.32, 36.27, 32.42, 32.23, 31.86, 14.37, 14.18; IR (KBr) 1586, 1478, 1461, 1445, 1378, 1362, 1331, 1240, 1178, 1118, 1087, 949, 891, 769, 673 cm^{-1}; CI MS *m/z*, 549 (MH+, ^{79}Br); HRMS. Calc'd for $C_{26}H_{30}BrI$ (^{79}Br): 548.0576. Found: 548.0580.

4-Bromo-2,7-di-*t*-butyl-9-phenylethynyl-*trans*-10b,10c-dimethyl-10b,10c-dihydro-pyrene (101)

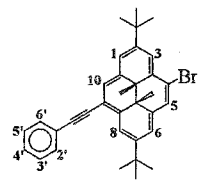

101

Phenylacetylene (61 mg, 0.598 mmol) was added to a solution of a mixture of the bromoiodopyrenes (**100** + **104**) (300 mg, 0.547 mmol) in THF (30 mL) and $HNEt_2$ (10

mL). Then catalyst $Pd(PPh_3)_2Cl_2$ (38 mg, 0.0542 mmol) and CuI (15 mg, 0.0789 mmol) were added. The reaction mixture was stirred overnight under argon in room temperature. The mixture was filtered through celite and the solvent was evaporated. The brownish residual was chromatographed over SiGel using firstly hexanes to elute starting materials, and secondly hexanes/CH_2Cl_2 (10:1) to elute the product, which was a mixture (241 mg, yield 84%) of bromophenylethynylpyrene (4,9- and 4,10-isomers). This mixture was used directly in the next step. A small portion of relatively pure 4-bromo-9-iodopyrene **100** (91%) was used to make pure 4-bromo-9-phenylethynylpyrene **101** for characterization, mp 158-161°C; ^{1}H NMR (360 MHz) δ 9.11 (d, J = 1.3 Hz, 1H, H-3), 8.79 (d, J = 1.2 Hz, 1H, H-1), 8.644 (s, 1H, H-5 or 10), 8.643 (s, 1H, H-5 or 10), 8.52 (d, J = 0.8 Hz, 1H, H-6), 8.48 (d, J = 0.9 Hz, 1H, H-8), 7.77-7.73 (m, 2H, H-2',6'), 7.47-7.38 (m, 3H, H-3',4' 5'), 1.71 (s, 9H, $C(CH_3)_3$), 1.69 (s, 9H, $C(CH_3)_3$), -3.75 (s, 3H, CH_3), -3.77 (s, 3H, CH_3); ^{13}C NMR (90.6 MHz) δ 148.38, 147.48, 138.40, 137.86, 136.22, 132.50, 132.21, 131.55, 128.54, 128.43, 128.13, 126.71, 126.35, 124.03, 122.47, 122.19, 121.16, 120.37, 116.95, 115.12, 95.25, 89.89, 36.31, 36.25, 32.04, 31.87, 30.51, 14.95, 14.56; IR (KBr) 2196, 1594, 1485, 1441, 1378, 1361, 1238, 1118, 892, 754, 687, 670 cm^{-1}; CI MS *m/z*, 523 (MH+, ^{79}Br); HRMS. Calc'd for $C_{34}H_{35}Br$ (M+, ^{79}Br): 522.1922. Found: 522.1920.

2,7-Di-*t*-butyl-9,12-epoxy-4-phenylethynyl-*trans*-12c,12d-dimethyl-9,12,12c,12d-tetrahydrobenzo[e]pyrene (102)

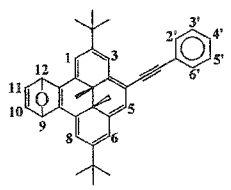

102

Distilled furan (8 mL) was added to a solution of the bromophenylethynylpyrene **101** (100 mg, 0.192 mmol) in dry THF (10 mL) under argon, and then $NaNH_2$ (600 mg, 15 mmol) and KO^tBu (5 mg) were added. The mixture was stirred overnight under argon. Methanol was added dropwise to quench excess base. The reaction mixture was extracted with water, was dried and evaporated. The brownish residual was chromatographed over deactivated SiGel using first hexane/benzene (6:1) to elute the reduced starting material phenylethynylpyrene and secondly hexane/EtOAc (6:1) to elute 71 mg (73%) of the product **102** as a mixture of two isomers, mp 214-215°C; ^{1}H NMR (360 MHz) δ 8.79-8.78 (m, 2H, H-3), 8.46 (s, 2H, H-5), 8.22-8.21 (m, 2H, H-6), 8.14-8.11 (m, 4H, H-1, 8), 7.73-7.70 (m, 4H, H-2',6'), 7.46-7.35 (m, 6H, H-3', 4',5'), 7.19-7.16 (m, 2H, H-10 or 11), 7.08-7.04 (m, 2H, H-10 or11), 6.56-6.51 (m, 4H, H-9,12), 1.656 & 1.653 (s, 9H each, $C(CH_3)_3$), 1.608 & 1.604 (s, 9H each, $C(CH_3)_3$), -3.158 & –3.162 (s, 3H each, CH_3), -3.416 & –3.424 (s, 3H each, CH_3); ^{13}C NMR (90.6 MHz) δ 146.33, 146.02, 145.73, 140.41, 140.30, 140.15, 140.03, 136.89, 136.57, 136.46, 136.35, 136.30, 136.27, 136.10, 135.86, 131.57, 128.94, 128.57, 128.51, 128.40, 128.36, 128.07, 127.94, 127.64, 124.05, 122.60, 122.55, 120.88, 120.80, 115.99, 115.89, 115.58, 115.31, 114.98, 94.52, 94.49, 89.85, 89.79, 81.22, 80.87, 80.82, 36.04, 35.78, 33.18, 32.65, 32.30, 31.75, 31.63, 31.52, 17.04, 16.54, 14.59, 14.11; IR (KBr) 2191, 1618, 1598, 1488, 1362, 1347, 1258,

1035, 875, 754, 690, 676 cm^{-1}; CI MS *m/z*, 511 (MH+); HRMS. Calc'd for $C_{38}H_{38}O$: 510.2923. Found: 510.2925.

2,7-Di-*t*-butyl-4-phenylethynyl-*trans*-12c,12d-dimethyl-12c,12d-dihydrobenzo-[e]pyrene (103)

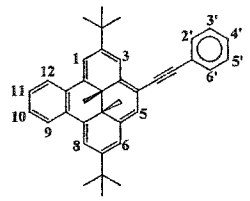

103

Distilled furan (3 mL) was added to a solution of the bromophenylethynylpyrene **101** (101 mg, 0.193 mmol) in dry THF (10mL) under argon, and then $NaNH_2$ (800 mg, 20 mmol) and KO^tBu (5mg) were added. The mixture was stirred under argon for two hours. The solution was settled, carefully decanted, and filtered through celite. More THF was used to rinse off all the product. The filtrate was dried and column chromatographed over deactivated SiGel using hexanes to elute first the yellowish green band, then the following pink band was collected and dried and gave the product **103** (47.2 mg) in 50% yield. The column was further washed with hexanes/ EtOAc (6:1) to elute 9% of the adduct **102** (9.2 mg); The dark pink solid of **103** has a mp 152-154°C; ^1H NMR (360 MHz) δ 8.74-8.70 (m, 2H, H-9,12), 8.28 (d, J = 1.3 Hz, 1H, H-1), 8.23 (d, J = 1.2 Hz, 1H, H-8), 8.03 (d, J = 1.3 Hz, 1H, H-3), 7.63-7.60 (m, 4H, H-10,11,2',6'), 7.40-7.36 (m, 2H, H-3',5'), 7.34-7.31 (m, 2H, H-6,4'), 7.25 (d, J = 0.9 Hz, 1H, H-5), 1.54 & 1.48 (s, 9H each, $C(CH_3)_3$), -1.40 & -1.42 (s, 3H each, CH_3); ^{13}C NMR (90.6 MHz) δ 147.30, 145.49, 141.89, 138.01, 136.89, 135.22, 131.59, 129.69, 129.47, 128.64,

128.00, 126.40, 126.24, 124.83, 124.73, 124.41, 122.95, 119.58, 118.50, 117.56, 117.41, 113.25, 94.61, 89.94, 36.78, 36.06, 35.63, 35.50, 30.80, 30.77, 18.17, 18.08; ; UV (cyclohexane) λ_{max} (ε_{max}) nm 236 (18,300), 264 (14,600), 312 (18,300), 325 (19,600), 342 (21,500), 377 (23,400), 395 (31,300), 509 (5,000), 624 (300); IR (KBr) 2189, 1593, 1473, 1367, 1255, 1117, 872, 753, 688 cm^{-1}; CI MS *m/z*, 495 (MH+); HRMS. Calc'd for $C_{38}H_{38}$: 494.2974. Found: 494.2980.

2,7-Di-*t*-butyl-4-phenyl-*trans*-12c,12d-dimethyl-12c,12d-dihydrobenzo[e]pyrene (105)

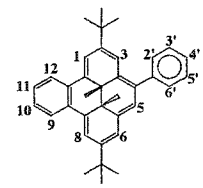

105

$Fe_2(CO)_9$ (52.9 mg, 0.145 mmol) was added to a solution of the phenylbenzopyrene adduct **109** (47.1 mg, 0.0969 mmol) in benzene (20 mL). The mixture was refluxed for 1 h in the dark and allowed cool to room temperature. The mixture was then filtered through SiGel in benzene and the solvent was evaporated. The residual was chromatographed over SiGel using hexanes/benzene (6:1) as eluant to give 37 mg (81%) of the product **105** as a bright reddish solid, mp 180-181°C; ^{1}H NMR (360 MHz) δ 8.80-8.74 (m, 2H, H-9,12), 8.31-8.29 (m, 2H, H-1,8), 7.64-7.59 (m, 2H, H-10,11), 7.58-7.55 (m, 3H, H-3,2',6'), 7.53-7.45 (m, 2H, H-3',5'), 7.39-7.34 (m, 2H, H-6,4'), 7.225 (d, J = 0.8 Hz, 1H, H-5), 1.49 (s, 9H, $C(CH_3)_3$), 1.39 (s, 9H, $C(CH_3)_3$), -1.453 (s, 3H, CH_3), -1.456 (s, 3H, CH_3); ^{13}C NMR (90.6 MHz) δ 144.84, 144.71, 141.89, 137.81, 134.90, 134.81, 133.54, 132.93, 129.95, 129.48, 129.17, 128.12, 126.62, 125.76, 125.68, 124.59,

124.44, 124.40, 119.69, 117.62, 117.03, 117.00, 35.77, 35.61, 35.40, 35.24, 30.64, 17.78, 17.60; IR (KBr) 1363, 1256, 891, 877, 871, 762, 752, 704, 694 cm^{-1}; UV (cyclohexane) λ_{max} (ε_{max}) nm 236 (18,900), 269 (14,500), 312 (23,100), 325 (24,900), 342 (27,700), 377 (31,400), 395 (42,700), 509 (6,900), 610 (500); CI MS *m/z*, 471(MH+); HRMS. Calc'd for $C_{36}H_{38}$: 470.2974. Found: 470.2974.

2,7-Di-*t*-butyl-4-phenyl-*trans*-10b,10c-dimethyl-10b,10c-dihydropyrene (106)

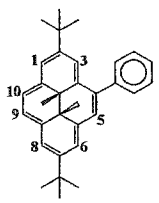

106

An aqueous solution of Na_2CO_3 (2M, 20 mL) was added to a mixture of $PhB(OH)_2$[79] (60 mg, 0.492 mmol) and the bromide **69** (104 mg, 0.246 mmol) in THF (30 mL), and then $Pd(PPh_3)_2Cl_2$ (6 mg) was added. The mixture was refluxed for 2 hr under argon and then cooled to room temperature. Hexanes (30 mL) were added to the mixture, which then was transferred to a separatory funnel. The organic phase was washed with water, dried and evaporated. The residual was chromatographed on SiGel using firstly hexanes as eluant. A very small amount of the green parent **20** eluted first. Secondly, hexanes/benzene (6:1) eluted the second bright green band to give 90 mg (87%) of the product **106**, mp 162-163 °C; ^{1}H NMR (360 MHz) δ 8.65 (d, J = 1.1 Hz, 1H, H-3), 8.52-8.53 (m, 3H, H-1,6,8), 8.48 (s, 1H, H-5), 8.440 & 8.438 (AB, J = 7.9 Hz, 2H, H-9,10), 7.85-7.81 (m, 2H, H-2',6'), 7.61-7.57 (m, 2H, H-3',5'), 7.50-7.46 (m, 1H, H-4'), 1.68 (s, 9H, $C(CH_3)_3$), 1.59 (s, 9H, $C(CH_3)_3$), -3.84 (s, 3H, CH_3), -3.86 (s, 3H, CH_3);

^{13}C NMR (90.6 MHz) δ 145.86, 145.59, 142.81, 137.00, 136.72, 136.30, 134.98, 133.29, 131.00, 128.10, 126.74, 124.88, 122.84, 122.51, 120.84, 120.54, 120.07, 36.06, 35.93, 31.93, 31.83, 30.05, 29.73, 14.79, 14.38; IR (KBr) 1597, 1477, 1461, 1446, 1382, 1359, 1344, 1231, 884, 700, 666 cm^{-1}; CI MS *m/z*, 421(MH+); Anal. Calc'd for $C_{32}H_{36}$: C, 91.37; H, 8.63. Found: C, 91.63; H, 8.81.

4-Bromo-2,7-di-*t*-butyl-9-phenyl-*trans*-10b,10c-dimethyl-10b,10c-dihydropyrene (107)

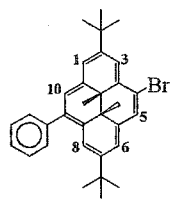

107

NBS (38 mg, 0.215 mmol) in dry DMF (10 mL) was added dropwise to a stirred solution of the phenylpyrene **106** (90 mg, 0.214 mmol) in dry CH_2Cl_2 (50 mL) cooled in a dry ice/acetone bath under argon with stirring. After the addition was complete, a small amount of CH_2Cl_2 (2 x 1 mL) was used to rinse the addition funnel in to the reaction mixture. The cooling bath was removed, and the reaction mixture was allowed to warm to room temperature and continued stirring for 1 hr. Hexanes (50 mL) was added to the mixture and the organic phase was extracted with water (6 x 100 mL) and dried. The green residual was chromatographed over SiGel using hexanes/CH_2Cl_2 (6:1) as eluant. ^{1}H NMR spectroscopy showed that product contained 3% starting material and the 4-bromo-10-phenylpyrene 12%. The total residual weighed 98 mg (92%) after chromatography. Some of the mixture was carefully washed with small amount of

pentane a few times. The residual dark green solid, **107**, was about 95% pure judging by ^{1}H NMR, mp (sublimes) 162°C; ^{1}H NMR (360 MHz) δ 8.77 (br. s, 1H, H-3), 8.62 (br. s, 1H, H-8), 8.60 (s, 1H, H-5), 8.52 (d, J ≅ 1.0 Hz, 1H, H-1), 8.47 (s, 1H, H-10), 8.44 (d, J ≅ 1.0 Hz, 1H, H-6), 7.80-7.78 (m, 2H, H-2',6'), 7.61-7.56 (m, 2H, H-3',5'), 7.51-7.46 (m, 1H, H-4'), 1.69 (s, 9H, $C(CH_3)_3$), 1.56 (s, 9H, $C(CH_3)_3$), -3.72 (s, 3H, CH_3), -3.75 (s, 3H, CH_3); ^{13}C NMR (90.6 MHz) δ 147.31, 147.00, 142.24, 137.38, 136.70, 135.82, 134.12, 131.70, 130.90, 128.20, 127.02, 126.11, 125.69, 121.96, 120.89, 120.86, 120.53, 115.43, 36.24, 36.11, 32.36, 31.88, 31.69, 30.26, 14.76, 14.36; IR (KBr) 1598, 1590, 1478, 1462, 1448, 1377, 1362, 1348, 1238, 953, 897, 761, 703, 666 cm^{-1}; CI MS *m/z*, 499 (MH+, ^{79}Br); HRMS. Calc'd for $C_{32}H_{35}Br$ (^{79}Br): 498.1922. Found: 498.1919.

2,7-Di-*t*-butyl-9,12-epoxy-4-phenyl-*trans*-dimethyl-9,12,12c,12d-tetrahydro-benzo[e]pyrene (109)

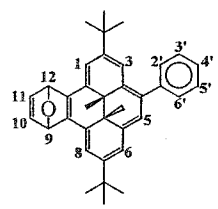

109

$NaNH_2$ (400 mg, 10 mmol) and KO^{t}Bu (5 mg) were added to a solution of the bromophenylpyrene **107** (100 mg, 0.201 mmol) in dried furan (7 mL) and THF (15 mL). The mixture was stirred at room temperature under argon for 5 hr. Methanol was added dropwise to quench the excess base. Hexanes (15 mL) were added and the mixture was transferred to a separatory funnel and the organic phase was extracted with water and dried and solvent was evaporated. The residual was chromatographed over deactivated

SiGel using hexanes/EtOAc (6:1) as eluant. The first portion was small amount of reduced phenylpyrene **106**. The second green band was collected to give 78 mg (80%) of the product **109** as equal mixture of two isomers, mp 212-214°C; ^{1}H NMR (360 MHz) δ 8.16 & 8.14 (s, 1H each, H-5), 8.10-8.07 (m, 4H, H-3,6), 8.03-8.01 (m, 4H, H-1,8), 7.74-7.71 (m, 4H, H-2',6'), 7.57-7.53 (m, 4H, H-3',5'), 7.48-7.43 (m, 2H, H-4'), 7.18-7.15 (m, 2H, H-10 or 11), 7.05-7.03 (m, 2H, H-10 or11), 6.55-6.50 (m, 4H, H-9,12), 1.602 & 1.599 (s, 9H each, $C(CH_3)_3$), 1.502 & 1.496 (s, 9H each, $C(CH_3)_3$), -2.88 & –2.90 (s, 3H each, CH_3), -3.13 & –3.17 (s, 3H each, CH_3); ^{13}C NMR (90.6 MHz) δ 145.75, 145.46, 145.38, 145.04, 142.30, 142.24, 139.96, 139.65, 137.01, 136.83, 136.44, 135.28, 135.20, 135.02, 134.87, 134.76, 130.72, 128.16, 128.04, 127.77, 127.63, 127.35, 126.96, 125.97, 121.67, 121.62, 121.44, 121.33, 114.69, 114.50, 114.42, 114.25, 81.08, 81.06, 80.76, 80.65, 35.83, 35.70, 33.61, 33.39, 32.69, 32.50, 31.40, 31.24, 17.21, 16.69, 14.69, 14.27; IR (KBr) 1618, 1600, 1476, 1461, 1443, 1361, 1344, 1258, 1033, 876, 858, 844, 765, 700, 676, 649 cm^{-1}; EI MS *m/z*, 486 (M+); Anal. Calc'd for $C_{36}H_{38}O$: C, 88.84; H, 7.87. Found: C, 88.54; H, 8.20.

Bis-isopyranofuran adduct (114)

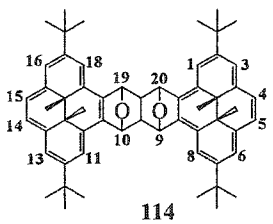

114

The isofuran **47**[31] (133 mg, 0.346 mmol) and adduct **70**[31] (116 mg, 0.283 mmol) were held under vacuum for 2 hr in an oven baked two neck round bottom flask. Dry toluene (8 mL) was then added to the flask under argon. The mixture was refluxed

overnight and then cooled in an ice bath. The solvent was carefully decanted and the green solid was washed with hexanes (4 X 4 mL) and air dried to give 168 mg (75%) of the product **114**. Crystallization from toluene gave fine green needles as a mixture of two isomers, mp (dec) 219-224 °C; ^{1}H NMR (360 MHz) δ 8.51, 8.48, 8.46, 8.44 (d, J = 1.2 Hz, 2H each, H-1,8,11,18), 8.39-8.37 (m, 8H total, H-3,6,13,16), 8.31-8.30 (m, 8H total, H-4,5,14,15), 6.667, 6.651, 6.640, 6.633 (s, 8H total, H-9,10,19,20), 2.503 (s, 2H, H-20a,20b, isomer I), 2.505, 2.413 (d, J = 6.5 Hz, 1H each, H-20a,20b, isomer II), 1.710, 1.659 (s, 18H each, $C(CH_3)_3$, isomer I), 1.681, 1.679 (s, 18H each, $C(CH_3)_3$, isomer II), -3.861, -4.29 (s, 6H each, CH_3, isomer I), -3.866, -4.34 (s, 6H each, CH_3, isomer II); ^{13}C NMR (90.6 MHz) δ 145.68, 145.61, 145.54, 138.56, 138.05, 138.01, 136.64, 136.59, 136.49, 136.40, 126.14, 125.95, 125.53, 125.47, 124.00, 123.94, 123.76, 123.71, 121.39, 121.28, 121.09, 121.03, 116.27, 116.22, 115.49, 115.43, 81.53, 81.49, 81.38, 81.34, 54.14, 53.92, 53.87, 36.10, 36.05, 31.95, 31.80, 29.32, 29.24, 15.04, 15.00, 14.19, 13.87; IR (KBr) 1603, 1461, 1345, 1262, 1225, 1007, 922, 886, 867 cm^{-1}; LSIMS *m/z* 794.4 (M+); HRMS. Calc'd for $C_{58}H_{66}O_2$ (M+): 794.5063. Found: 794.5100.

2,7,12,17-Tetra-*t*-butyl-*trans*-19c,19d,20c,20d-tetramethyl-19c,19d,20c,20d-tetrahydrotetrabenzo[de,yz,lm,qr]hexaphene (116)

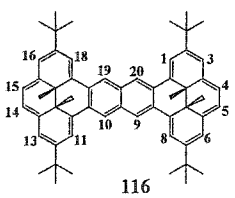

116

P_2S_5 (50.0 mg, 0.225 mmol) was added to the solution of the adduct **114** (50.0 mg, 0.063 mmol) in CS_2 (20 mL) under argon. The mixture was stirred for 2 hr and then was

filtered through celite. The solvent was removed and the solid was chromatographed over SiGel using firstly hexanes to elute the red band, and secondly hexanes/benzene (10:1) to elute the green band which was collected to give 15 mg (31%) of the product **116** as two isomers in equal amount. The product was washed by hexanes (4 x 4 mL) and then the ratio of the two isomers was about 2:3, which allowed assignment of the ^{1}HNMR for the two isomers. This sample showed mp (dec) 173-178 °C; ^{1}H NMR, isomer I, (360 MHz) δ 9.196 (s, 4H, H-9,10,19,20), 8.05 (d, J = 1.2 Hz, 4H, H-1,8,11,18), 6.843 (d, J = 1.0 Hz, 4H, H-3,6,13,16), 6.594 (s, 4H, H-4,5,14,15), 1.474 (s, 36H, $C(CH_3)_3$), -0.325 (s, 12H, CH_3). Isomer II, δ 9.190 (s, 4H, H-9,10,19,20), 8.03 (d, J = 1.2 Hz, 4H, H-1,8,11,18), 6.835 (d, J = 1.0 Hz, 4H, H-3,6,13,16), 6.587 (s, 4H, H-4,5,14,15), 1.470 (s, 36H, $C(CH_3)_3$), -0.310 (s, 12H, CH_3). ^{13}C NMR (90.6 MHz) δ 144.72, 139.48, 136.11, 129.34, 129.29, 128.79, 122.25, 121.11, 119.92, 117.75, 117.66, 38.17, 35.16, 31.52, 30.32, 30.25, 25.61, 19.69, 19.62; UV (cyclohexane) λ_{max} (ε_{max}) nm 235 (15,100), 260 (14,600), 331 (13,100), 346 (18,300), 417 (27,100), 441 (43,600), 624 (2,100); IR (KBr) 1622, 1474, 1431, 1359, 1228, 1155, 898, 870 cm^{-1}; LSIMS *m/z* 760.6 (M+); HRMS. Calc'd for $C_{58}H_{64}$ (MH+): 761.5086. Found: 761.5064.

2,7-Di-*t*-butyl-9,18-epoxy-18c,18d-dimethyl-9,18,18c,18d-tetrahydrotetrabenzo-[cd,i,k,pq]naphthacene (118)

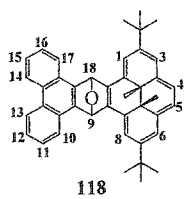

118

$NaNH_2$ (570 mg, 14.6 mmol) and KO^tBu (2 mg) were added to a stirred solution of the isofuran **47**[31] (84.3 mg, 0.220 mmol) and 9-bromophenanthrene **117**[84] (281.8 mg, 1.097 mmol) in dried THF (25 mL) under argon. The mixture was stirred overnight and then methanol (5 mL) and hexanes (25 mL) were added. The organic phase was washed, dried and evaporated. The solid was chromatographed over deactivated SiGel using benzene/hexanes (1:1) as eluant. The green band was collected and gave 104 mg (85%) of the adduct **118**, which on recrystallization from toluene gave dark green crystals, mp 221-222 °C; ^{1}H NMR (360 MHz) δ 8.59 (d, J = 8.3 Hz, 2H, H-13,14), 8.43, 8.40 (d, J ~ 1.2 Hz, 1H each, H-1 or 8), 8.41, 8.27 (dd, J = 8.1 Hz, 1.1 Hz, 1H each, H-10 or 17), 8.13, 8.10 (d, J = 1.2 Hz, 1H each, H-3 or 6), 8.07 (s, 2H, H-4,5), 7.63, 7.61 (s, 1H each, H-9 or 18), 7.72-7.64, 7.59-7.52 (m, 2H each, H-11,16 or 12,15), 1.66, 1.63 (s, 9H each, $C(CH_3)_3$), -3.14, -4.12 (s, 3H each, CH_3); ^{13}C NMR (90.6 MHz) δ 145.52, 145.30, 145.01, 144.66, 137.28, 136.22, 136.18, 135.76, 129.61, 129.47, 127.81, 127.22, 126.78, 126.75, 126.67, 126.62, 126.04, 125.97, 124.47, 124.36, 124.23, 124.03, 123.57, 121.23, 115.47, 114.70, 81.72, 81.14, 35.74, 35.69, 34.21, 33.32, 31.54, 31.51, 16.50, 14.25; IR (KBr) 1616, 1448, 1363, 1343, 1260, 883, 865, 777, 755, 745, 721, 716, 671, 632 cm^{-1}; CI MS *m/z*, 561(MH+); Anal. Calc'd for $C_{42}H_{40}O$: C, 89.96; H, 7.19. Found: C, 89.66; H, 7.34.

2,7-Di-*t*-butyl-*trans*-18c,18d-dimethyl-18c,18d-dihydrotetrabenzo[cd,i,k,pq]-naphthacene (119)

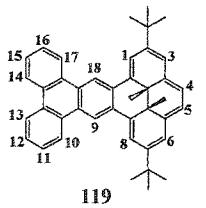

119

A mixture of the epoxide **118** (88 mg, 0.157 mmol) and $Fe_2(CO)_9$ (88 mg, 0.242 mmol) in benzene (30 mL), was refluxed under argon in the dark for 5 hr. After cooling to room temperature, the mixture was filtered through a short column (5 cm) of deactivated SiGel, using benzene as eluant. The solvent was then removed and the dark purple solid product was carefully washed with pentane until the initial brownish color disappeared and gave 73 mg (86%) of the product **119**. Slow evaporation from hexanes/CH_2Cl_2 yield dark purple crystals, mp (dec) 188-193 °C; ^{1}H NMR (360 MHz) δ 9.92 (s, 2H, H-9,18), 8.92 (dd, J = 8.2 Hz, 1.3 Hz, 2H, H-10,17), 8.67 (dd, J = 8.2 Hz, 1.2 Hz, 2H, H-13,14), 8.40 (d, J = 1.3 Hz, 2H, H-1,8), 7.78-7.74 (m, 2H, H-11,16), 7.71-7.67 (m, 2H, H-12,15), 7.23 (d, J = 1.2 Hz, 2H, H-3,6), 6.99 (s, 2H, H-4,5), 1.55 (s, 18H, $C(CH_3)_3$), -1.07 (s, 6H, CH_3); ^{13}C NMR (90.6 MHz) δ 144.51, 138.81, 135.19, 130.15, 130.06, 128.59, 127.54, 127.46, 127.37, 123.53, 123.33, 121.26, 120.15, 118.57, 117.43, 36.47, 35.39, 30.63, 18.31; UV ($CHCl_3$) λ_{max} (ε_{max}) nm 284 (43,200), 337 (38,600), 374 (22,200), 392 (46,200), 412 (72,400), 529 (5,700), 644 (600); IR (KBr) 1627, 1605, 1490, 1434, 1360, 1227, 886, 872, 754, 719, 673 cm^{-1}; CI MS *m/z*, 545(MH+); Anal. Calc'd for $C_{42}H_{40}$: C, 92.60; H, 7.40. Found: C, 92.58; H, 7.64.

Phenyl-tris-pyrene (120)

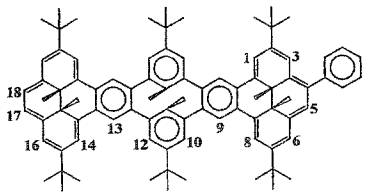

120

The impure phenyltrisDHP precursor **121** (15 mg, 0.013 mmol) and $Fe_2(CO)_9$ (10 mg, 0.027 mmol) were refluxed in benzene (15 ml) under argon for 1h. The mixture was slowly cooled to room temperature and the solvent was evaporated. The residual was chromatographed over alumina using hexanes/benzene (6:1) and gave 4 mg (27%) of the product **120** as a red solid, mp (dec) 168-172°C; ^{1}H NMR (360 MHz), similar groups of peaks were observed as for trisDHP **72**. group I: δ 9.01 (br. s, 4H, H-9,13,22,26), 8.40-8.37 (m, 4H, H-1,8,14,21), 7.74-7.61(m, 2H, H-2',6') 7.54-7.49 (m, 2H, H-3',5'), 7.43-7.39 (m, 5H, H-3,6,16,19,4'), 7.19-7.18 (m, 7H, H-5,17,18,10,12,23,25), 1.57(s), 1.54(s), 1.47(s), 1.44(s), 1.370-1.363(m) (108H total, $C(CH_3)_3$), 1.30 (br. s, 6H, CH_3 from cyclophane), -1.23, -1.36 (br. s, 12H total, CH_3 from DHPs).

^{1}H NMR (360 MHz), group II: δ 9.16-9.15 (m, 4H, H-9,13,22,26), 8.59-8.57 (m, 4H, H-1,8,14,21), 7.74-7.61(m, 2H, H-2',6') 7.54-7.49 (m, 6H, H-3,6,16,19,3',5'), 7.43-7.39 (m, 1H, H-4'), 7.32 (br. s, 3H, H-5,17,18), 7.19-7.18 (m, 4H, H-10,12,23,25),), 1.57(s), 1.54(s), 1.47(s), 1.44(s), 1.370-1.363(m) (108H total, $C(CH_3)_3$), 1.30 (br. s, 6H, CH_3 from cyclophane), -1.49, -1.62 (br. s, 12H total, CH_3 from DHPs). LSIMS *m/z,* 1153.6 (MH+); HRMS. Calc'd for $C_{88}H_{96}$ (MH+): 1153.7590. Found: 1153.7576.

Phenyltris-pyrene precursor (121)

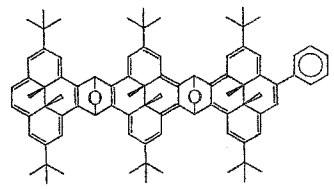

121

$NaNH_2$ (400 mg, 10 mmol) and KO^tBu (5 mg) were added to a solution of the furan **79** (50 mg, 0.065 mmol) and the phenylbromide **107** (100 mg, 0.201 mmol) in dry THF (15 mL). The reaction mixture was stirred under argon for 2.5 hr and was filtered through celite. The solvent was evaporated and the residual was chromatographed on alumina over a short column (5 cm) using first hexanes/benzene (1:1) to elute the reduced starting material and second using hexanes/EtOAc (6:1) to elute 18 mg (23%) of the product **121** which was a mixture of isomers and some impurities which could not be separated from the product. The product **121** was not stable in $CDCl_3$. A crude ^1H NMR (300 MHz) spectrum was quickly taken in C_6D_6. The three groups of internal methyl proton chemical shifts were: -2.67 to -3.00 & -4.14 to -4.32 & -4.97 to -5.03. The material was used directly in the next step.

5.3 Photochromic and Thermochromic Kinetic Studies

For first order reactions: $\ln(c_t) = kt + \text{constant}$

From Beer's law: $c = A/\varepsilon d$

c ----- concentration (mol L^{-1})

A ----- absorbance

d ----- path length (cm)

Thus: $\ln(A_t/\varepsilon d) = kt + \text{constant}$

At a particular wavelength, ε is constant and d is 1 cm. The above equation can then be re-written as: $\ln(A_t) = kt + \text{Constant'}$.

For photo openings, the measured absorption is due to the reactant, and thus the above equation was used directly for the calculation. In the following graphs: $x = A_t$.

For photo closings and thermal return reactions, the measured absorption is from the product. Thus, the concentration of reactant $c_r = c_0 - c_t$; c_0 is the initial reactant concentration, which can be measured in terms of absorbance (A_0) before the sample is bleached. The above equation becomes:

$\ln(A_0 - A_t) = kt + \text{constant'}$. In the following graphs: $x = A_0 - A_t$.

5.4 Experimental Error Determination

Triphenyleno-DHP **119** has a medium thermal return rate, and a moderate photo opening rate as well, thus we thought **119** could serve as a model compound for experimental error determination.

5.4.1 Thermal Return Reaction of CPD to DHP

The thermal return reaction of triphenyleno-CPD to DHP in toluene was monitored by UV-Vis spectroscopy. Three independent runs, in which each run included three temperatures, 46°C, 60°C and 70°C, were performed. The experiment results were monitored at two different wavelengths, and the thermal return rates were calculated according to first order kinetics.

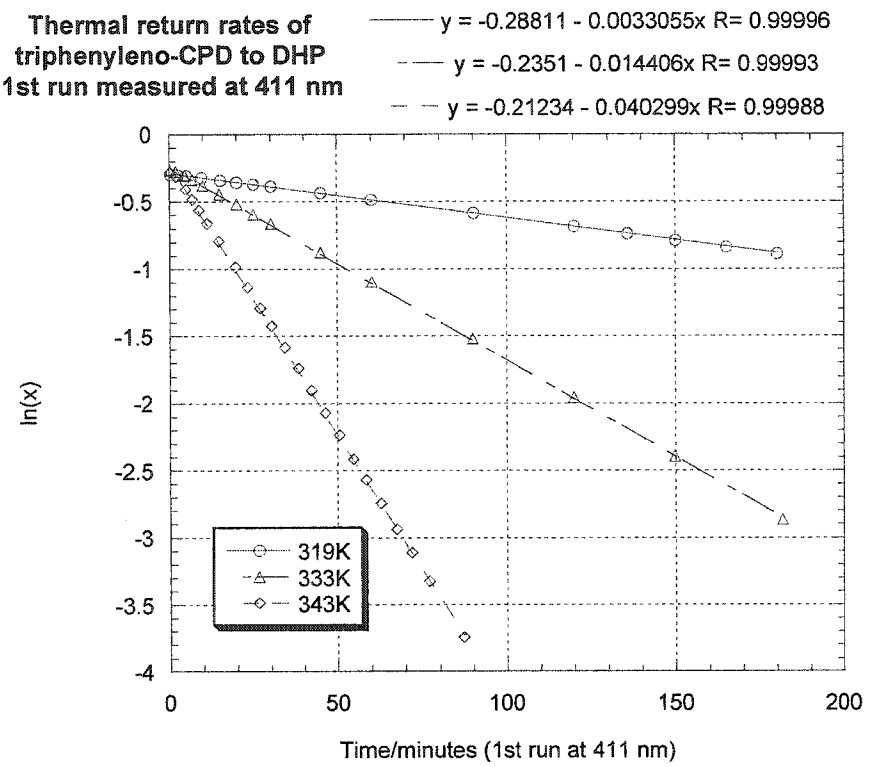
Thermal return rates of
triphenyleno-CPD to DHP
1st run measured at 411 nm
y = -0.28811 - 0.0033055x R= 0.99996
y = -0.2351 - 0.014406x R= 0.99993
y = -0.21234 - 0.040299x R= 0.99988
ln(x)
0
-0.5
-1
-1.5
-2
-2.5
-3
-3.5
-4
0
50
100
150
200
319K
333K
343K
Time/minutes (1st run at 411 nm)

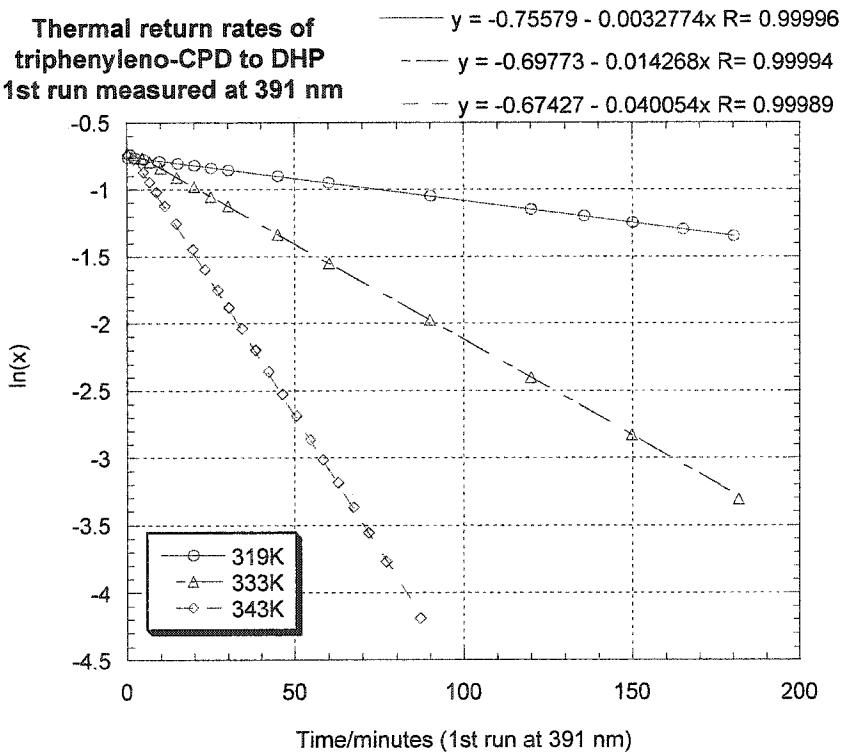
Thermal return rates of
triphenyleno-CPD to DHP
1st run measured at 391 nm
y = -0.75579 - 0.0032774x R= 0.99996
y = -0.69773 - 0.014268x R= 0.99994
y = -0.67427 - 0.040054x R= 0.99989
ln(x)
-0.5
-1
-1.5
-2
-2.5
-3
-3.5
-4
-4.5
0
50
100
150
200
319K
333K
343K
Time/minutes (1st run at 391 nm)

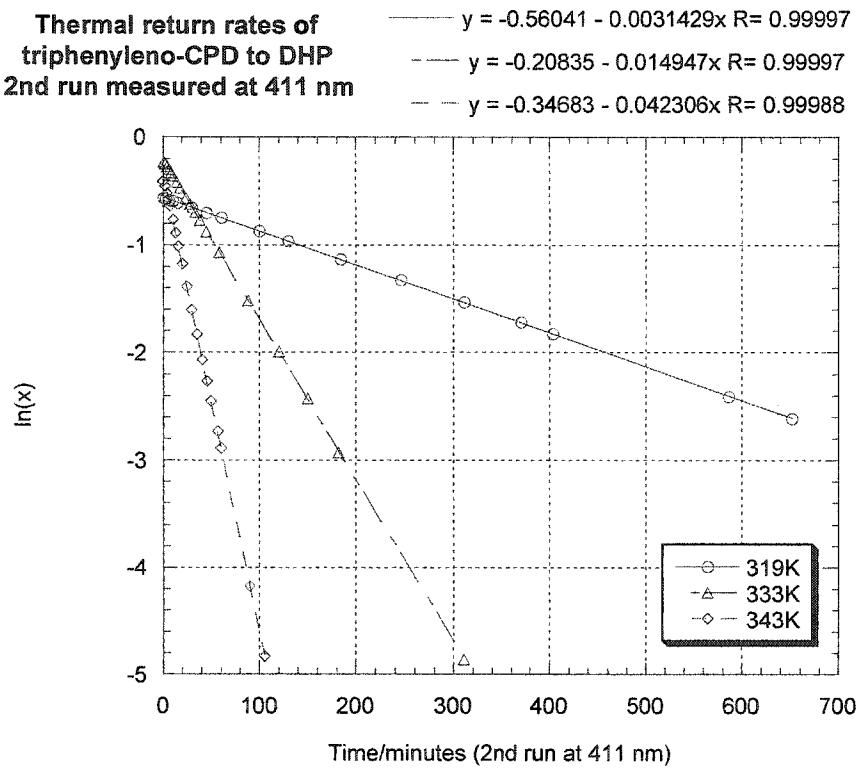
Thermal return rates of triphenyleno-CPD to DHP 2nd run measured at 411 nm
y = -0.56041 - 0.0031429x R= 0.99997
y = -0.20835 - 0.014947x R= 0.99997
y = -0.34683 - 0.042306x R= 0.99988
ln(x)
0
-1
-2
-3
-4
-5
0
100
200
300
400
500
600
700
319K
333K
343K
Time/minutes (2nd run at 411 nm)

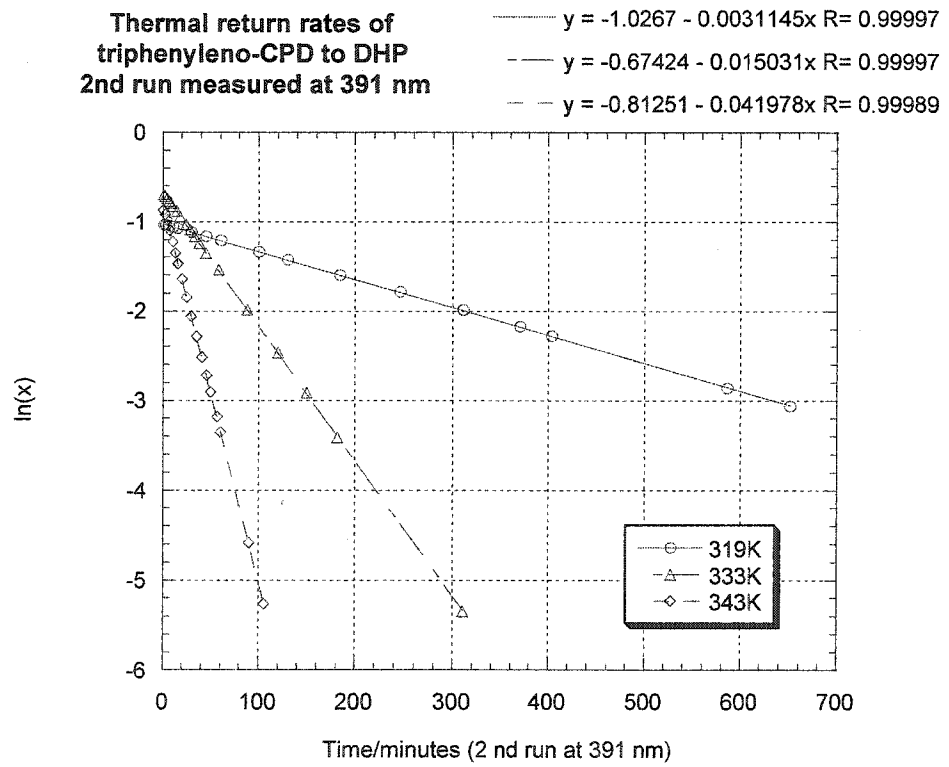
Thermal return rates of triphenyleno-CPD to DHP 2nd run measured at 391 nm
y = -1.0267 - 0.0031145x R= 0.99997
y = -0.67424 - 0.015031x R= 0.99997
y = -0.81251 - 0.041978x R= 0.99989
ln(x)
0
-1
-2
-3
-4
-5
-6
0
100
200
300
400
500
600
700
319K
333K
343K
Time/minutes (2 nd run at 391 nm)

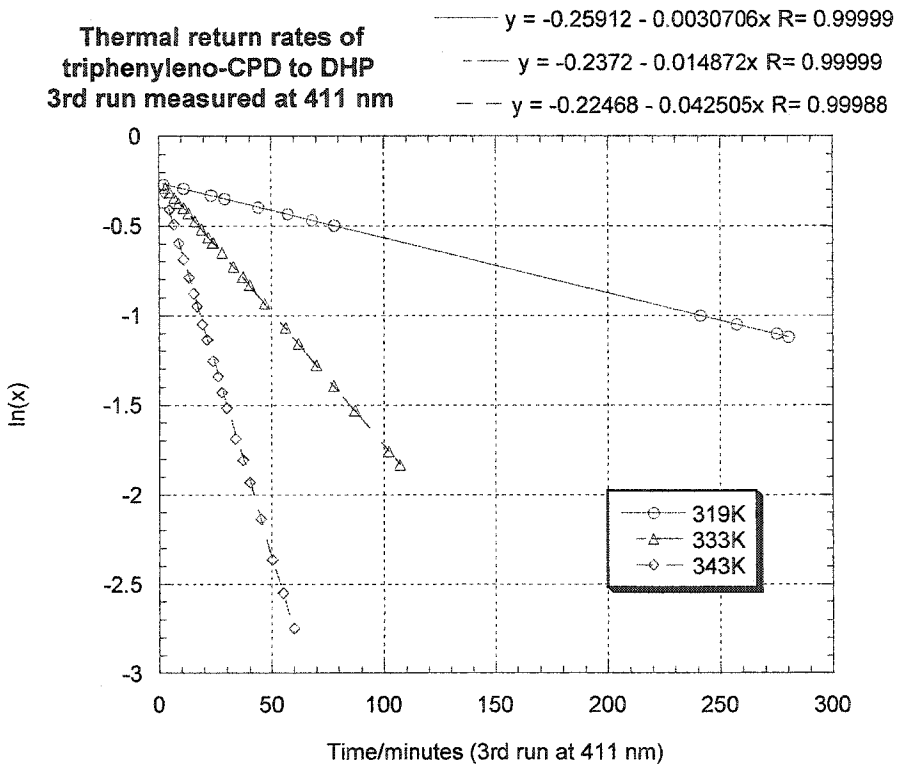
Thermal return rates of
triphenyleno-CPD to DHP
3rd run measured at 411 nm
y = -0.25912 - 0.0030706x R= 0.99999
y = -0.2372 - 0.014872x R= 0.99999
y = -0.22468 - 0.042505x R= 0.99988
ln(x)
0
-0.5
-1
-1.5
-2
-2.5
-3
0
50
100
150
200
250
300
319K
333K
343K
Time/minutes (3rd run at 411 nm)

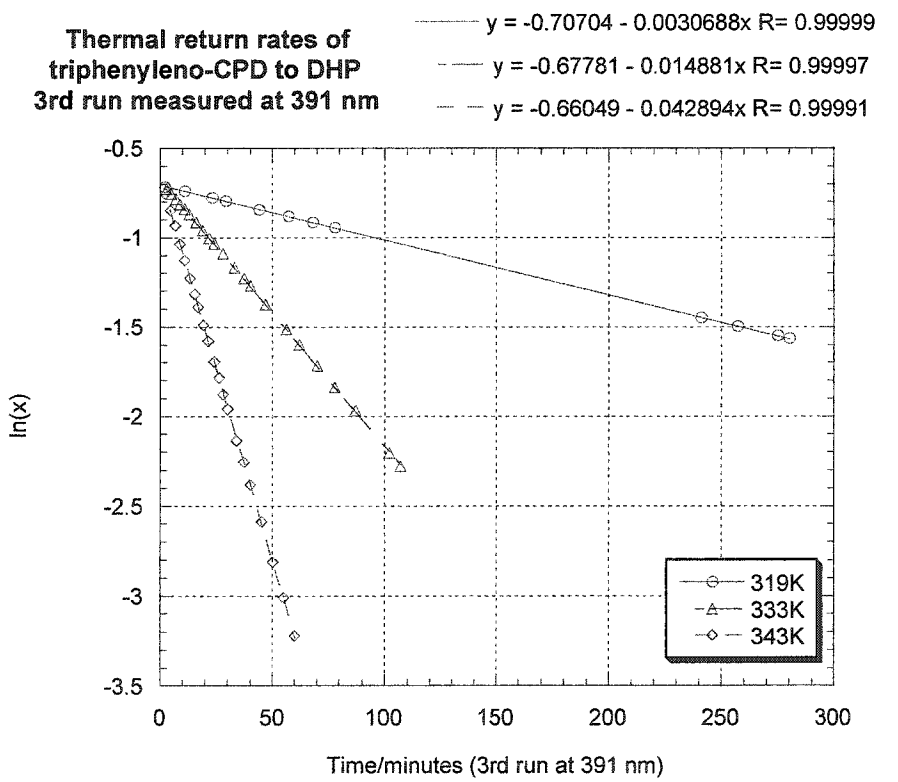
Thermal return rates of
triphenyleno-CPD to DHP
3rd run measured at 391 nm
y = -0.70704 - 0.0030688x R= 0.99999
y = -0.67781 - 0.014881x R= 0.99997
y = -0.66049 - 0.042894x R= 0.99991
ln(x)
-0.5
-1
-1.5
-2
-2.5
-3
-3.5
0
50
100
150
200
250
300
319K
333K
343K
Time/minutes (3rd run at 391 nm)

Rates measured at 411nm wavelength

k(411 nm)	319K	333K	343K
1st Run	0.0033055	0.014406	0.040299
2nd Run	0.0031429	0.014947	0.042306
3rd Run	0.0030706	0.014872	0.042505
sd	0.000120308	0.000293105	0.001220252
sd%	3.8	2.0	2.9

Rates measured at 391nm wavelength

k(391 nm)	319K	333K	343K
1st Run	0.0032774	0.014268	0.040054
2nd Run	0.0031145	0.015031	0.041978
3rd Run	0.0030688	0.014881	0.042894
sd	0.00010965	0.000404235	0.001449508
sd%	3.5	2.7	3.5

The tables above summarized the rate constants and calculated the relative standard deviations. The maximum value of which is 3.8%, and was used in the calculation of deviations of rate constants in the text.

The E_{act} , $H^{\neq}$ and $S^{\neq}$ were calculated with each run at two wavelengths as follows.

Plots of E_{act} for the thermal return reaction of triphenyleno-CPD to DHP

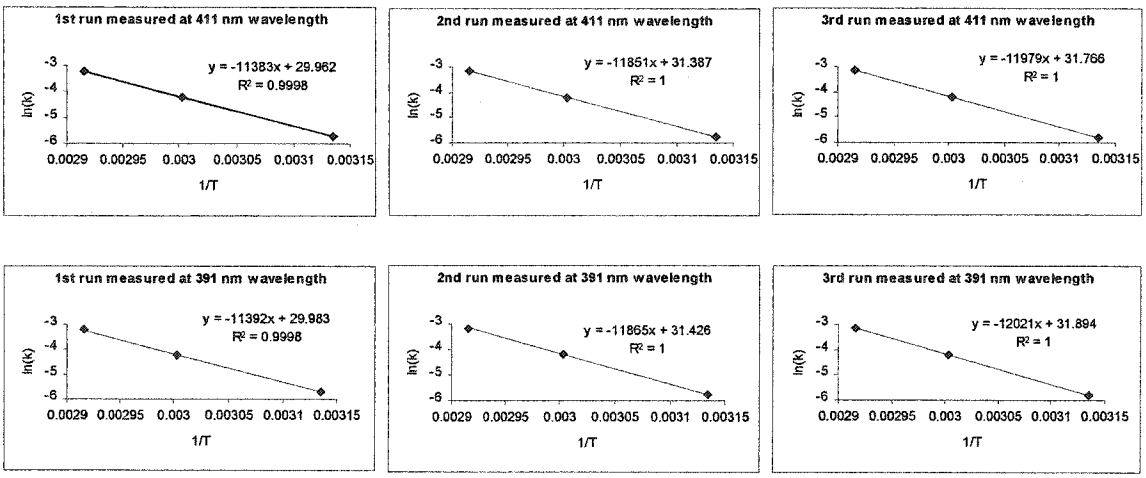

Calculations of E_{act} and relative standard deviations

Measured at 411nm wavelength		
	slope	Eact
1st Run	11383	22.63
2nd Run	11851	23.56
3rd Run	11979	23.81
sd		0.6237
sd%		2.7

Measured at 391nm wavelength		
	slope	Eact
1st Run	11392	22.65
2nd Run	11865	23.59
3rd Run	12021	23.90
sd		0.6512
sd%		2.8

The maximum value, 2.8%, was used to calculate the deviations for E_{act} in the text.

Plots of $H^{\neq}$ and $S^{\neq}$ for the thermal return reaction of triphenyleno-CPD to DHP

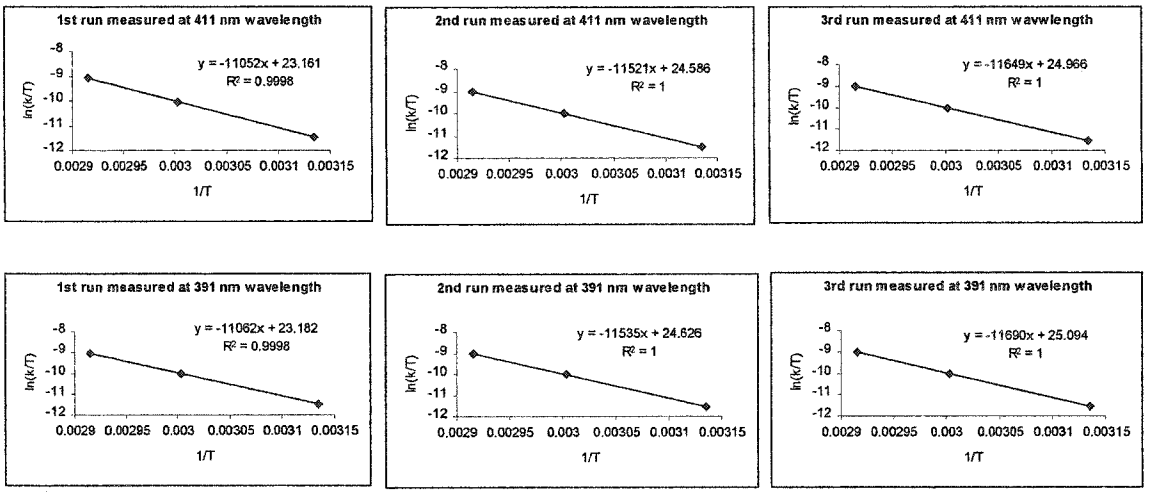

Calculations of $H^{\neq}$ and $S^{\neq}$, and relative standard deviations

	Measured at 411nm wavelength			
	Slope	$H^{\neq}$	intercept	$S^{\neq}$
1st Run	11052	21.97	23.161	-1.13
2nd Run	11521	22.90	24.586	1.70
3rd Run	11649	23.16	24.966	2.46
sd		0.6249		0.6652
sd%		2.8		37.7

	Measured at 391nm wavelength			
	slope	$H^{\neq}$	intercept	$S^{\neq}$
1st Run	11062	21.99	23.182	-1.09
2nd Run	11535	22.93	24.626	1.78
3rd Run	11690	23.24	25.094	2.71
sd		0.6504	0.9967	0.8140
sd%		2.9	4.1	43.7

Thus, 2.9% and 44% were used to calculate the deviations of $H^{\neq}$ and $S^{\neq}$ in the text, respectively.

5.4.2 Photo Opening Reaction of DHP to CPD

1. Concentration effect

Three samples, C1, C2, C3 of triphenyleno-DHP, **119** in dry THF in quartz UV cells, with initial absorbances at 410 nm as 0.6672, 1.0531 and 1.8721, and one benzo-DHP, **21** in THF with a initial absorbance at 388 nm as 0.8712, were placed side by side.

A 500 W tungsten lamp was used as a light source, and a 590 nm cut-off filter was used. The samples were irradiated at various time intervals, the results were plotted according to first order kinetics.

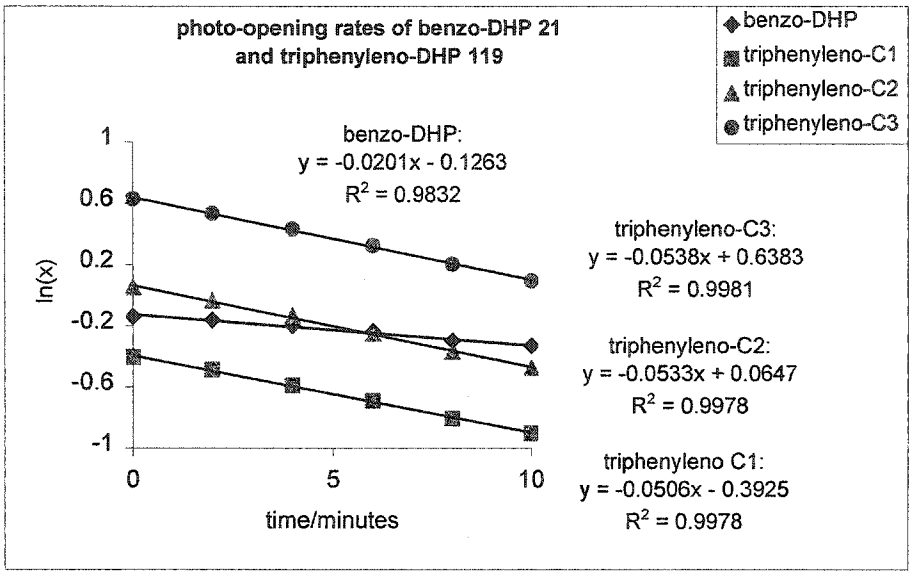

	rate constant	rate ratio
triphenyleno-C1	0.0506	2.52
triphenyleno-C2	0.0533	2.65
triphenyleno-C3	0.0538	2.68
benzo-DHP	0.0201	1
sd	0.00172	0.0856
sd%	3.3	3.3

The above table lists the photo-opening rates of **21** and **119** at different concentrations and the relative photo-opening rate ratios. The relative deviation of 3.3% suggests that the photo-opening rate does not depend on the sample concentration.

2. Distance between lamp and sample

A fresh pair of samples of triphenyleno-DHP and benzo-DHP in dry THF were irradiated with a 500 W tungsten lamp using a 590 nm cut-off filter. Three distances between the samples and the lamp were chosen as 115cm, 70cm and 40cm. The absorbance was monitored at 410 nm and 388 nm for triphenyleno-DHP and benzo-DHP, respectively.

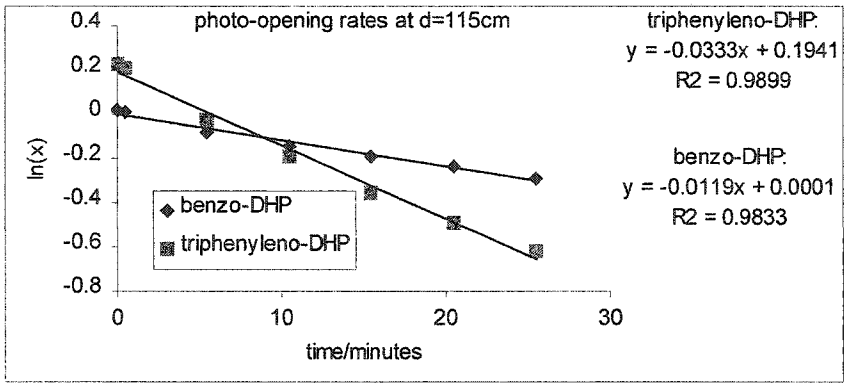

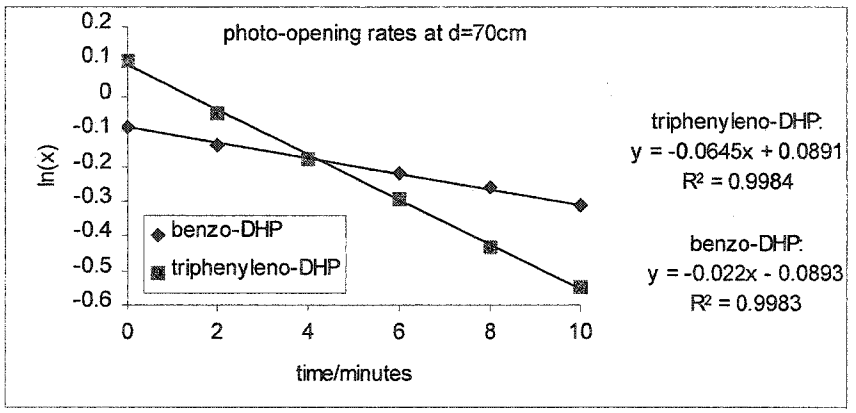

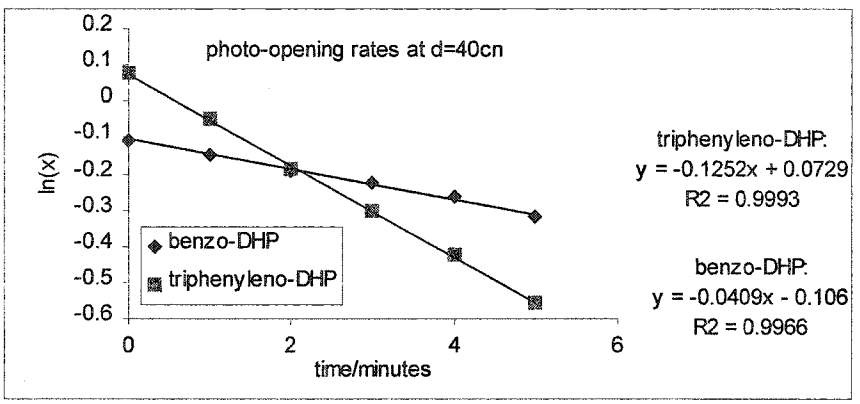

Rate constants were listed below, and rate ratios were calculated accordingly.

	d=115cm	d=70cm	d=40cm	sd	sd%
rate constant (triphenyleno-DHP)	0.0333	0.0645	0.1252		
rate constant (benzo-DHP)	0.0119	0.0220	0.0409		
rate ratio	2.80	2.93	3.06	0.13140826	4.5
sd%					

The rate constants for both triphenyleno-DHP and benzo-DHP increase dramatically with decrease in distance between lamp and sample. However, the rate ratio does not show a significant change, in fact, the relative standard deviation is only 4.5%.

In order to check the change of rate ratio with the change of light source, a 300 nm cut-off filter was used, the distance between the lamp and sample was kept 115 cm.

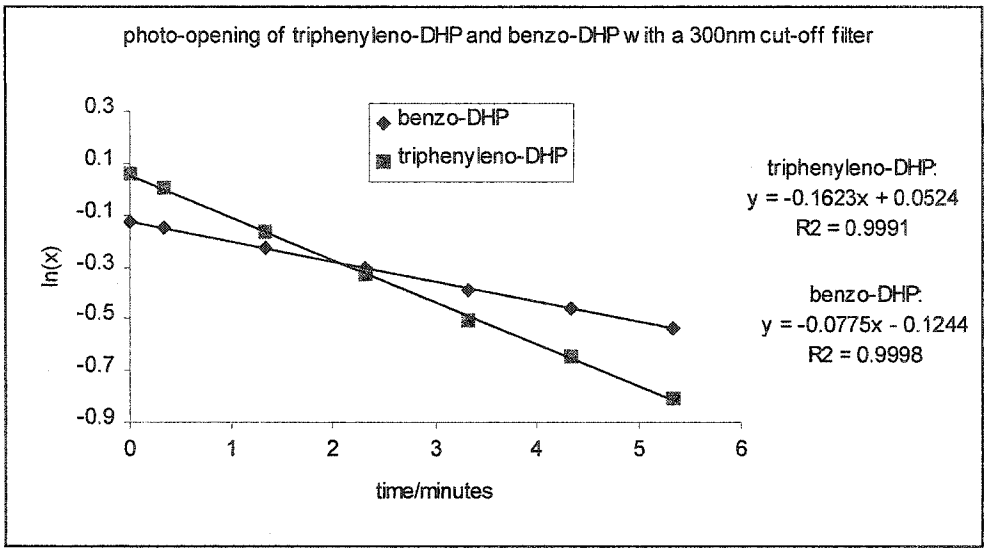

The rate constants increased for both the samples compared to the same sample lamp distance using a 590 nm cut-off filter. Also, the ratio changes from 2.8 to 2.1.

The change of concentration and distance between the lamp and the sample did not seem to affect the relative rate ratio very much. Within each experiment, the relative standard deviation is within 5%. When the two experiment results calculated together, the overall standard deviation is 7.1%.

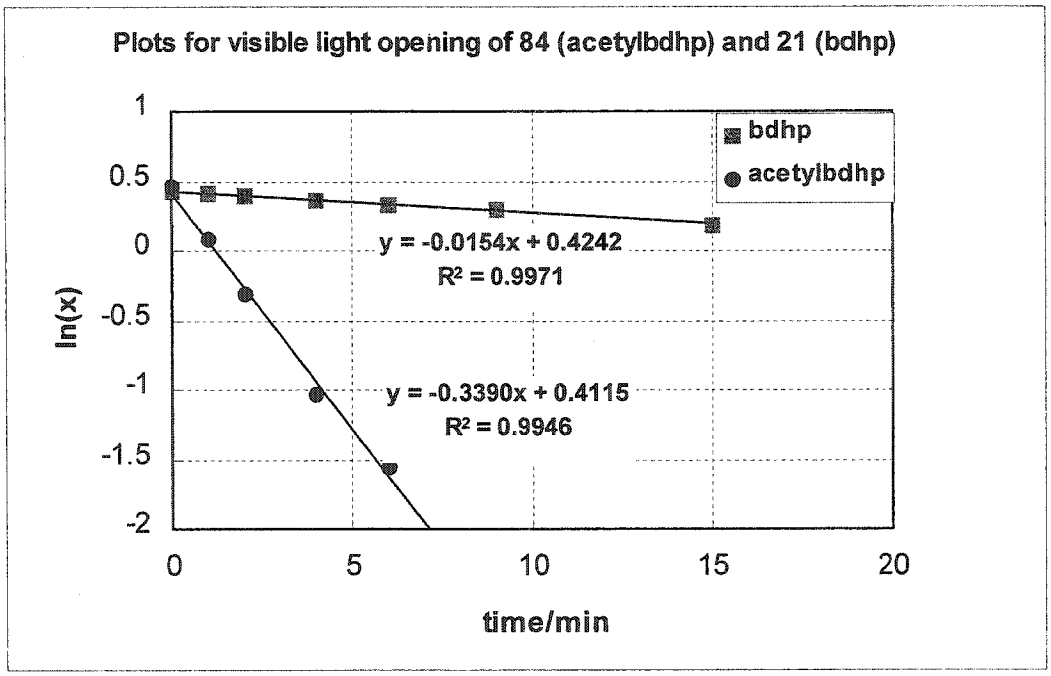
Plots for visible light opening of 84 (acetylbdhp) and 21 (bdhp)
bdhp
acetylbdhp
y = -0.0154x + 0.4242
R² = 0.9971
y = -0.3390x + 0.4115
R² = 0.9946
ln(x)
time/min
1
0.5
0
-0.5
-1
-1.5
-2
0
5
10
15
20

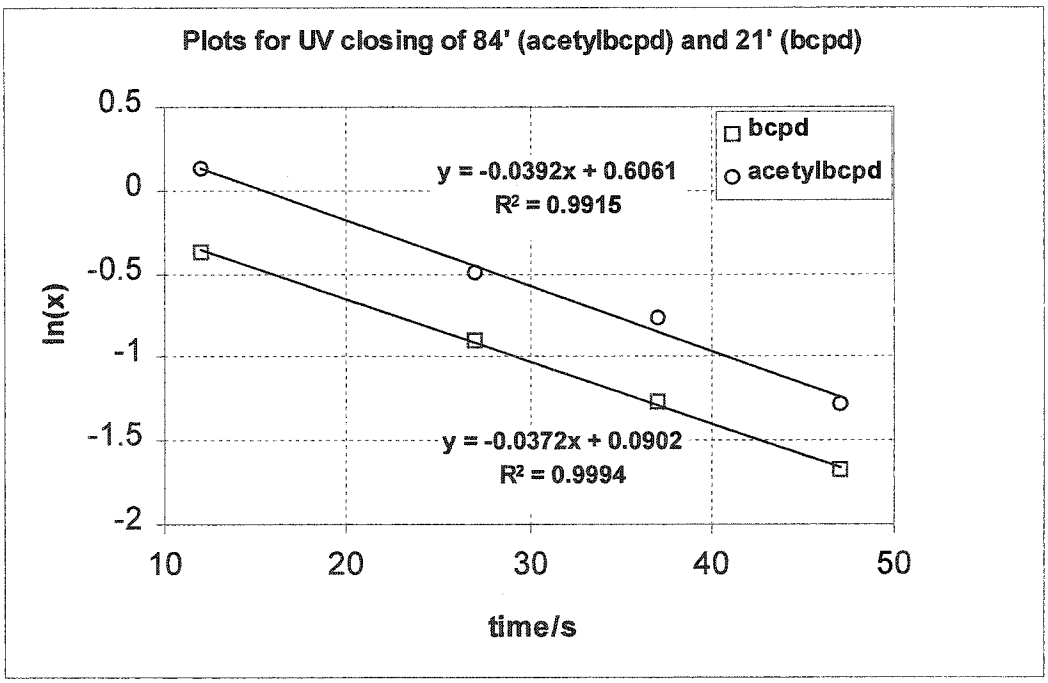
Plots for UV closing of 84' (acetylbcpd) and 21' (bcpd)
bcpd
acetylbcpd
y = -0.0392x + 0.6061
R² = 0.9915
y = -0.0372x + 0.0902
R² = 0.9994
ln(x)
time/s
0.5
0
-0.5
-1
-1.5
-2
10
20
30
40
50

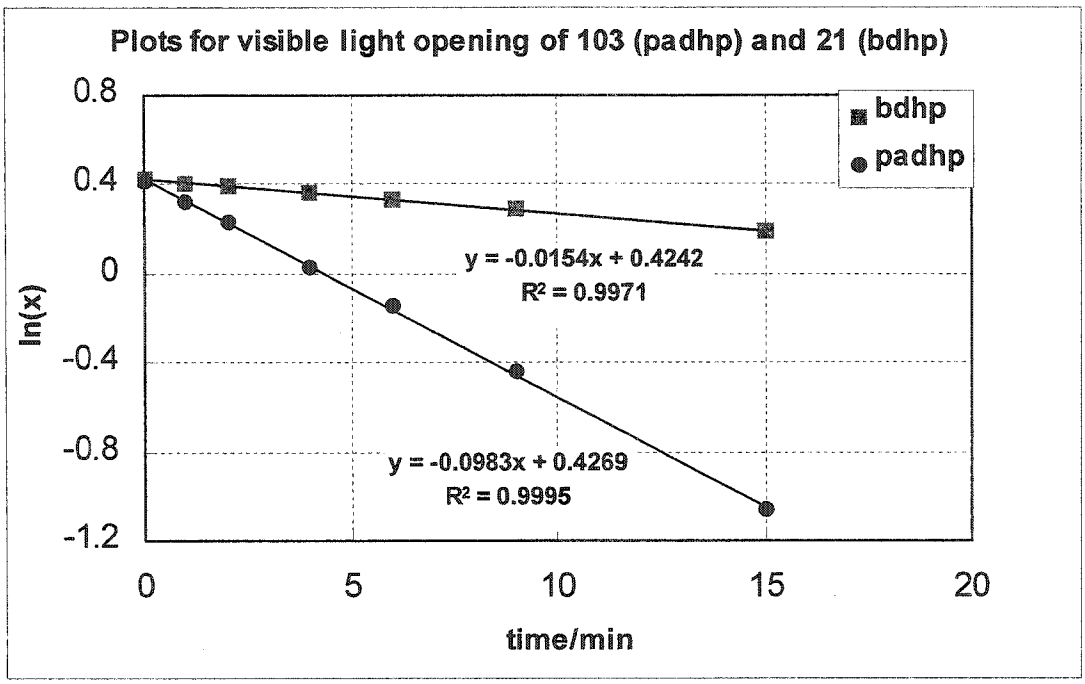
Plots for visible light opening of 103 (padhp) and 21 (bdhp)
0.8
0.4
0
-0.4
-0.8
-1.2
ln(x)
0
5
10
15
20
time/min
bdhp
padhp
y = -0.0154x + 0.4242
R² = 0.9971
y = -0.0983x + 0.4269
R² = 0.9995

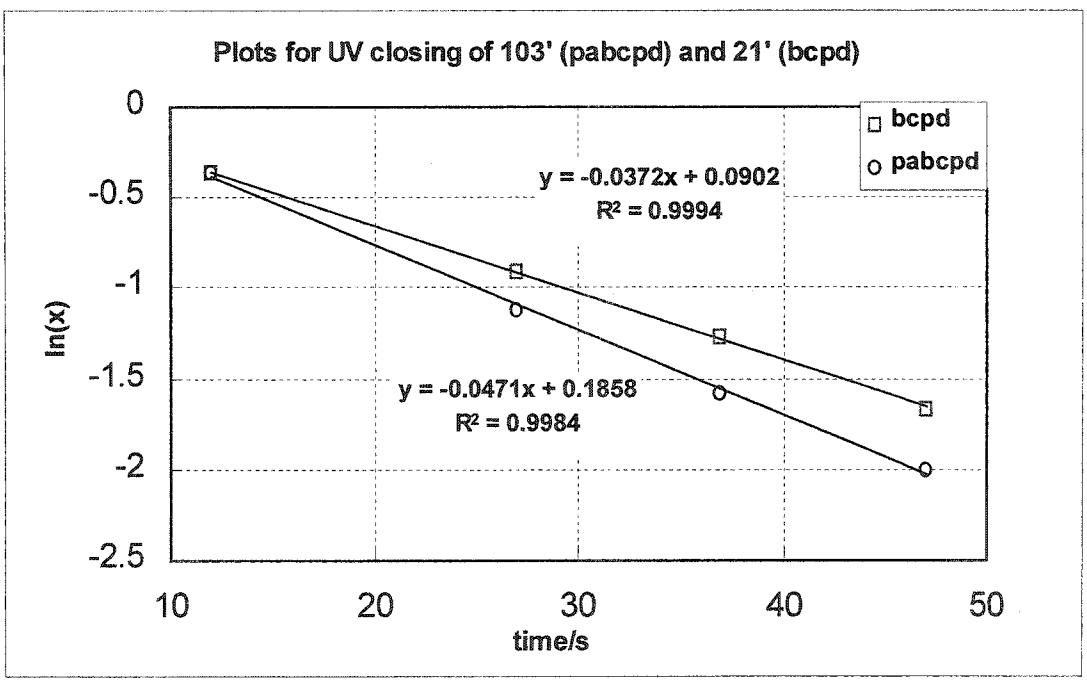
Plots for UV closing of 103' (pabcpd) and 21' (bcpd)
0
-0.5
-1
-1.5
-2
-2.5
ln(x)
10
20
30
40
50
time/s
bcpd
pabcpd
y = -0.0372x + 0.0902
R² = 0.9994
y = -0.0471x + 0.1858
R² = 0.9984

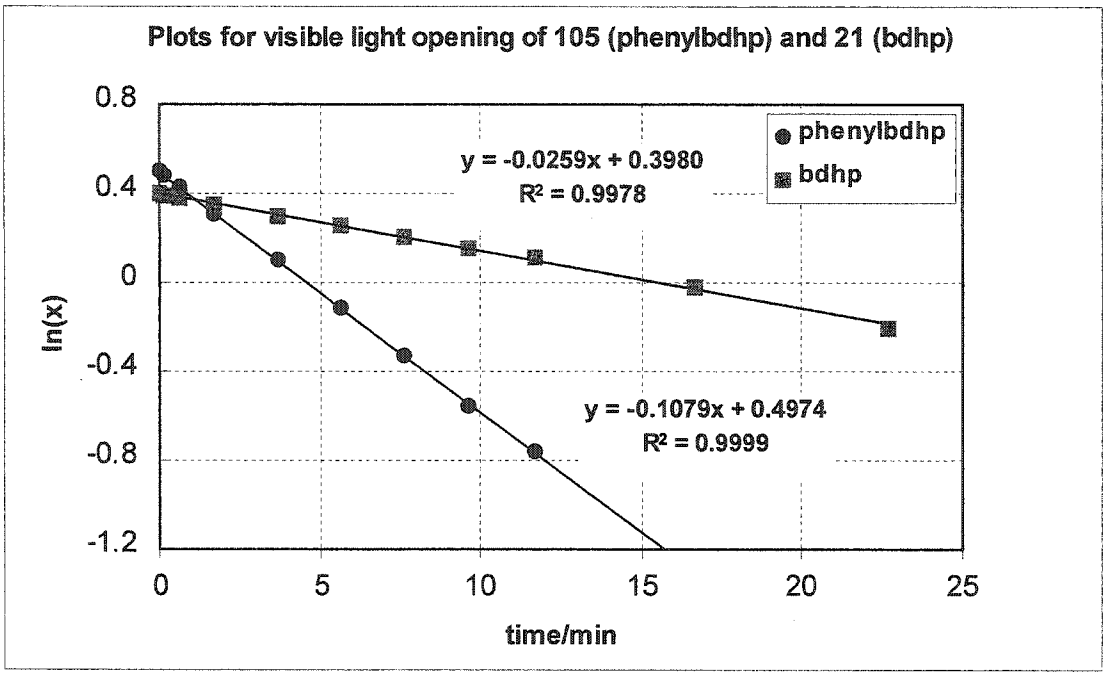
Plots for visible light opening of 105 (phenylbdhp) and 21 (bdhp)
0.8
0.4
0
-0.4
-0.8
-1.2
ln(x)
0
5
10
15
20
25
time/min
phenylbdhp
bdhp
y = -0.0259x + 0.3980
R² = 0.9978
y = -0.1079x + 0.4974
R² = 0.9999

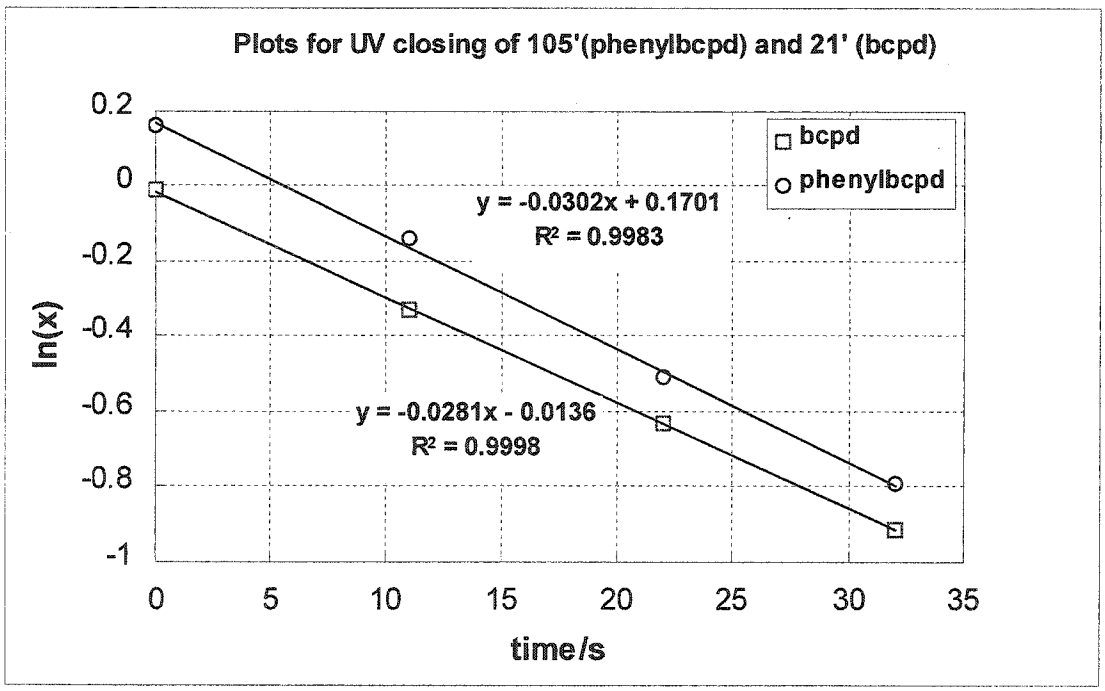
Plots for UV closing of 105'(phenylbcpd) and 21' (bcpd)
0.2
0
-0.2
-0.4
-0.6
-0.8
-1
ln(x)
0
5
10
15
20
25
30
35
time/s
bcpd
phenylbcpd
y = -0.0302x + 0.1701
R² = 0.9983
y = -0.0281x - 0.0136
R² = 0.9998

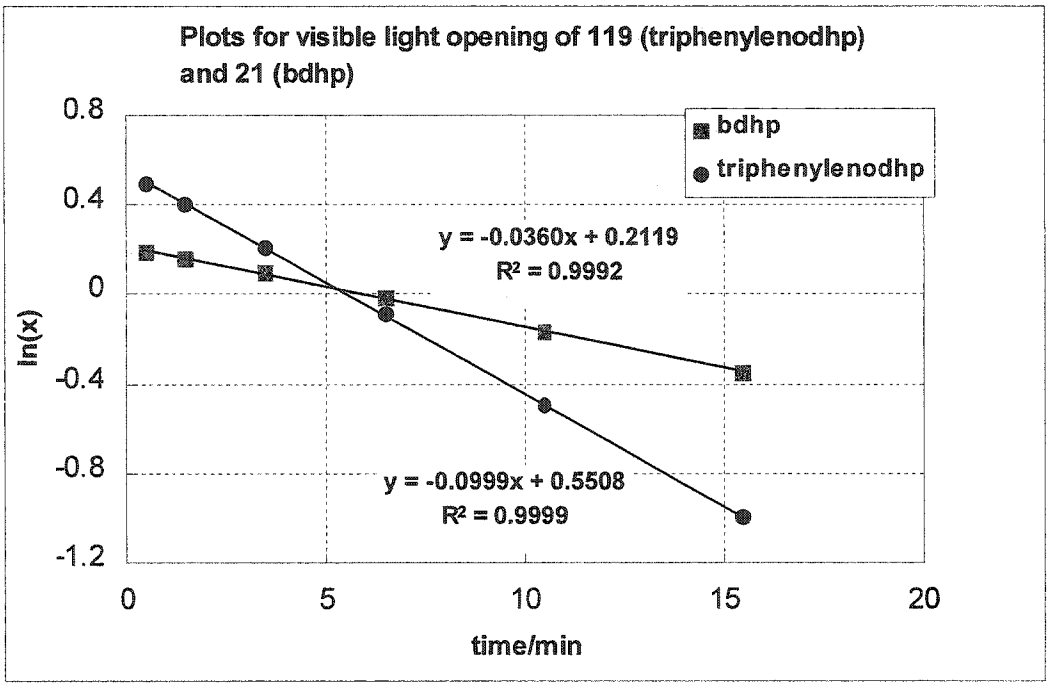
Plots for visible light opening of 119 (triphenylenodhp) and 21 (bdhp)
bdhp
triphenylenodhp
y = -0.0360x + 0.2119
R² = 0.9992
y = -0.0999x + 0.5508
R² = 0.9999
ln(x)
time/min
0.8
0.4
0
-0.4
-0.8
-1.2
0
5
10
15
20

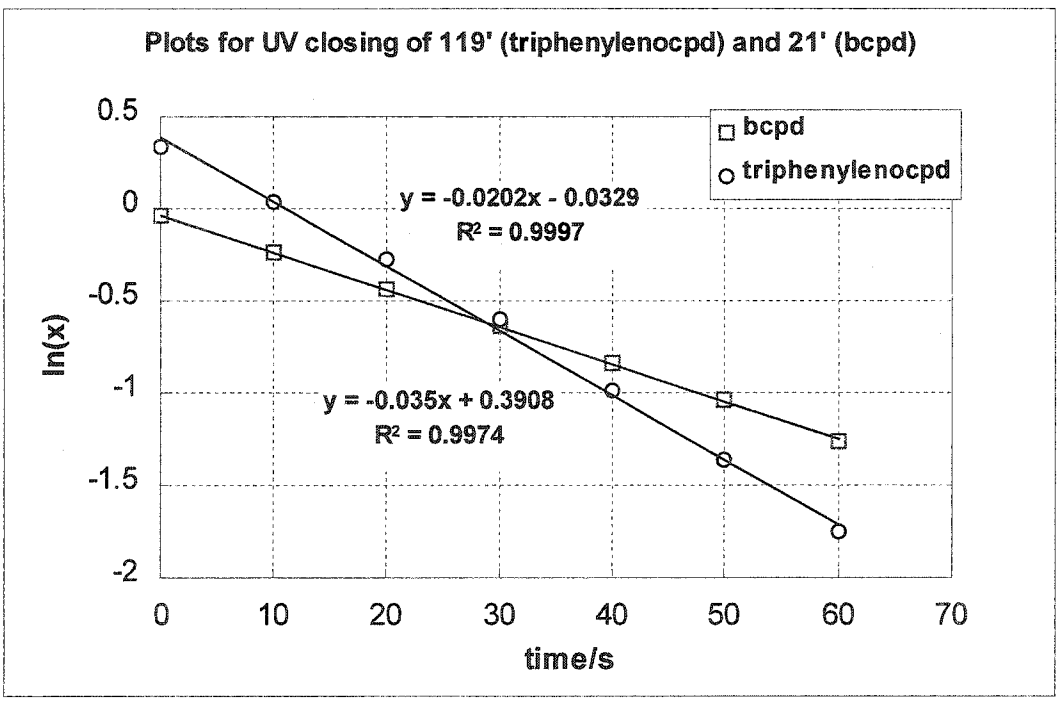
Plots for UV closing of 119' (triphenylenocpd) and 21' (bcpd)
bcpd
triphenylenocpd
y = -0.0202x - 0.0329
R² = 0.9997
y = -0.035x + 0.3908
R² = 0.9974
ln(x)
time/s
0.5
0
-0.5
-1
-1.5
-2
0
10
20
30
40
50
60
70

Thermal decay plots of acetylbenzo-CPD 84' closing to DHP 84

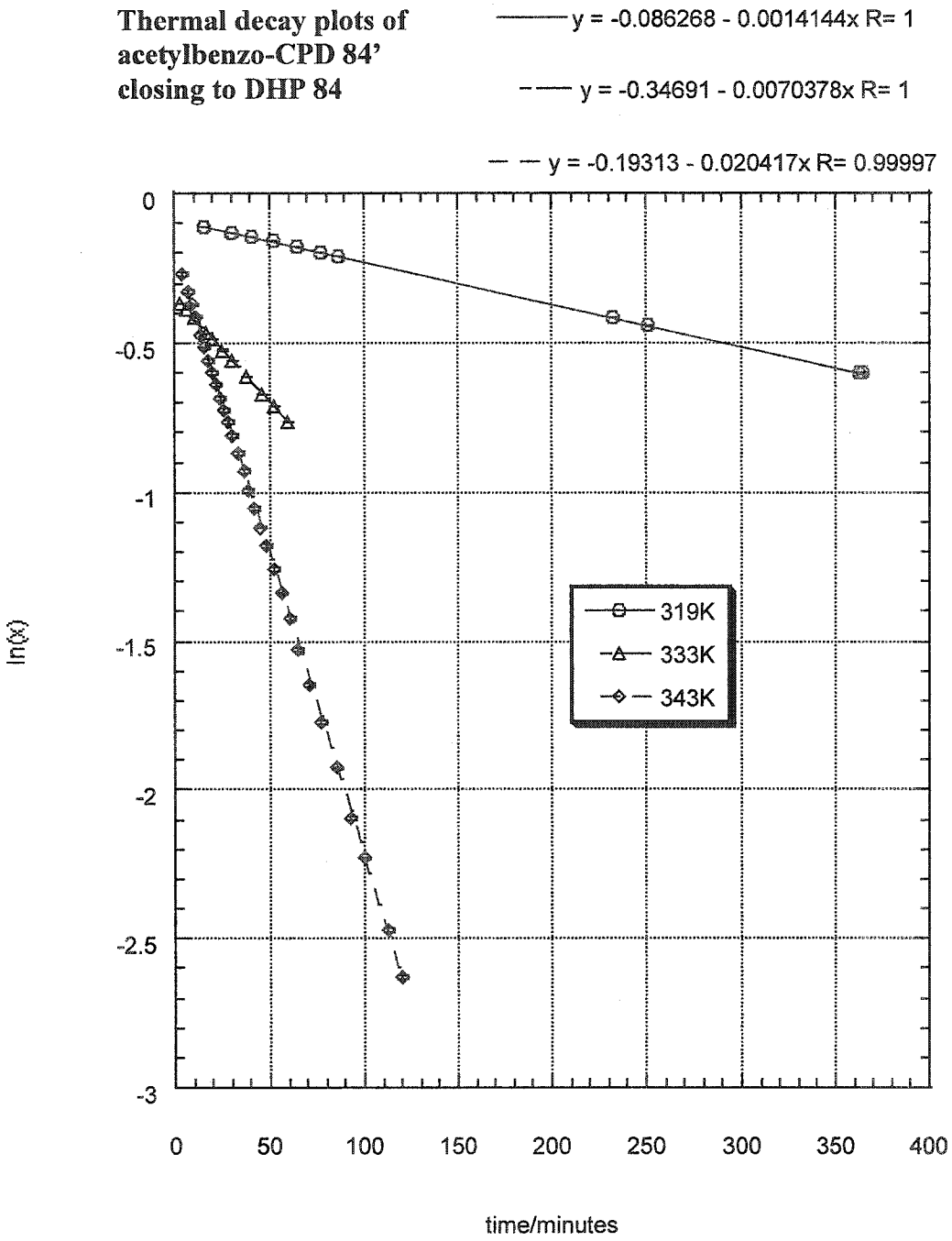

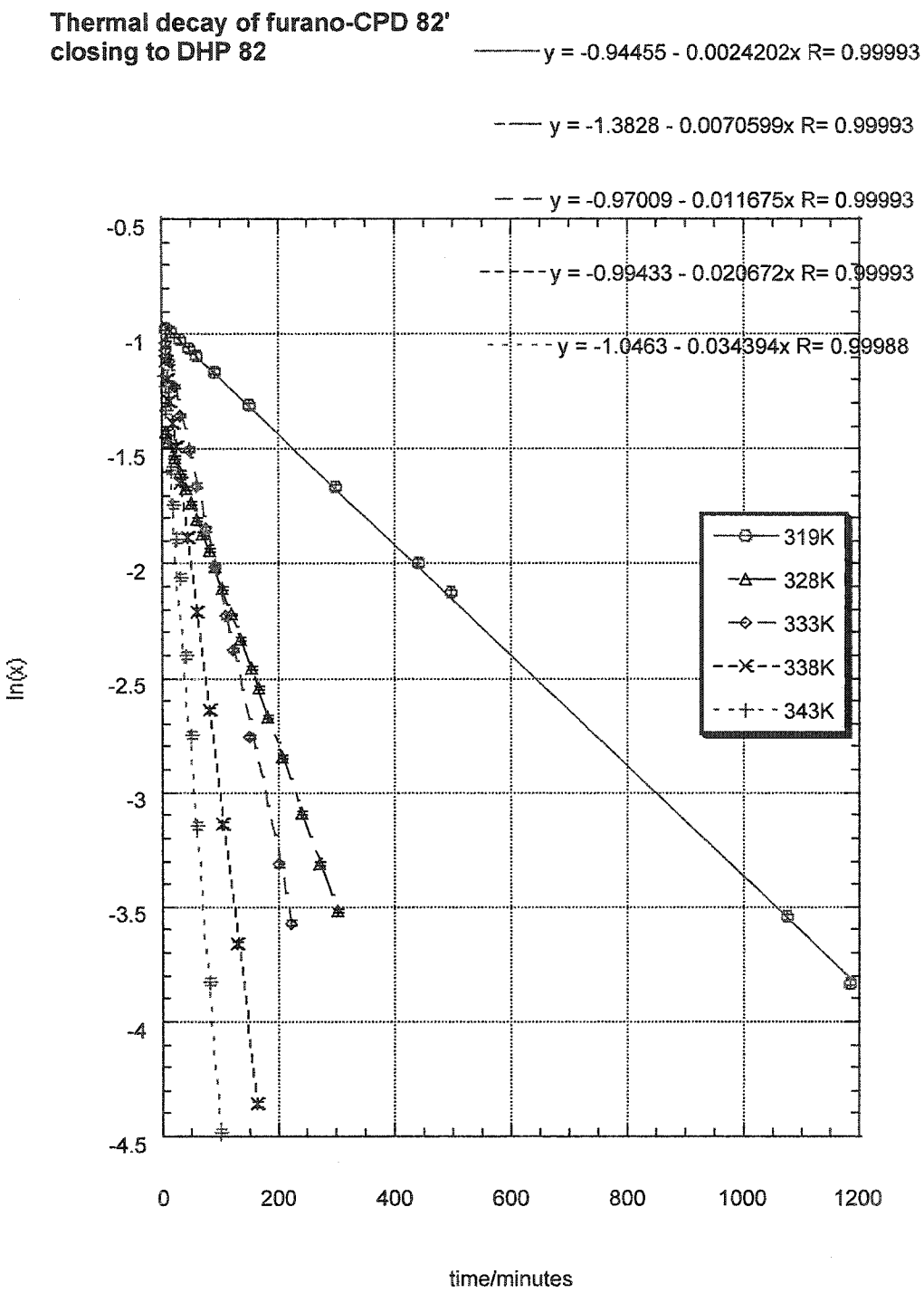
Thermal decay of furano-CPD 82'
closing to DHP 82
y = -0.94455 - 0.0024202x R= 0.99993
y = -1.3828 - 0.0070599x R= 0.99993
y = -0.97009 - 0.011675x R= 0.99993
y = -0.99433 - 0.020672x R= 0.99993
y = -1.0463 - 0.034394x R= 0.99988
319K
328K
333K
338K
343K
ln(x)
-0.5
-1
-1.5
-2
-2.5
-3
-3.5
-4
-4.5
0
200
400
600
800
1000
1200
time/minutes

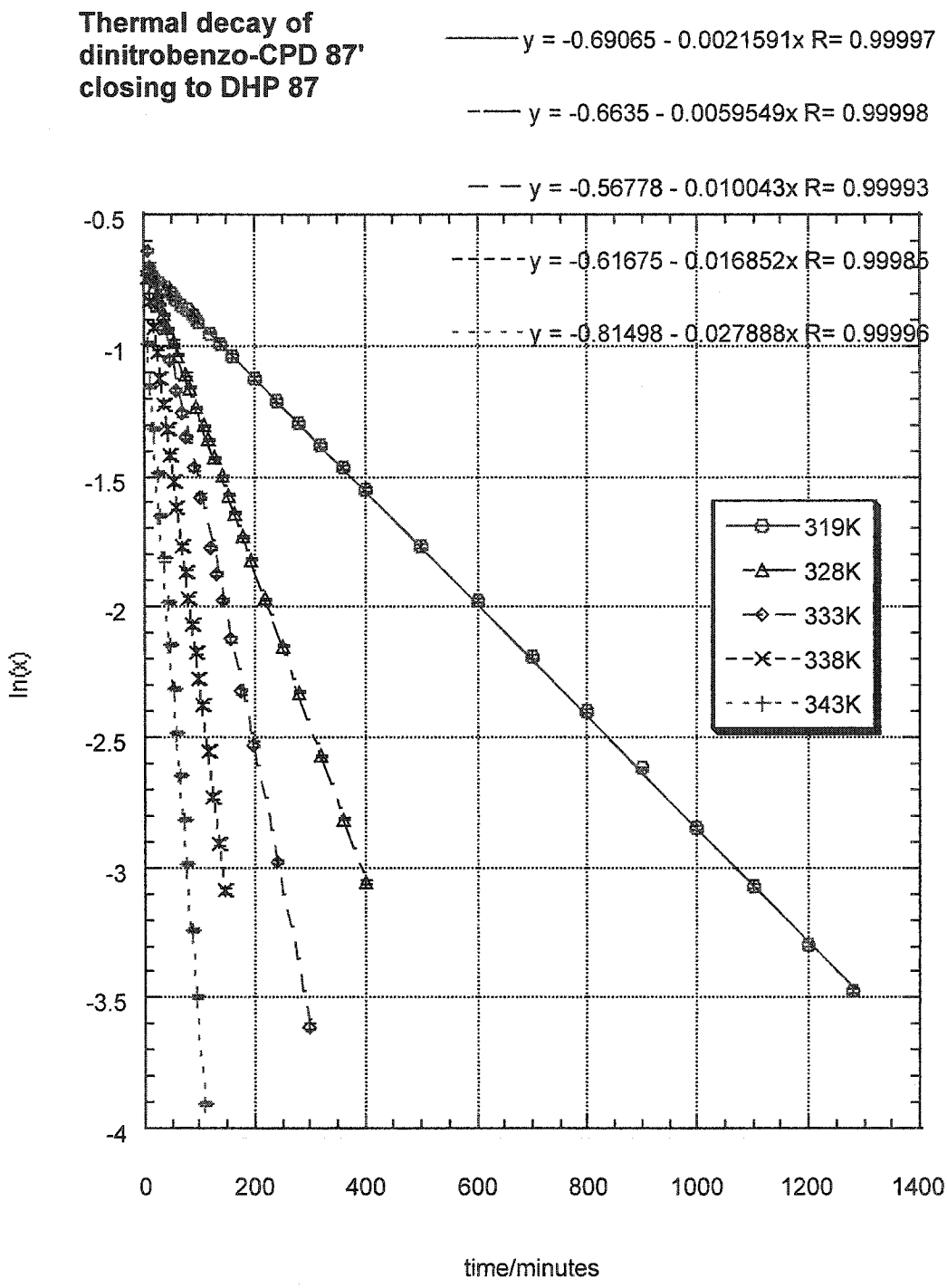
Thermal decay of dinitrobenzo-CPD 87' closing to DHP 87
y = -0.69065 - 0.0021591x R= 0.99997
y = -0.6635 - 0.0059549x R= 0.99998
y = -0.56778 - 0.010043x R= 0.99993
y = -0.61675 - 0.016852x R= 0.99985
y = -0.81498 - 0.027888x R= 0.99996
319K
328K
333K
338K
343K
ln(x)
-0.5
-1
-1.5
-2
-2.5
-3
-3.5
-4
0
200
400
600
800
1000
1200
1400
time/minutes

**Thermal decay of nitrobenzo-CPD 86'
closing to DHP 86**

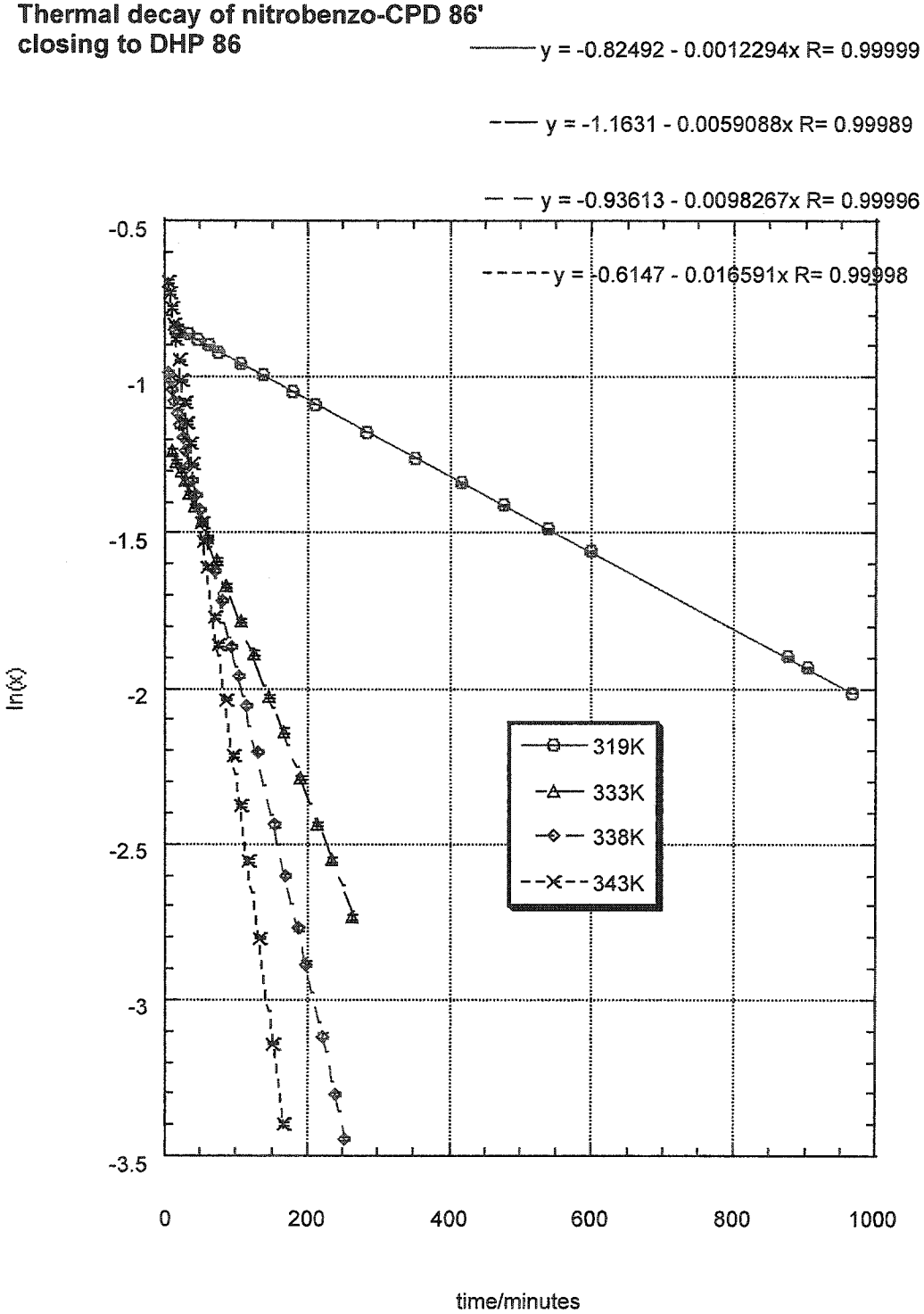

Thermal decay plots of phenylethynylbenzo-CPD 103' closing to DHP 103

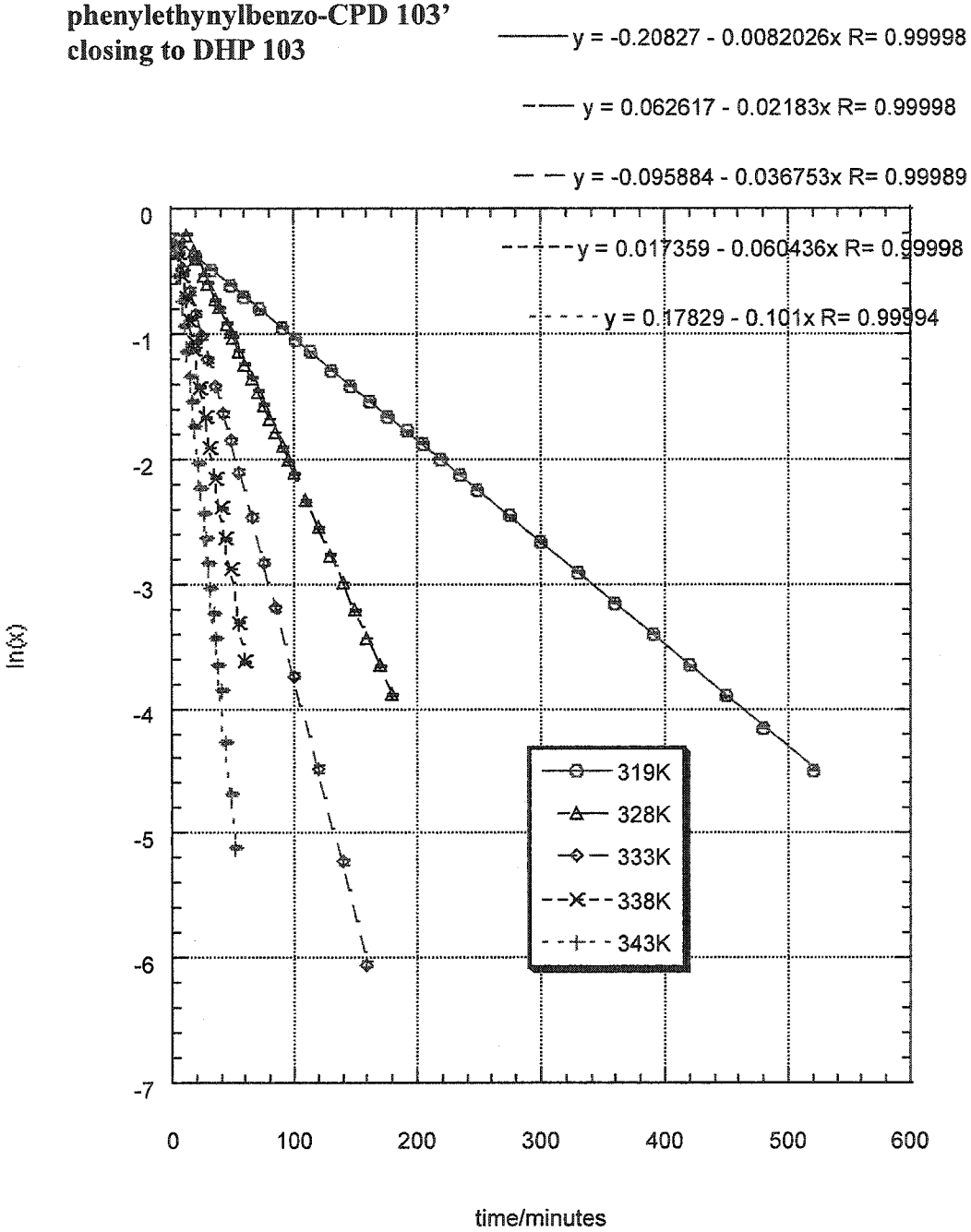

Thermal decay plots of phenylbenzo-CPD 105' closing to DHP 105

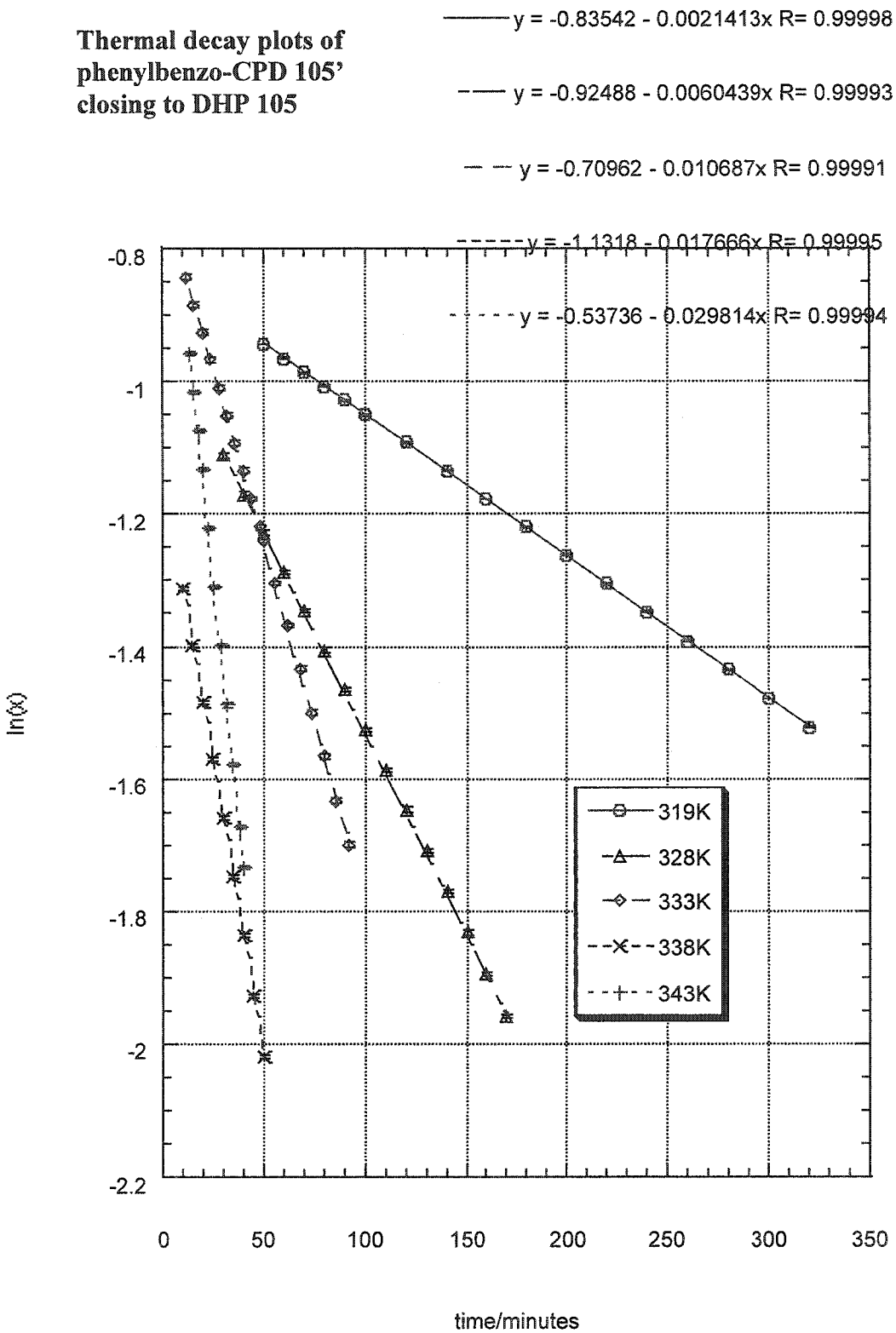

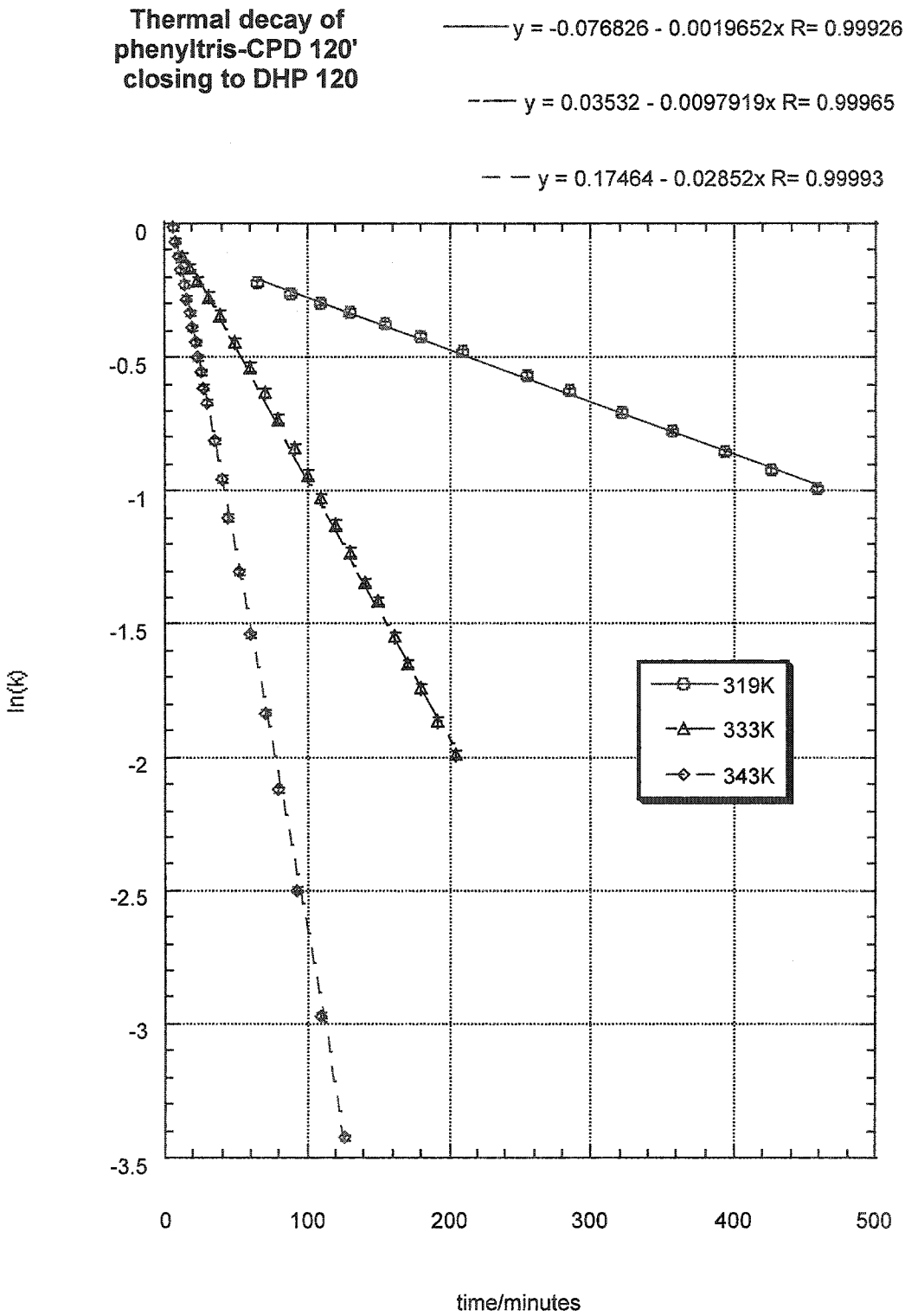
Thermal decay of phenyltris-CPD 120' closing to DHP 120
y = -0.076826 - 0.0019652x R= 0.99926
y = 0.03532 - 0.0097919x R= 0.99965
y = 0.17464 - 0.02852x R= 0.99993
0
-0.5
-1
-1.5
-2
-2.5
-3
-3.5
ln(k)
0
100
200
300
400
500
time/minutes
319K
333K
343K

Thermal decay plots of tris-CPD 72' closing to DHP 72

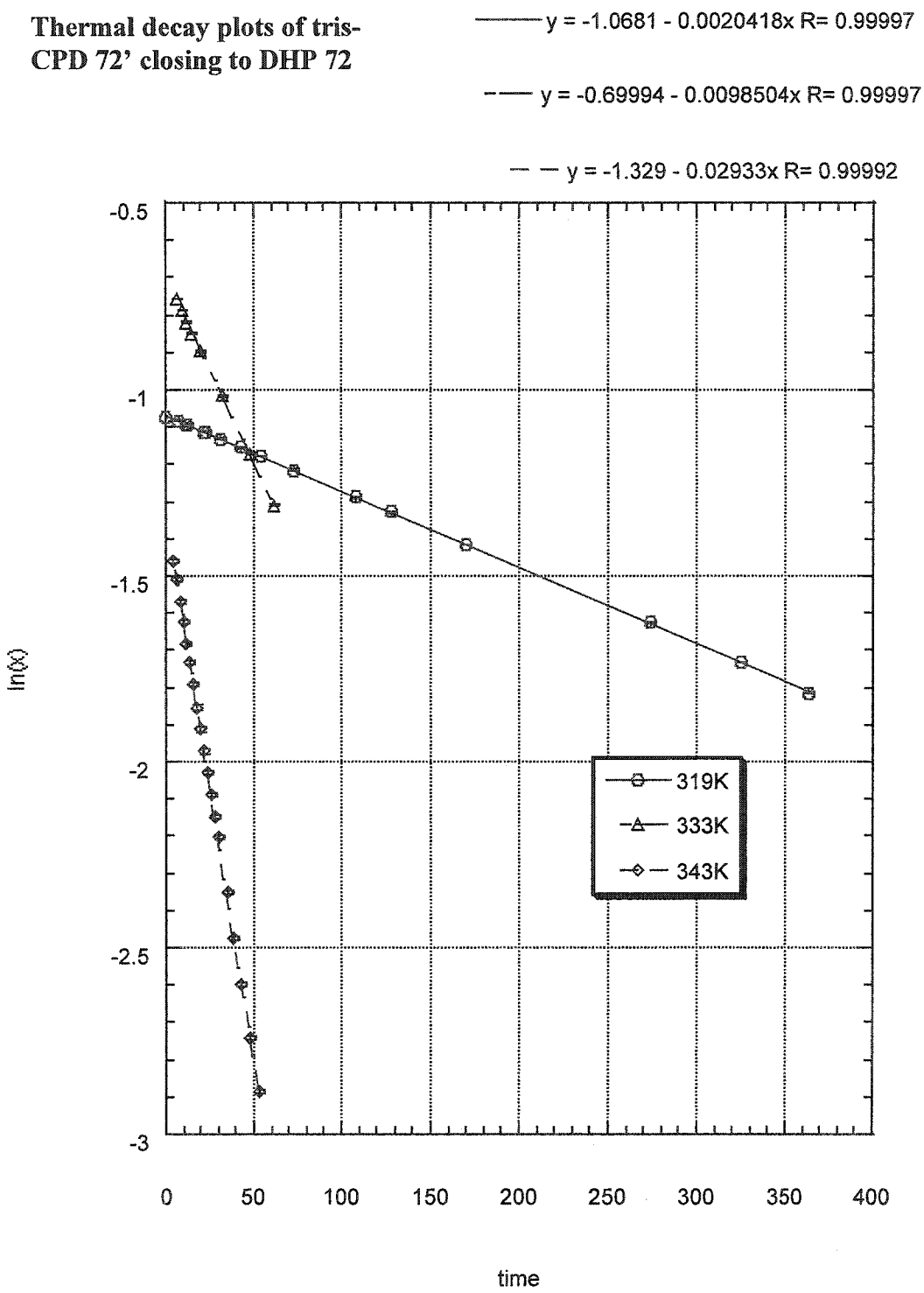

Arrhenius plots for the thermal return of CPD to DHP

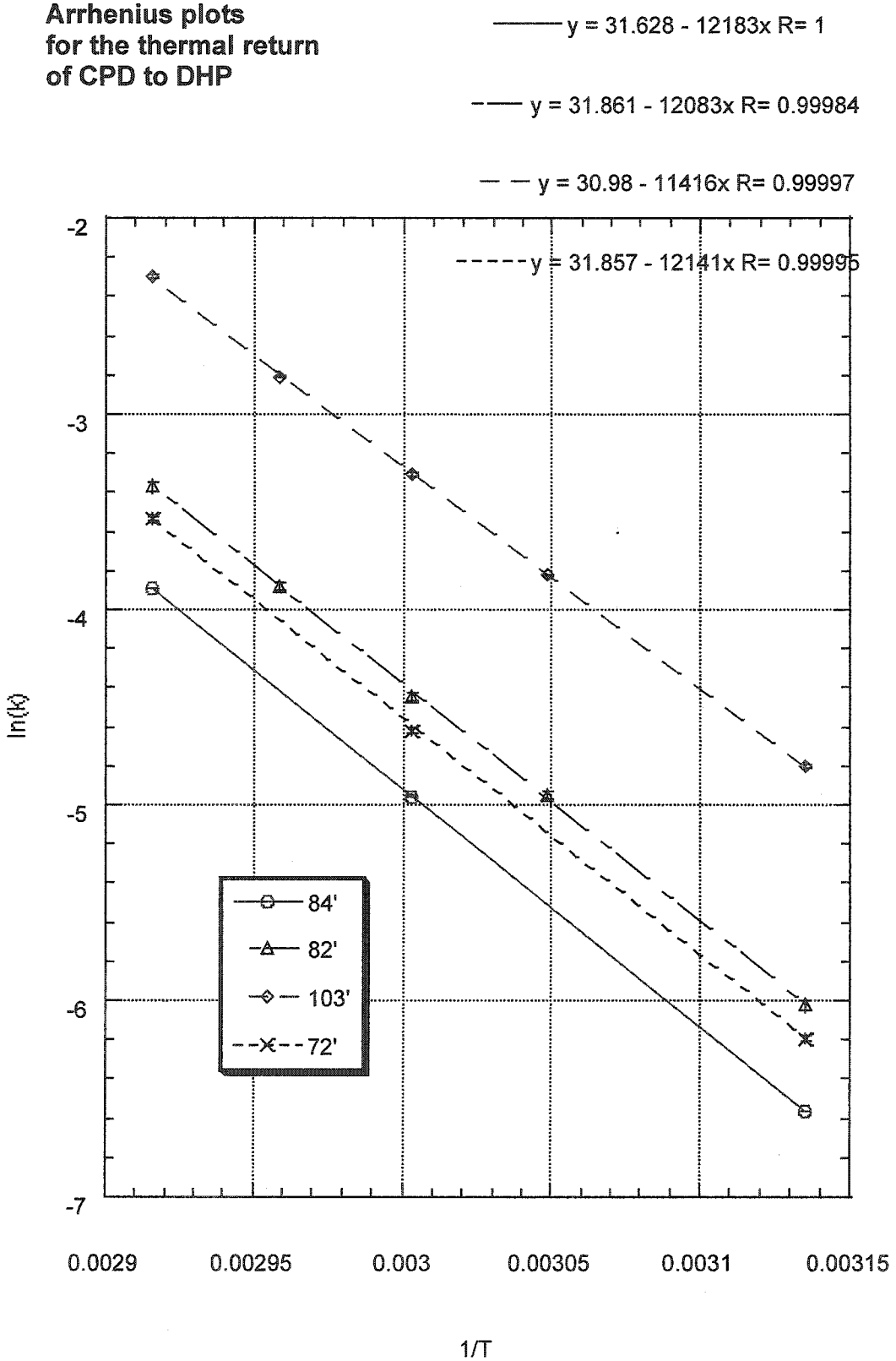

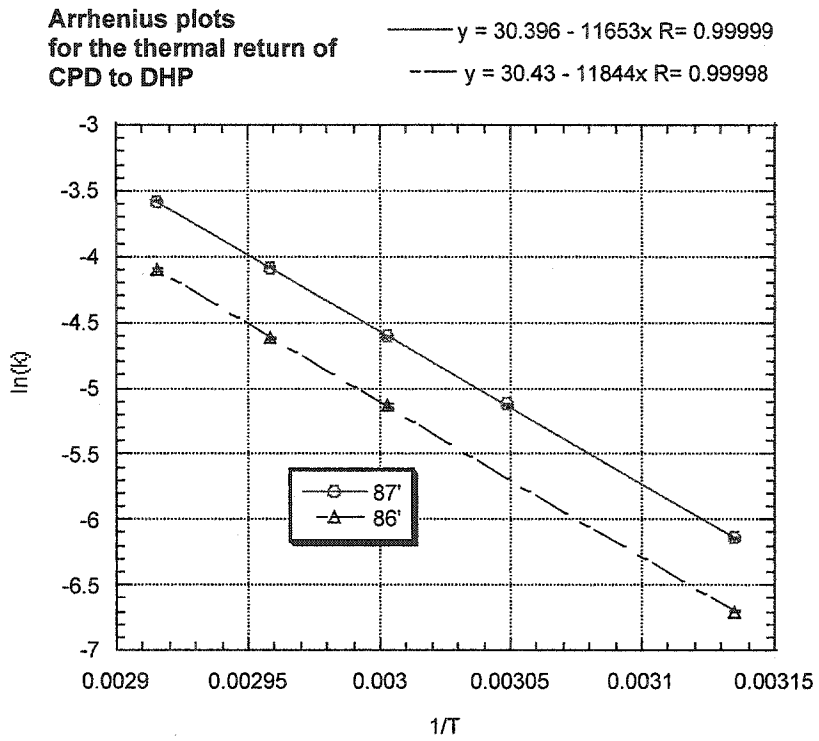
Arrhenius plots for the thermal return of CPD to DHP
y = 30.396 - 11653x R= 0.99999
y = 30.43 - 11844x R= 0.99998
-3
-3.5
-4
-4.5
-5
-5.5
-6
-6.5
-7
ln(k)
87'
86'
0.0029
0.00295
0.003
0.00305
0.0031
0.00315
1/T

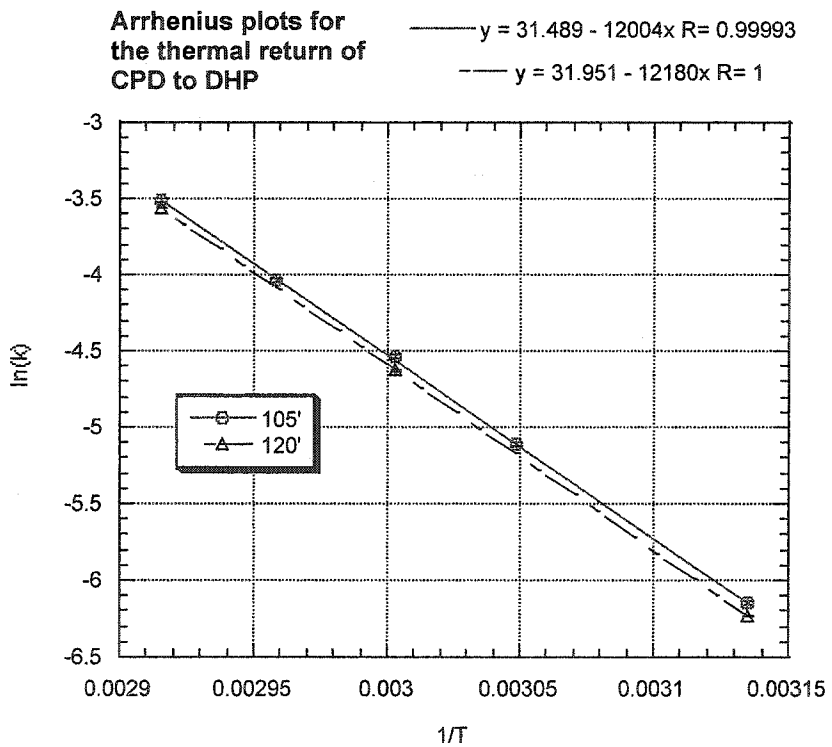
Arrhenius plots for the thermal return of CPD to DHP
y = 31.489 - 12004x R= 0.99993
y = 31.951 - 12180x R= 1
-3
-3.5
-4
-4.5
-5
-5.5
-6
-6.5
ln(k)
105'
120'
0.0029
0.00295
0.003
0.00305
0.0031
0.00315
1/T

Eyring plots for the thermal return reactions of CPD to DHP

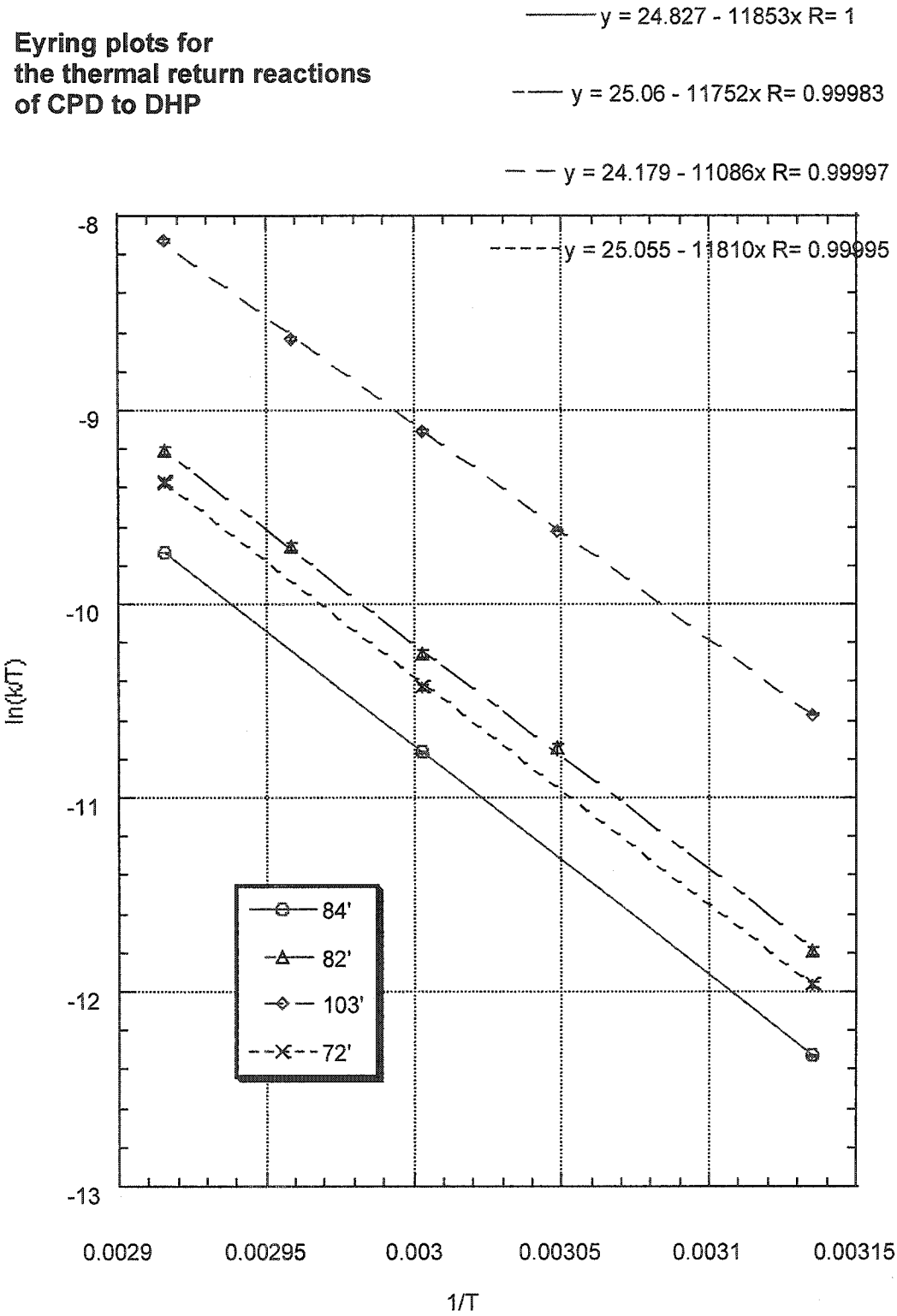

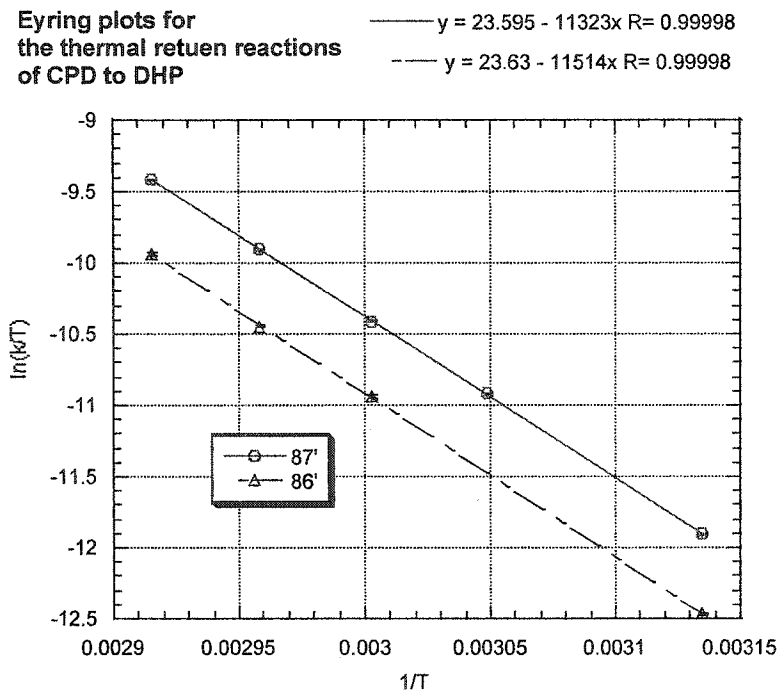
Eyring plots for
the thermal retuen reactions
of CPD to DHP
y = 23.595 - 11323x R= 0.99998
y = 23.63 - 11514x R= 0.99998
-9
-9.5
-10
-10.5
-11
-11.5
-12
-12.5
ln(k/T)
87'
86'
0.0029
0.00295
0.003
0.00305
0.0031
0.00315
1/T

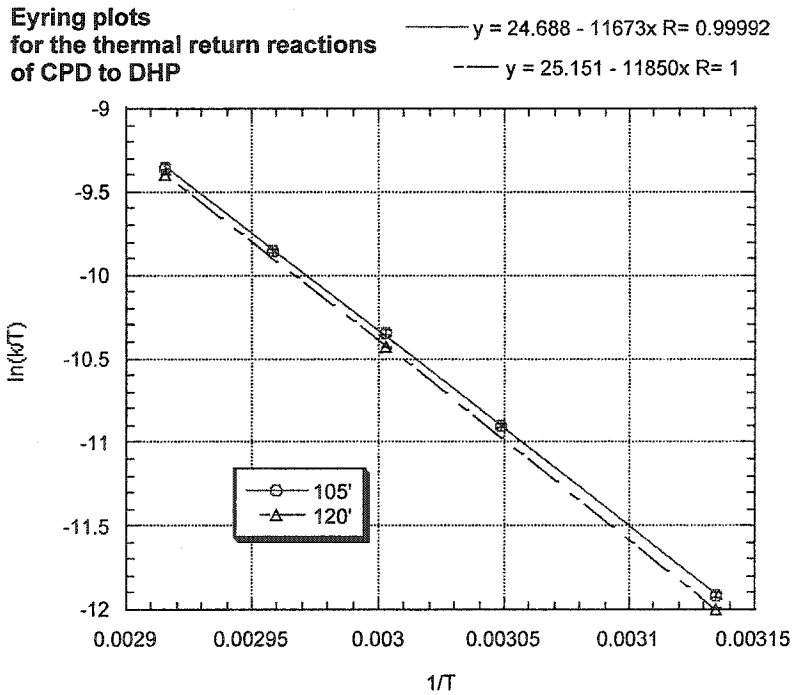
Eyring plots
for the thermal return reactions
of CPD to DHP
y = 24.688 - 11673x R= 0.99992
y = 25.151 - 11850x R= 1
-9
-9.5
-10
-10.5
-11
-11.5
-12
ln(k/T)
105'
120'
0.0029
0.00295
0.003
0.00305
0.0031
0.00315
1/T

Chapter Six Thesis References

(1) Faraday, M. *Phil. Trans. Roy. Soc.* **1825**, *115*, 440-466.

(2) Kekule, A. *Bull. Soc. Chim. Fr.* **1865**, *3*, 98.

(3) Lloyd, D. *J. Chem. Inf. Comput. Sci.* **1996**, *36*, 442-447.

(4) Willstaetter, R.; Waser, E. *Ber.* **1911**, *44*, 3424-3445.

(5) Huckel, E. Z. *Phys.* **1931**, *70*, 204-286.

(6) Sondheimer, F. *Pure Appl. Chem.* **1963**, *7*, 363-388.

(7) Breslow, R.; Brown J.; Gajewski, J. J. *J. Am. Chem. Soc.* **1967**, *89*, 4383-4390.

(8) Flygare, W. H. *Chem. Rev.* **1974**, *74*, 653-687.

(9) Dauben, H. J.; Wilson, J. D.; Laity, J. L. Nonbenzenoid Aromatics, Vol. 2, Academic Press, **1971**, pp 167.

(10) Burnham, A. K.; Lee, J.; Schmalz, T. G. *J. Am. Chem. Soc.* **1977**, *99*, 1836-1844.

(11) Gorelik, M. V. *Russ. Chem. Rev.* **1990**, *59*, 116-133.

(12) Haigh, C. W.; Mallion, R. B. *Mol. Phys.* **1970**, *18*, 737-750.

(13) Breslow, R.; Groves, J. *J. Am. Chem. Soc.* **1970**, *92*, 984-988.

(14) Schaefer, T.; Schneider, W. G. *Can. J. Chem.* **1963**, *41*, 966-982.

(15) Grasselli, J. G. *Atlas of Spectral Data and Physical Constants for Organic Compounds:* CRC press, **1973**, pp B460.

(16) Pouchert, C. J.; Behnke, J. *The Aldrich Library of ^{13}C and ^{1}H FT NMR Spectra,* Edn., 1; Vol. III; **1993**, pp 1.

(17) Vogel, E.; Roth, H. D. *Angew. Chem. Int. Ed. Engl.* **1964**, *3*, 228-229. Vogel, E.; Boll, W. A. *Angew. Chem. Int. Ed. Engl.* **1964**, *3*, 642-643.

(18) Schafer-Ridder, M.; Wagner, A.; Schwamborn, M.; Schreiner, H.; Devront, E.; Vogel, E. *Angew. Chem. Int. Ed. Engl.* **1978,** *17,* 853-855.

(19) Grimme, W.; Kanfhold, M.; Dettmeier, U.; Vogel, E., *Angew. Chem. Int. Ed. Engl.* **1966,** *5,* 604-605.

(20) Vogel, E.; Konigshofen, H.; Mullen, K.; Oth, J. F. M. *Angew. Chem. Int. Ed. Engl.* **1974**, *13*, 281-283.

(21) Oth, J. F. M. *Pure Appl. Chem.* **1971,** *25*, 573-622.

(22) Boekelheide, V.; Pepperdine, W. *J. Am. Chem. Soc.* **1970,** *92,* 3684-3688.

(23) Boekelheide, V.; Phillips, J. B. *J. Am. Chem. Soc.* **1967**, *89*, 1695-1704.

(24) Mitchell, R. H.; Klopfenstein, C.; Boekelheide, V. *J. Am. Chem. Soc.* **1969**, *91,* 4931-4932.

(25) Vogler, H. *J. Am. Chem. Soc.* **1978,** *100*, 7464-7500.

(26) Memory, J. D.; Wilson, N. K. *NMR of Aromatic Compounds;* John Wiley & Sons; New York; **1982**, pp30-33.

(27) Pauling, L. *J. Chem. Phys.* **1936**, *4*, 673-677.

(28) Pople, J. A. *J. Chem. Phys.* **1956**, *24,* 1111-1116.

(29) Haddon, R. C. *Tetrahedron* **1972**, *28*, 3613-3633. Haddon, R. C. *Tetrahedron,* **1972**, *28*, 3635-3655.

(30) Mitchell, R. H.; Iyer, V. S.; Khalifa, N.; Mahadevan, R.; Venugopalan, S.; Weerawarna, S. A.; Zhou, P. *J. Am. Chem. Soc.* **1995**, *117*, 1514-1532.

(31) Mitchell, R. H.; Ward, T. R. *Tetrahedron* **2001**, *57*, 3689-3695

(32) Bouas-Laurent, H.; Durr, H. *Pure Appl. Chem.* **2001**, *73*, 639-665.

(33) Irie, M. *Chem. Rev.* **2000,** *100*, 1685-1716.

(34) Henry, A. J. *J. Chem. Soc.* **1946**, 1156-1164.

(35) Beveridge, D. J.; Jaffe, H. H. *J. Am. Chem. Soc.* **1965**, *87*, 5340-5346.

(36) Dyck, R. H.; McClure, D. S. *J. Chem. Phys.* **1962**, *36*, 2326-2345.

(37) Muszkat, K. A.; Fischer, E. J. Chem. Soc. (B) **1967**, 662-678.

(38) Gegiou, D.; Muszkat, K. A.; Fischer, E. *J. Am. Chem. Soc.* **1968**, *90*, 3907-3918.

(39) Malkin, S.; Fischer, E. *J. Phys. Chem.* **1962**, *66*, 2482 Zimmerman, G.; Chow, L. Y.; Paik, U. J. *J. Chem. Phys.* **1958,** *80*, 3528-3531.

(40) Fischer, E.; Frei, Y. *J. Chem. Phys.* **1957**, *27*, 328-330.

(41) Saltiel, J. *J. Am. Chem. Soc.* **1967**, *89*, 1036-1037.

(42) Waldeck, D. H. *Chem. Rev.* **1991**, *91*, 415-436.

(43) Irie, M.; Mohri, M. *J. Org. Chem.* **1988**, *53*, 803-808.

(44) Nakamura, S.; Irie, M. *J. Org. Chem.* **1988**, *53,* 6136-6138.

(45) Blattmann, H. R.; Schmidt, W. *Tetrahedron* **1970**, *26*, 5885-5899.

(46) Blattmann, H. R.; Meuche, D.; Heilbronner, E.; Molyneux, R. J.; Boekelheide, V. *J. Am. Chem. Soc.* **1965**, *87*, 130-131.

(47) Murakami, S.; Tsutsui, T.; Saito, S.; Yamato, T.; Tashiro, M. *Nippon Kagukukai Shi*, **1988**, 221-229.

(48) Mitchell, R. H.; Iyer, V. S.; Mahadevan, R.; Venugopalan, S.; Zhou, P. *J. Org. Chem.* **1996**, *61*, 5116-5120.

(49) Mitchell, R. H. *Eur. J. Org. Chem.* **1999**, 2695-2703.

(50) Mitchell, R.H.; Ward, T.R.; Chen, Y.; Wang, Y.; Weerawarna, S. A.; Dibble, P. W.; Marsella, M. J.; Almutairi, A; Wang, Z.Q. *J. Am. Chem. Soc.* **2003**, *125*, 2974-2988.

(51) Ward, T. R. Ph.D. Thesis, University of Victoria, **2000**.

(52) Mitchell, R. H.; Chen, Y. *Tetrahedron lett.*, **1996**, *37*, 5239-5242.

(53) Mitchell, R. H.; Ward, T. R.; Wang, Y.; Dibble, P. W. *J. Am. Chem. Soc.* **1999**, *121*, 2601-2602.

(54) Marsella, M.J.; Wang, ZQ.; Mitchell, R. H. *Org. Lett.* **2000**, *2*, 2979-2982.

(55) Yokoyama, Y. *Chem. Rev.* **2000**, *100*. 1717-1739.

(56) Chakraborty, D. P.; Sleigh, T.; Stevenson, R.; Swoboda, G. A.; Weinstein, B. *J. Org. Chem.* **1966**, *31*, 3342-3345.

(57) Santiago, A.; Becker, R. S. *J. Am. Chem. Soc.* **1968**, *90*, 3654-3658.

(58) Heller, H. G. *IEE Proc.* **1983**, *130*, Pt. I, 209-211.

(59) Glaze, A. P.; Heller, H. G.; Whittall, J. *J. Chem. Soc., Perkin Trans. 2.* **1992**, 591-594.

(60) Kaneko, A.; Tomoda, A.; Ishizuka, M.; Suzuki, H.; Matsushima, R. *Bull. Chem. Soc. Jpn.* ***1988***, *61*, 3569-3573.

(61) Berkovic, G.; Krongauz, V.; Weiss, V. *Chem. Rev.* **2000**, *100*, 1741-1753.

(62) Hirshberg, Y. *J. Am. Chem. Soc.* **1956**, 78, 2304-2312. Bercovici, T.; Fischer, E. *J. Am. Chem. Soc.* **1964**, 86, 5687-5688.

(63) Brown, G. H. *Photochromism*, John Wiley & Sons; New York; **1971**, pp98-99, pp440-444, pp569-578.

(64) Mitchell, R. H.; Yan, J. S. H. *Can. J. Chem.* **1977**, *55*, 3347-3348.

(65) Mitchell, R. H.; Zhou, P. *Tetrahedron. Lett.* **1990**, *31*, 5277-5280.

(66) Tashiro, M.; Yamato, T. *J. Am. Chem. Soc.* **1982**, *104*, 3701-3707.

(67) Zhou, P. Ph.D. Thesis, University of Victoria, **1990**.

(68) Jung, K.; Koreeda, M., *J. Org. Chem.* **1989**, *54*, 5667-5675.

(69) McMurry, J. E.; Silvestri, M. G.; Fleming, M. P.; Hoz, T.; Grayston, M. W., *J. Org. Chem.* **1978**, *43*, 3249-3255.

(70) Girard, P.; Namy, H. B.; Kagan, H. B. *J. Am. Chem. Soc.* **1980**, *102*, 2693-2698.

(71) Chen, Y. Ph.D. Thesis, University of Victoria, **1997**.

(72) Mitchell, R. H.; Ward, T. R.; Wang, Y. Heterocycles, **2001**, *54*, 249-257.

(73) Geldard, J. F.; Lions, F. *J. Org. Chem.* **1965**, *30*, 318-319.

(74) Phillips, J. B.; Molyneux, R. J.; Sturm, E.; Boekelheide, V. *J. Am. Chem. Soc.* **1967**, *89*, 1704-1709.

(75) Mitchell, R. H.; Yan, J. S. H.; Dingle, T. W. *J. Am. Chem. Soc.* **1982**, *104*, 2551-2559.

(76) Tashiro, M.; Yamato, *T. Org. Prep. Proced. Int.* **1982**, *14*, 216-219.

(77) Sheepwash, M.A., Ph.D. Thesis, University of Victoria, **2002**.

(78) Lemieux, R. H.; Morgan, A. R. *Can. J. Chem.* **1965**, *43*, 2190-2199.

(79) Aldrich, P2000-9, 97% [98-80-6], mp 217-220°C.

(80) Slee, J. D.; LeGoff, E. *J. Org. Chem.* **1970**, *35*, 3897-3901.

(81) Cava, M. P.; Scheel, F. M. *J. Org. Chem.* **1967**, *32*, 1304-1307.

(82) PCMODEL V. 7.0, Serena Software, Bloomington, IN 47402-3076.

(83) Sheepwash, M. A.; Mitchell, R. H.; Bohne, C. *J. Am. Chem. Soc.* **2002,** *124*, 4693-4700.

(84) Aldrich, B7540-9, 96% [573-17-1], mp 60-64°C